

A Modulatory Role for Alpha-Synuclein During Ectopic Neuronal  
Cell Cycle Re-Entry: Implications for Alzheimer's Disease and  
Parkinson's Disease

Shahzad S. Khan  
Miami, FL

B.S., The Florida State University, 2011

A Dissertation presented to the Graduate Faculty of the  
University of Virginia in Candidacy for the Degree of Doctor of  
Philosophy

Department of Neuroscience

University of Virginia  
July, 2018

# Abstract

Alpha-synuclein ( $\alpha$ Syn) is enriched in presynaptic terminals of neurons where it maintains synaptic vesicle stores, promotes SNARE complex assembly, and regulates exocytosis. Under diseased conditions such as Alzheimer's disease (AD) and Parkinson's disease (PD), soluble  $\alpha$ Syn is associated with neurodegeneration. However, the precise mechanism(s) by which  $\alpha$ Syn causes neuron loss are ill-defined. The purpose of this thesis was to investigate the functional role of  $\alpha$ Syn during the induction of ectopic neuronal cell cycle re-entry (CCR), a prelude to neuron loss in AD. The results show that  $\alpha$ Syn bi-directionally modulates the Amyloid- $\beta$  oligomer-induced increase in cyclin D1 in primary neuronal cultures and also ameliorates neuronal cyclin D1 expression in mutant Amyloid Precursor Protein (APPJ20) animals. Moreover,  $\alpha$ Syn modulation of CCR directly correlated to the increase production of OC- and A11-positive Amyloid- $\beta$  assemblies. Furthermore, MC1-tau in primary neurons and transgenic mice were found to be bi-directionally modulated by  $\alpha$ Syn. Upon overexpression of human  $\alpha$ Syn in APPJ20 mice, a decline in Barnes maze performance was observed when compared to the APPJ20 parental strain. By contrast, genetic ablation of  $\alpha$ Syn in APPJ20 restored Barnes maze performance to comparative levels found in non-transgenic mice. Although this thesis will discuss limitations of the results and potential future directions, our conclusions underscore a central role for  $\alpha$ Syn in AD pathogenesis and offer novel insight into  $\alpha$ Syn neurotoxicity.

# Acknowledgements

I would like to acknowledge my PhD advisor, Dr. George S. Bloom, for his guidance and mentorship throughout my graduate training. I would also like to express my gratitude to my thesis committee members: Drs. Scott O. Zeitlin, Benjamin W. Purow, James W. Mandell, and Alev Erisir for their input on this research, and their individual contributions to my personal and professional development. I thank The Bloom laboratory for the passionate discussions we shared on research projects, experiments, and the many words of encouragement throughout my training. Finally, I want to acknowledge my family and in particular my son David and wife Sadai, for motivating me to be the person I am today.

# Table of Contents

Abstract	Page 1
Acknowledgements	Page 2
Table of Contents	Page 3
Abbreviations	Page 5
<b>Chapter 1: Introduction</b>	Page 7
Introduction to Alzheimer's disease	Page 7
The Synuclein Family	Page 10
Subcellular Localization of Alpha-Synuclein.	Page 10
Alpha-Synuclein Structure	Page 11
Alpha-Synuclein Function.	Page 13
Alpha-synuclein and Alzheimer's disease.	Page 15
Alpha-synuclein and Parkinson's disease.	Page 16
The Building Blocks of Plaques and Tangles.	Page 17
Amyloid Precursor Protein (APP).	Page 18
APP Mutations are Linked to AD.	Page 19
Amyloid- $\beta$ (A $\beta$ ) function.	Page 20
Amyloid- $\beta$ oligomers.	Page 21
Amyloid- $\beta$ fibrils.	Page 22
Background on Tau.	Page 22
Tau Function.	Page 23

Tau phosphorylation.	Page 24
Tau aggregation.	Page 25
Non-Alzheimer Disease Tauopathies.	Page 26
Amyloid- $\beta$ Toxicity in AD is Tau-Dependent.	Page 26
Cell Cycle Re-Entry in AD.	Page 27
<b>Chapter 2: Bidirectional modulation of Alzheimer phenotype by alpha-synuclein in mice and primary neurons.</b>	Page 29
<b>Chapter 3: Future Directions</b>	Page 87
<b>Chapter 4: References</b>	Page 92

# Abbreviations

AD = Alzheimer's disease

A $\beta$  = Amyloid- $\beta$

$\alpha$ Syn = Alpha-synuclein

APP = Amyloid- $\beta$  precursor protein

Akt = Protein kinase B/Akt

KO = Knockout

syntaptobrevin-2 = syb2

ER = Endoplasmic reticulum

NAC = Non-amyloid component

SNARE = Soluble N-ethylmaleimide-sensitive factor attachment protein receptor

PD = Parkinson's disease

LBD = Lewy body dementia

MSA = multiple systems atrophy

sAPP $\alpha$  = secreted Amyloid Precursor Protein  $\alpha$

CTF- $\alpha$  = C-terminal fragment  $\alpha$

p3 = 3kDa peptide

$\alpha$ AICD = amyloid intracellular domain  $\alpha$

sAPP $\beta$  = secreted Amyloid Precursor Protein  $\beta$

CTF- $\beta$  = C-terminal fragment  $\beta$

LTP = Long-term potentiation

A $\beta$ Os = A $\beta$  oligomers

MAP = Microtubule-associated protein

PHF = Paired helical filament

FTDP-17 = Frontotemporal dementia with parkinsonism linked to chromosome-17

HD = Huntington's disease

CCR = neuronal cell cycle re-entry

CaMK II = Ca<sup>2+</sup>/calmodulin-dependent protein kinase II

PKA = Protein kinase A

WT = wildtype

# Chapter 1: Introduction

# Introduction

***Introduction to Alzheimer's disease.*** Alzheimer's disease (AD) was originally identified over 100 years ago by Alois Alzheimer (Hippius and Neundörfer, 2003). His patient, Auguste Deter, presented with severe cognitive decline at the later stages of her life. Upon her death, Alois Alzheimer observed the presence of two histopathological features in her brain – large extracellular inclusions that we now know are composed primarily of Amyloid- $\beta$  (A $\beta$ ) peptides, and intra-neurofibrillary tangles that were eventually identified to be composed primarily of the microtubule associated protein tau. Decades later, the disease severity was found to strongly correlate to the abundance of the proteinaceous assemblies (Blessed et al., 1968), and thus these plaques and tangles would later become a defining feature of disease that now bears his name. To date, much more is known regarding Alzheimer's onset and histopathology. AD is characterized by the progressive and insidious loss of synapses and neurons throughout the brain. The disease is believed to begin in the entorhinal cortex, where at later stages it affects the hippocampal and then higher cortical structures of the brain (Braak and Braak, 1991). The loss of these synapses and neurons precedes and likely causes cognitive deficits in patients, which can be clinically described as a mild cognitive impairment (Petersen et al., 2001). During the stages of early AD, memory impairment becomes worse and executive brain function becomes impacted. In the United States, AD accounts for approximately 25 deaths per 100,000 individuals per year, making AD the most lethal neurodegenerative disorder (Kochanek et al., 2016).

Despite its prevalence, there are no effective treatment strategies that slow or reverse AD progression. One reason for this is because the disease likely begins decades before the first signs of symptoms in patients. For instance, brain alterations are detectable in the brains of young individuals at risk to develop AD later on in life (Reiman et al., 2012). However, it is often very difficult to identify individuals at the pre-clinical stages for intervention due to their lack of the aforementioned memory impairment and thus, treatment strategies may begin too late. Previously, the FDA required patients to have a diagnosis of dementia before they could enroll in clinical trials. There are efforts now to begin clinical trials earlier during the preclinical stages of AD, however this is difficult because there are no early detection methods for patients that precede the onset of symptoms. Nevertheless, early detection and intervention hold the most promise for many of the current treatment strategies being developed.

Despite a plethora of research on AD a consensus into the underlying causes of neurodegeneration remain subjective. Again, A $\beta$  plaques and Tau tangles are pathological signatures of AD, and yet they are not directly believed to be the cause of neurodegeneration. Instead, the soluble protein intermediates that precede these filamentous inclusions, termed oligomers, are believed to be primarily neurotoxic. For instance, there are some cases of patients who have had amyloid plaque or neurofibrillary tangle accumulation without any sign of cognitive decline (Nelson et al., 2009). Finally, emerging work implicates  $\alpha$ -Synuclein ( $\alpha$ Syn) in AD etiology, suggesting that amyloid- $\beta$ , tau, and  $\alpha$ Syn are working in unison to promote neurodegeneration (discussed below).

The following section provides a background on  $\alpha$ Syn, A $\beta$ , the amyloid- $\beta$  precursor protein (APP), and tau, and discusses how they may contribute to AD pathogenesis.

***The Synuclein Family.***  $\alpha$ Syn was originally identified in non-mammalian cells by two independent groups. The original antibody used to identify  $\alpha$ Syn was generated by the purification of cholinergic vesicles (Maroteaux et al., 1988). A few years later a separate study in zebra finches reported an alteration in  $\alpha$ Syn mRNA during periods of song acquisition (George et al., 1995). Additionally, two other members of the synuclein family,  $\beta$ - and  $\gamma$ -synuclein, were also identified (Tobe et al., 1992; Nakajo et al., 1994; Ji et al., 1997).  $\beta$ -synuclein and  $\gamma$ -synuclein share 74% and 67% homology with  $\alpha$ Syn, respectively, suggesting that some functional features are conserved across the family - this is further supported by the mild phenotype reported for various double KO synuclein mice. Furthermore,  $\beta$ -synuclein has been proposed to provide protection against  $\alpha$ Syn toxicity, likely via  $\beta$ -synuclein regulation of Akt activity (Hashimoto et al., 2004). However, despite over two decades of research since the discovery of synucleins many questions regarding synuclein neurobiology remain. Our lack of knowledge on the synuclein family as a whole could be attributed to the narrow focus of the field on  $\alpha$ Syn pathophysiology, given the conspicuous accumulation of  $\alpha$ Syn into large  $\beta$ -sheet inclusions in a myriad of neurodegenerative disorders.

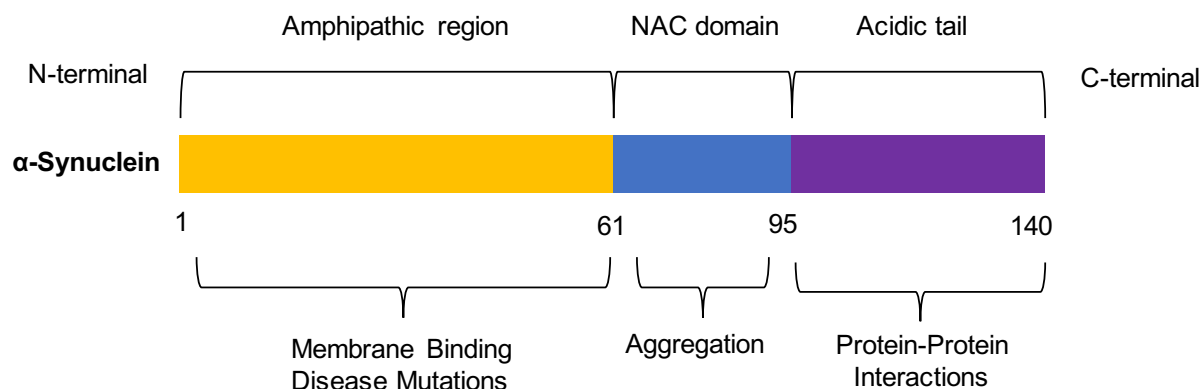
### ***Subcellular Localization of $\alpha$ Syn.***

At the time of its initial discovery,  $\alpha$ Syn was localized in what appeared to be distal synapses and the nucleus (Maroteaux et al., 1988). Subsequent work has confirmed that  $\alpha$ Syn sequesters to the presynaptic terminals in vertebrate animals, although the reason for its subcellular distribution to presynaptic terminals remains largely unknown. One

potential explanation for  $\alpha$ Syn preference to the presynaptic terminal is its interaction with syntaptobrevin-2. For instance,  $\alpha$ Syn is less associated with presynaptic terminals in syntaptobrevin-2 KO neurons (Burré et al., 2010). Although presynaptic terminal  $\alpha$ Syn is well established, the distribution of  $\alpha$ Syn at the nucleus has not been consistently observed (Mori et al., 2002; Yu et al., 2007). Nevertheless, some studies have corroborated the initial observation of nuclear  $\alpha$ Syn (Kontopoulos et al., 2006; Outeiro et al., 2007; Schell et al., 2009). Importantly,  $\alpha$ Syn occupies the somatic compartment of immature neurons before synapses are formed (Withers et al., 1997; Hsu et al., 1998). Therefore, inconsistencies in the literature may be due to differences in neuronal maturity at the time of experimental analysis. On the other hand, given the size of  $\alpha$ Syn at 14 kDa, it has been proposed that  $\alpha$ Syn could readily enter nuclear pores by simple diffusion (Bendor et al., 2013), however this has not been rigorously tested. There have been reports of  $\alpha$ Syn in other subcellular compartments such as the ER-Golgi network and the mitochondria, but because  $\alpha$ Syn overexpression was used in many of these studies the observations may not reflect  $\alpha$ Syn behavior under physiological conditions. Thus, it is generally accepted that  $\alpha$ Syn is primarily a presynaptic protein.

**$\alpha$ Syn Structure.**  $\alpha$ Syn comprises three distinct domains – it contains a seven repeat, 11-residue sequence (XKTKEGXXXX) within its N-terminal domain, a non-amyloid component (NAC) region, and an acidic C-terminal domain (**Introductory Figure 1**). Soluble cytosolic pools and purified recombinant  $\alpha$ Syn are natively unfolded. However, upon binding to phospholipid membranes  $\alpha$ Syn adopts an  $\alpha$ -helical structure within the N-terminal domain (Davidson et al., 1998). The  $\alpha$ -helical structure results from an

interaction among lysine residues across the helix. Interestingly, the NAC region (residues 61-95) received its name due to its accumulation into amyloid- $\beta$  ( $A\beta$ ) plaques found in AD (Uéda et al., 1993). Independently of plaques, the NAC region is hydrophobic, and accounts for the propensity of  $\alpha$ Syn to aggregate under disease conditions. The C-terminal region of  $\alpha$ Syn is considered to be unstructured (Bertini et al., 2007; Wu et al., 2008) and the primary site of post-translational modifications. Although it lacks a defined structure, modifications of the C-terminal domain have been implicated in modulation of  $\alpha$ Syn membrane binding and aggregation (Crowther et al., 1998; Davidson et al., 1998; Jo et al., 2000; Perrin et al., 2000; Eliezer et al., 2001; Volles et al., 2001; Cole et al., 2002; Park et al., 2002; Bussell and Eliezer, 2003; Chandra et al., 2003; Fortin et al., 2004; Nuscher et al., 2004; Park et al., 2004; Bussell et al., 2005).



**Introductory Figure 1.** Structural Features of  $\alpha$ -Synuclein.

Furthermore, tetrameric assemblies of  $\alpha$ -helical  $\alpha$ Syn have been reported under native conditions (Bartels et al., 2011). These tetrameric structures are proposed to increase  $\alpha$ Syn membrane binding and reduce its propensity to form disease-associated

filamentous inclusions, however there is some controversy surrounding these reports. In response to the initial Bartels et al. report, work from the Südhof lab was only able to observe a negligible amount of tetrameric  $\alpha$ Syn from mouse brain (see the Burré et al., 2011 comment in reference to Bartels et al., 2011). Conversely, the Lesné lab recently reported an increase in multimeric  $\alpha$ Syn, that was consistent in molecular weight to a tetrameric assembly, under conditions where human wildtype  $\alpha$ Syn is moderately overexpressed in amyloid Precursor Protein (APP) transgenic mice (Larson et al., 2017). However, the tetrameric species observed by Lesné and colleagues coincided with increased pathology, suggesting that these tetrameric species cause a deleterious gain of toxicity for  $\alpha$ Syn. Therefore, the physiological relevance and abundance of tetrameric  $\alpha$ Syn remains unresolved.

***$\alpha$ Syn Function.*** First, given the affinity for  $\alpha$ Syn to bind highly curved membranes and its enrichment in presynaptic terminals, one of the putative functions of  $\alpha$ Syn centers around its maintenance of synaptic vesicle stores. Indeed, in primary hippocampal neurons,  $\alpha$ Syn reduces inter-neuronal trafficking of synaptic vesicles, resulting in larger recycling pools (Scott and Roy, 2012). Subsequent work has shown that  $\alpha$ Syn multimers can associate to clusters of synaptic vesicles, and this association may account for slower vesicle trafficking (Wang et al., 2014).  $\alpha$ Syn multimers that form upon membrane binding are not considered to be neurotoxic and they are instead likely generated to enhance the interaction between  $\alpha$ Syn and curved membranes (Wang et al., 2011). Further strengthening the functional role of  $\alpha$ Syn on synaptic vesicle maintenance,  $\alpha$ Syn binds to synthetic synaptic vesicles through an interaction with synaptobrevin-2, and this

interaction prevents the vesicles from associating to synthetic plasma membranes in vitro (Diao et al., 2013). Taken together, there is strong support for the putative function of  $\alpha$ Syn as a modulator of vesicle stores and inhibitor of vesicle fusion at the synapse.

Second, strong evidence exists supporting a role for  $\alpha$ Syn as a regulator of soluble N-ethylmaleimide-sensitive factor attachment protein receptor (SNARE) complex assembly. SNARE complex assembly and disassembly are essential for neurotransmitter release at presynaptic nerve terminals. Genetic ablation of  $\alpha$ -,  $\beta$ -, and  $\gamma$ -Synuclein results in reduced SNARE complex assembly (Burré et al., 2010). By contrast, overexpression of  $\alpha$ Syn has also been shown to accelerate SNARE complex assembly. In order for  $\alpha$ Syn to function as a regulator of SNAREs,  $\alpha$ Syn must first bind to synaptobrevin-2. Interestingly, membrane binding of  $\alpha$ Syn during SNARE-complex assembly seems to promote the production of multimeric  $\alpha$ Syn (Burré et al., 2014), although the multimeric  $\alpha$ Syn described in this study is distinctively different than the tetrameric species first observed from protein purified from human erythrocytes (Bartels et al., 2011).

Third,  $\alpha$ Syn may also regulate exocytosis and neurotransmitter release at the synapse. Although  $\alpha$ Syn-KO mice are viable and do not display overt neuropathology, there is evidence of increased exocytosis, along with elevated levels of extracellular dopamine (Abeliovich et al., 2000). However, the effect appears to be specific to dopaminergic neurons, as glutamate levels appear to be unchanged (Abeliovich et al., 2000). Furthermore, synaptic vesicle exocytosis is delayed when  $\alpha$ Syn is overexpressed (Nemani et al., 2010). However, the precise mechanism that accounts for  $\alpha$ Syn modulation of vesicle exocytosis remains unclear.

In summary, the association of  $\alpha$ Syn to membranes appears to be important to its native function. The hydrophobic core of  $\alpha$ Syn appears to be essential to its gain of function in neurodegenerative diseases (described in the next section). Finally, although C-terminal modifications are reported to alter  $\alpha$ Syn structure and protein-protein interactions, the functional aspects of these changes along the C-terminal still remain to be elucidated.

**$\alpha$ Syn and AD.**  $\alpha$ Syn misfolding and accumulation can result in the formation of intracellular inclusions called Lewy bodies, which classically define Parkinson's disease (PD), Lewy body dementia (LBD), and Multiple Systems Atrophy (MSA). Research on  $\alpha$ Syn intensified following the revelation that  $\alpha$ Syn inclusions characterize these neurodegenerative diseases which are now classified as synucleinopathies. However,  $\alpha$ Syn also contributes to histopathology in AD. The NAC hydrophobic core of  $\alpha$ Syn was initially identified as a major component of the large, extracellular plaques found in the brain parenchyma of AD (Uéda et al., 1993). Furthermore, Lewy bodies are detected in over 50% of AD cases (Hamilton, 2000), although it should be noted that the Lewy bodies typically localize to the amygdala. Although  $\alpha$ Syn contributes to these two histopathological features of AD, the precise role of the soluble protein is still unclear. There is also a strong link between memory deficits and  $\alpha$ Syn in AD, PD and LBD, suggesting an intrinsic role for  $\alpha$ Syn in during memory retention and acquisition (Aarsland et al., 2003; Hely et al., 2008; Overk et al., 2014; Adamowicz et al., 2017; Larson et al., 2017). Several classical studies have also demonstrated that  $\alpha$ Syn overexpression can exacerbate neurodegeneration, as defined by behavioral deficiencies, in APP transgenic mice (Masliah et al., 2001; Larson et al., 2017). A recent study looking at  $\alpha$ Syn genetic

ablation found a rescue of memory in APP mice (Spencer et al., 2016), supporting the notion of bidirectional control of memory deficiencies by  $\alpha$ Syn in APP mice. However, this was not investigated in a controlled setting prior to the work described in this thesis.

***$\alpha$ Syn and Parkinson's disease.*** Although important questions remain unanswered for  $\alpha$ Syn within the context of AD, it is perhaps best understood in the context of Parkinson's disease (PD). PD is clinically defined by the presence of Lewy body inclusions, named after Dr. Fritz Lewy. Lewy bodies are proposed to originate in the substantia nigra pars compacta in PD. Symptoms include motor deficits that result in rigidity and resting tremors. Over 10 million people worldwide are currently afflicted with PD, making it the second most prevalent neurodegenerative disorder. At later stages motor deficits intensify to chorea, which is described as involuntary movement of the body and a compromised gait. Eventually,  $\alpha$ Syn pathology spreads from the midbrain region to higher ordered structures in the brain, such as the hippocampus and neocortex. This spread of  $\alpha$ Syn aggregates throughout the brain is associated with dementia onset in approximately 80% of PD patients (Hely et al., 2008). There is a strong genetic association regarding  $\alpha$ Syn and PD.  $\alpha$ Syn gene mutations are associated with an increased risk for PD. Interestingly, these mutations are all contained within the N-terminal region of the protein (see **Introductory Figure 1**), suggesting that a decrease in the propensity of  $\alpha$ Syn to adopt the alpha-helical structure or bind highly curved membranes plays a role in PD. Furthermore, duplication or triplication in the *SNCA* gene that encodes  $\alpha$ Syn are also penetrant for PD (Singleton et al., 2003; Ahn et al., 2008). The precise mechanisms

behind  $\alpha$ Syn neurotoxicity are still being elucidated, although mitochondria deficits have been implicated. Since  $\alpha$ Syn is a presynaptic protein, and the mitochondria are not generally found in the presynaptic terminal, there is some debate surrounding this proposed mechanism.

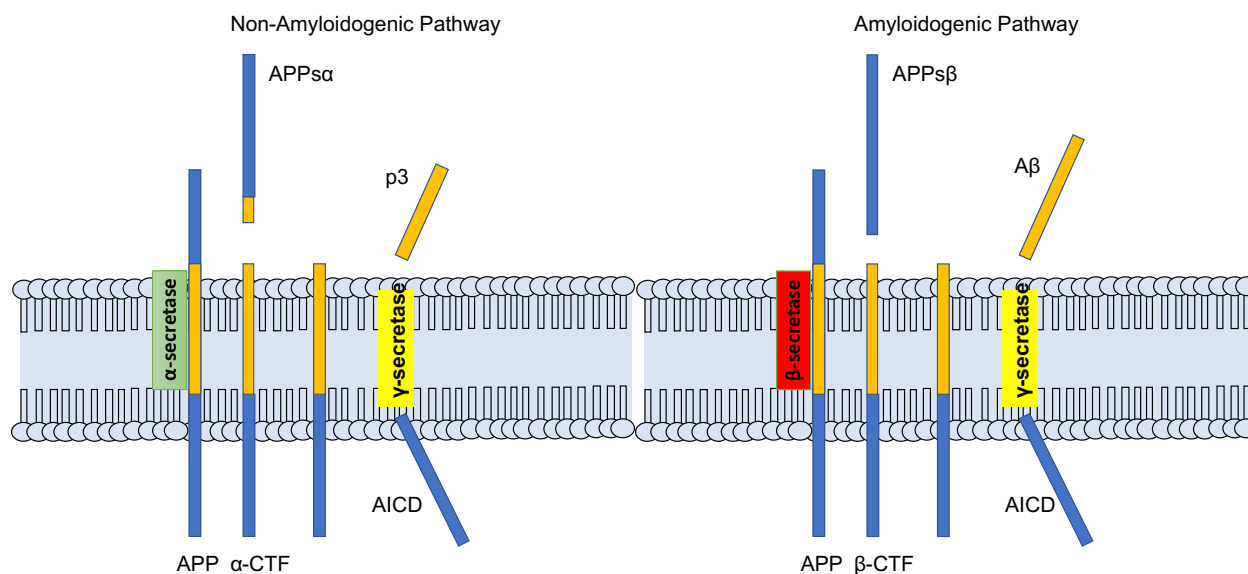
***The Building Blocks of Plaques and Tangles.*** Although the identification of AD took place over 100 years ago, the major protein components of senile plaques and neurofibrillary tangles began to be elucidated in the 1980s. To characterize the components of senile plaques they were isolated from human brains (Allsop et al., 1983). Subsequent analysis identified the primary component of senile plaques to be Amyloid- $\beta$ , a small, 42 amino-acid peptide. The discovery of A $\beta$  and its amino-acid sequence then allowed researchers to identify its gene of origin. The A $\beta$  domain was localized within a gene encoding sequence for a larger unknown protein, and therefore the larger protein was named the Amyloid- $\beta$  precursor protein, or APP (Glenner and Wong, 1984a; 1984b). A similar methodology was employed to determine the protein composition of neurofibrillary tangles. Ultimately, two independent studies observed that tau, a recognized microtubule associated protein (MAP), was the major component of neurofibrillary tangles (Kosik et al., 1986; Wood et al., 1986).

***Amyloid Precursor Protein (APP).*** APP is a type-1 transmembrane glycoprotein and is encoded by the *APP* gene located on chromosome 21 (Goldgaber et al., 1987; Kang et al., 1987; Tanzi et al., 1987). In humans there are three APP splicing variants, however the 695 amino-acid variant is predominantly expressed in the brain. Although a precise

function for APP remains elusive, its enzymatic cleavage and turnover are relatively well-defined, as a result of extensive work that was performed to understand A $\beta$  production. APP is generally follows one of two pathways: (1) APP is predominately cleaved by a pathway that precludes the formation of Amyloid- $\beta$  peptide (non-amyloidogenic) or (2) a less frequent pathway that results in the secretion of Amyloid- $\beta$  (amyloidogenic) (**Introductory Figure 2**). The distinguishing cleavage events for both pathways are carried out by enzymatic secretases. In the non-amyloidogenic pathway,  $\alpha$ -secretase initiates the non-amyloidogenic cleavage of APP in contrast to  $\beta$ -secretase, which initiates the amyloidogenic pathway. Both pathways culminate in cleavage event catalyzed by  $\gamma$ -secretase, a multi-subunit protease complex.

APP proteolysis by secretases results in the production of several cleavage products.  $\alpha$ -secretase cleaves APP at K16 and L17 of the A $\beta$  domain that begins with the amino acids DAE and therefore prevents the production of full length A $\beta$  peptides. Instead, a large secreted Amyloid Precursor Protein  $\alpha$  (sAPP $\alpha$ ) ectodomain is generated while the C-terminal fragment  $\alpha$  (CTF- $\alpha$ ) remains tethered to the membrane. Following  $\gamma$ -secretase cleavage, the C-terminal fragment is broken down into a 3kDa peptide (p3) and an amyloid intracellular domain ( $\alpha$ AICD) which is eventually released from the membrane. By contrast, the amyloidogenic pathway results in the formation of the sAPP $\beta$  fragment which does not incorporate the 1-16 amino acid region of the A $\beta$ . The remaining portion of APP that is tethered to the membrane, CTF- $\beta$ , produces A $\beta$  peptides of varying lengths (predominantly A $\beta$ <sub>1-40</sub> and A $\beta$ <sub>1-42</sub>), depending on the precise site of  $\gamma$ -secretase cleavage. The two alloforms differ in their propensity to aggregate (A $\beta$ <sub>1-42</sub> > A $\beta$ <sub>1-40</sub>).

**APP Mutations are Linked to AD.** Several *APP* familial mutations have been identified in AD patients (Goate et al., 1991; Murrell et al., 1991; Mullan et al., 1992). These mutations are rare (1-5%), but when inherited these APP mutations are usually fully penetrant for early-onset AD. The mutations that have been linked to AD are generally near the A $\beta$ -encoding region of the gene and have been experimentally shown to increase either the production of A $\beta$  or the A $\beta_{x-42}$  to A $\beta_{x-40}$  ratio. Similarly, over 286 mutations in the catalytic subunits of the  $\gamma$ -secretase complex, presenilin 1 or 2, have been identified as risk factors for early onset AD. Many of the presenilin mutations are also proposed to promote an increased A $\beta$  production. Conversely, an A673T mutation of APP was identified in human populations with a lower rate of AD (Jonsson et al., 2012). In vitro studies of this mutation report an approximate 40% reduction in A $\beta$  peptide levels, which may account for the lower disease rate.



**Introductory Figure 2.** APP cleavage through the Non-Amyloidogenic and Amyloidogenic Pathways.

**A $\beta$  function.** A $\beta$  can range in size from 15-43 amino acids, depending on which sites are cleaved along APP. Although A $\beta$  is monomeric by nature, in AD it gains the propensity to aggregate. The aggregates can range in size from oligomers (dimers, trimers, hexamers, nonamers, and dodecamers [A $\beta$ 56\*]) to protofibrils and fibrils (Lesné et al., 2006). Like many other disease-associated proteins, the basic function of A $\beta$  in healthy brains is ill-defined. Nevertheless, A $\beta$  has been implicated in cholesterol transport, synaptic plasticity, and the antimicrobial response. Specifically, studies have shown that A $\beta$  can facilitate the retrograde transport of cholesterol (Igbavboa et al., 2009). Loss of this function was speculated to compromise lipid rafts, which are central to membrane trafficking and require cholesterol. With regards to synaptic plasticity, ablation of either APP or  $\beta$ -secretase in mice results in a reduction in long-term potentiation (LTP) (Ma et al., 2007; Tyan et al., 2012). Since the APP or  $\beta$ -secretase would result in a reduction of A $\beta$ , these results imply a role for A $\beta$  production in synaptic plasticity. However, since there are other APP cleavage products, and other targets of  $\beta$ -secretase, A $\beta$  may not be the sole contributor to the observed phenotype. Additionally, studies have found that A $\beta$  may produce an antimicrobial response (Kumar et al., 2016). Aggregation of the A $\beta$  may therefore increase brain susceptibility to infection. Importantly, however, more basic research is needed in these in order for the functional features of A $\beta$  to be fully extrapolated.

**A $\beta$  oligomers.** Brain levels of A $\beta$  oligomers strongly correlate with cognitive decline in AD. Experimentally, A $\beta$  oligomers (A $\beta$ Os) have been shown to promote memory impairment in mice, decrease LTP, increase synapse loss, initiate neuronal cell cycle re-

entry, and activate kinases that in turn phosphorylate tau (Shankar et al., 2008; Varvel et al., 2008; Bhaskar et al., 2009; Reed et al., 2011; Seward et al., 2013; Bhaskar et al., 2014; Norambuena et al., 2017). Interestingly, many of the pathogenic features of A $\beta$ Os require tau expression, suggesting that A $\beta$ Os are signaling upstream of tau to promote neuronal dysfunction. How extracellular A $\beta$ Os initiate the signaling cascade that results in AD pathogenesis is currently unclear and in some cases contradictory. One potential explanation for these discrepancies in the literature is that oligomers formed from synthetic A $\beta$  elicit a different cellular response than brain-derived A $\beta$ Os. For instance, synthetic A $\beta$ Os were shown to be bioactive at 1.3 $\mu$ M whereas brain-derived A $\beta$ Os generated a response in the nanomolar range (Reed et al., 2011). Hence, standardization of A $\beta$ Os may help elucidate their signaling properties.

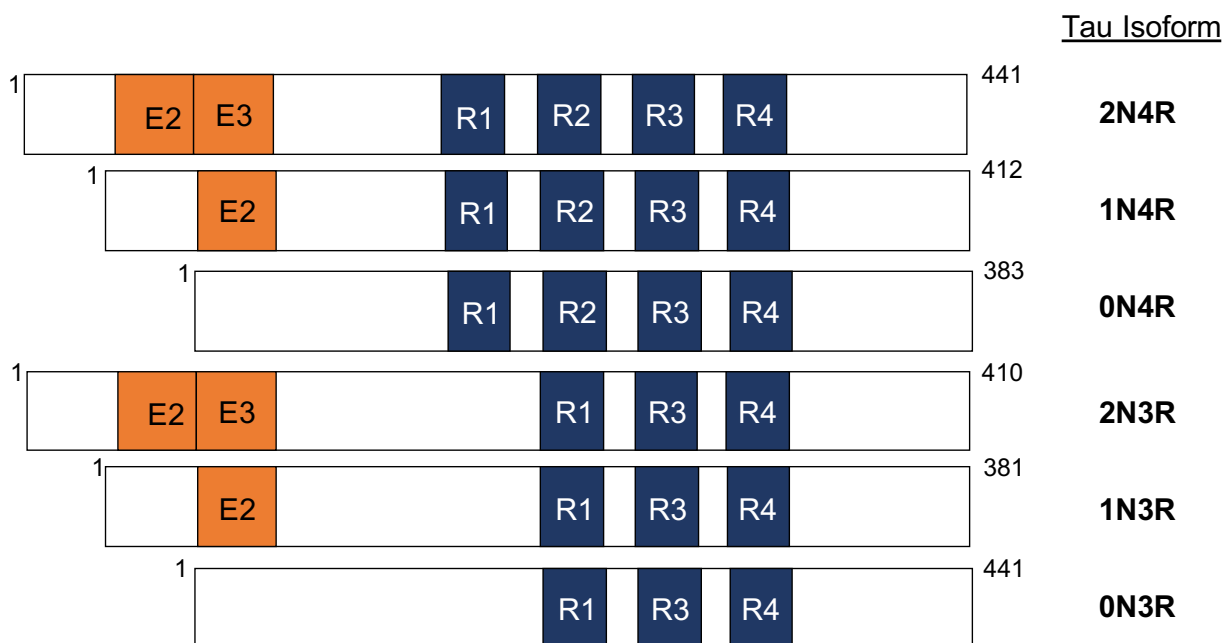
**A $\beta$  fibrils.** Although A $\beta$  fibrils are the principal constituent of amyloid plaques in AD, several revelations have questioned their causality to AD symptomology. First, amyloid plaques are poor correlates of cognitive decline (Engler et al., 2006). Second, robust amyloid plaque pathology has been observed postmortem in individuals who were cognitively normal (Rentz et al., 2010). APP transgenic mice perform memory tasks normally despite an increase in amyloid plaque deposition (Lesne et al., 2008). Finally, targeting of amyloid plaques in human clinical trials did not improve or halt disease progression, and instead, appeared to worsen symptoms (Nicoll et al., 2003). From these observations, there has been a paradigm shift on the belief that A $\beta$  fibrils are causative for AD. In fact, consensus is growing for the assertion that amyloid plaques function as a

“sink-hole” whereby plaques sequester smaller toxic assemblies of A $\beta$ , thereby neutralizing oligomer bioactivity and subsequent neurotoxicity.

**Background on Tau.** Tau was originally isolated from purified porcine brain tubulin (Weingarten et al., 1975). In that report, purified tau was shown to promote unassembled tubulin to polymerize into microtubules. Subsequent studies have substantiated these initial observations, and thus tau is generally described as a microtubule-associated protein or MAP. Tau is expressed throughout the brain during development. The *MAPT* gene that encodes tau is located on chromosome 17q21 (Neve et al., 1986). In the central nervous system, tau exists as six isoforms as a result of *MAPT* splice variation (Goedert et al., 1989a) (**Introductory Figure 3**). The six isoforms differ in the number of exons expressed at the N-terminus (0,1, or 2) and by the number of microtubule binding repeat domains near the C-terminus (3 or 4). During early development, there is greater expression of 3 repeat tau, and it is heavily phosphorylated (Goedert et al., 1989b). However, as mammals mature into adulthood the ratio of 3 repeat to 4 repeat tau is 1 to 1 (Spires-Jones et al., 2009).

**Tau Function.** In mature mammals neurons, tau localizes to axons where it is tightly associated to microtubules. Purified recombinant tau is generally considered natively unfolded. However, when it is associated to microtubules some there is evidence that it adopts a hairpin structure, where the N- and C- terminal ends are in close proximity (Jeganathan et al., 2006). As mentioned earlier, tau can stabilize microtubules, likely by promoting tubulin polymerization (Witman et al., 1976). When it is microtubule-bound, tau

may function as a “speed bump” via its regulation of organelle transport dynamics (Dixit et al., 2008). Interestingly, Tau-KO mice are viable with no obvious alterations in their behavior, fecundity, or physical appearance (Dawson et al., 2001; Tucker et al., 2001). However, milder changes in neuronal morphology and migration were observed in the developing mouse brain. Consistent with its putative function in organelle transport, a deficit in mitochondria transport was reported in Tau-KO mice (Sapir et al., 2012).



**Introductory Figure 3.** The six isoforms of tau in the CNS. E = exons or R = microtubule binding domain.

***Tau phosphorylation.*** Tau phosphorylation is the most well-characterized post-translational modification for the protein. Around the time when filamentous tau was determined to be the principle component of the neurofibrillary tangles found in AD, it was also noted to be substantially phosphorylated (Grundke-Iqbal et al., 1986). Subsequent analysis of tau has determined that there are ~85 potential phosphorylation sites and

nearly 40 known kinases for the longest isoform of tau (4R/2N). Although a detailed understanding of the biological response of site-directed tau phosphorylation remain to be determined, some information has been elucidated for certain phosphorylation events. For instance, phosphorylation of tau within its microtubule binding domain results in a reduced affinity for microtubules (Merrick et al., 1997; Jenkins and Johnson, 1998; Leugers and Lee, 2010). Furthermore, as mentioned earlier, tau is proposed to adopt a hairpin structure upon binding to microtubules under native conditions (Horowitz et al., 2006), and this structure is postulated to contribute to microtubule stability. Increased phosphorylation would adversely generate a greater concentration of negative charge within the confines of the hairpin structure and may therefore promote its disruption and compromise microtubule integrity. Coincidentally, A $\beta$ O<sub>s</sub> act through tau within its N-terminal domain to elicit microtubule disassembly (King et al., 2006). Since the N-terminal domain is located distally to the microtubule binding region of tau, it is tempting to suspect that A $\beta$ O<sub>s</sub> may compromise the hairpin structure of tau via a similar N-terminal domain modification.

***Tau aggregation.*** Under disease conditions Tau aggregates into ordered assemblies, forming soluble oligomer intermediates that eventually generate the paired helical filaments that are found in neurofibrillary tangles. Tau does not readily aggregate in solution. However, studies have shown that incubating monomeric tau with the anticoagulant heparin seeds the formation of oligomers and paired helical filaments (PHFs) in vitro (Woerman et al., 2015). Interestingly, tau assembly into toxic aggregates can also be initiated when tau is incubated with small amounts of  $\alpha$ Syn oligomers

(Castillo-Carranza et al., 2018). Extracellular tau oligomers were recently shown to promote tau redistribution to the somatodendritic compartment, and also resulted in fast axonal transport deficits in primary neurons (Swanson et al., 2017). These results are consistent with the putative role of tau during organelle transport across microtubules. Unlike the robust neurotoxicity of tau oligomers, the larger fibrils and paired helical filaments are relatively benign, which supports the idea that larger assemblies are generated to sequester more toxic tau intermediates, analogous to the observations made for A $\beta$  fibrils. Importantly, while many tau phosphorylations have been implicated in its aggregation, a recent study demonstrated a neuroprotective effect when tau was phosphorylated at threonine 205 (Ittner et al., 2016). Hence, a greater understanding of tau neurobiology will be possible once tau phosphorylation is better understood.

***Non-Alzheimer Disease Tauopathies.*** Other than AD, neurofibrillary tangles have been observed in other neurodegenerative diseases. The onset of these tau-related neurodegenerative disorders, or non-Alzheimer's tauopathies, is proposed to occur independently of A $\beta$  pathology (Lee et al., 2001). Tauopathies include Frontotemporal dementia with parkinsonism linked to chromosome-17 (FTDP-17), sporadic corticobasal degeneration, progressive supranuclear palsy, and Pick's disease. Tau pathology is also observed in Huntington's disease (HD) (Gratuze et al., 2016) and Parkinson's disease (PD) (Duka et al., 2006; Haggerty et al., 2011; Duka et al., 2013), but the contribution of tau to these diseases is only beginning to be appreciated.

***A $\beta$  Toxicity in AD is Tau-Dependent.*** Although it was well established that amyloid- $\beta$  and tau are the respective building blocks of plaques and tangles found in AD, the functional link between the two proteins and disease etiology remained elusive. It was not until the early 2000s that two independent studies reported the first evidence that A $\beta$  toxicity is tau-dependent (Götz et al., 2001; Lewis et al., 2001). Genetic crossbreeding of human tau containing P301L familial mutation linked to FTDP17 and mutant APP mice with both the Swedish mutations (K670N and M671L) resulted in no difference in plaque formation but a substantial enhancement in tangle pathology when compared to the P301L parental strain. In the other study, rather than crossbreeding, P301L mice received brain injections with synthetic Amyloid- $\beta$ , which resulted in a robust increase in tangle pathology. Another seminal study investigated the consequence of partial or complete tau ablation in APPJ20 mice, which contain Swedish and Indiana familial mutations (KM670/671NL, APP V717F). Amyloid plaque deposition was unchanged in the APP mice that were either heterozygous or homozygous for tau ablation. However, tau reduction or complete KO protected mice from memory deficits, increased survival, and reduced synapse loss (Roberson et al., 2007). Taken together, these results provided the foundation for the “amyloid cascade hypothesis” - the assertion that A $\beta$  is signaling through tau to drive AD pathogenesis.

***Cell Cycle Re-Entry in AD.*** Cell culture experiments and analysis of human disease brain sections, in combination with animal studies as described above, have allowed investigators to unravel the molecular underpinnings of the A $\beta$  to tau signaling pathway. One of the more compelling pathways elucidated from these approaches involves the

seemingly aberrant activation of the cell cycle machinery within terminally differentiated neurons. In general, once a neuronal progenitor completes the maturation process to neuronal differentiation, it exits the cell cycle, and thus is in  $G_0$ . The maintenance of quiescence likely requires the active function of cell cycle regulation and inhibition by the neuron. In neurodegenerative disease including AD, cell cycle regulation is compromised and reactivated. Rather than resulting in the production of new neurons however, this cell cycle re-entry (CCR) is proposed to cause neuron death accounting for up to 90% of the neuron loss in the neocortex (Bussi re et al., 2003) and 67% of CA1 neurons of the neocortex (West et al., 1994). The strongest evidence for this was demonstrated in postmortem sections of human brains, where elevated expression levels of cell cycle proteins were described (Herrup and Yang, 2007; Arendt et al., 2010). Additionally, work using primary cortical neurons treated with A $\beta$ O recapitulated the CCR phenotype in vitro, providing an experimental paradigm with which CCR could be further studied (Varvel et al., 2008). Subsequent work demonstrated that CCR could be ameliorated by treatment with the mTOR inhibitor rapamycin, that CCR induced dendritic arborization, and CCR preceded neuron death (Bhaskar et al., 2009). Most notably, A $\beta$ O induced CCR is tau dependent, since A $\beta$ O do not induce CCR in primary neurons from Tau-KO mice, or APPJ20/Tau-KO mice (Seward et al., 2013).

How precisely does A $\beta$ O initiate CCR, and why is CCR tau-dependent? The results suggest that A $\beta$ O function as activators of kinases that in turn ectopically phosphorylate tau. Specifically, work from our lab has shown that A $\beta$ O can activate mTORC1 at plasma membranes, Ca<sup>2+</sup>/calmodulin-dependent protein kinase II (CaMKII), protein kinase A (PKA), and Fyn, which in turn results in the phosphorylation of tau at S262, S416, S409,

and Y18, respectively (Seward et al., 2013; Norambuena et al., 2017). All of these sites are required for neuronal CCR since re-expression of phospho-null tau at any of these sites precludes CCR. Importantly, however, it is still unknown why tau expression is required by A $\beta$ O $_2$ s or why tau must be phosphorylated at these sites for CCR.

**Chapter 2: Bidirectional modulation of  
Alzheimer phenotype by alpha-  
synuclein in mice and primary  
neurons.**

*Note: The methods, project rationale, results and discussion sections are adapted from the Khan-Lacroix-Boyle et al. submitted research manuscript entitled “Bidirectional modulation of Alzheimer phenotype by alpha-synuclein in mice and primary neurons. **My direct contributions to this research are represented in Figures 6, 7 and Supplementary Figures 8, 9, and 10. These results and my other contributions are highlighted for additional emphasis in this chapter.**”*

## **Bidirectional modulation of Alzheimer phenotype by alpha-synuclein in mice and primary neurons**

**Shahzad S. Khan<sup>1,2,\*</sup>, Michael LaCroix<sup>5,6,7\$,\*</sup>, Gabriel Boyle<sup>5,6,7\*</sup>, Mathew A. Sherman<sup>5,6,7</sup>, Jennifer L. Brown<sup>5,6,7</sup>, Fatou Amar<sup>5,6,7,\$</sup>, Jacqueline Aldaco<sup>5,6,7,¶</sup>, Michael K. Lee<sup>5,7,8</sup>, George S. Bloom<sup>1,2,3,4</sup> & Sylvain E. Lesné<sup>5,6,7,#</sup>**

<sup>1</sup>Neuroscience Graduate Program, The University of Virginia, Charlottesville, VA, USA

<sup>2,3,4</sup>Departments of Biology, Cell Biology and Neuroscience, The University of Virginia, Charlottesville, VA, USA

<sup>5</sup>Department of Neuroscience, The University of Minnesota, Minneapolis, MN, USA

<sup>6</sup>N. Bud Grossman Center for Memory Research and Care, The University of Minnesota, Minneapolis, MN, USA

<sup>7</sup>Institute for Translational Neuroscience, The University of Minnesota, Minneapolis, MN, USA

<sup>8</sup>Center for Neurodegenerative Disease, The University of Minnesota, Minneapolis, MN, USA

\*These authors contributed equally

\$Present address: University of Texas Southwestern Medical School, Dallas, TX 75390.

§Present address: Taub Institute, Columbia University, New York, NY 10032.

¶Present address: University of Houston, Houston, TX 77004.

#Correspondence: [lesne002@umn.edu](mailto:lesne002@umn.edu)

### **Author Contributions**

**S.S.K.**, M.L., M.A.S., F.A. and S.E.L. performed experiments; S.E.L., G.S.B. and **S.S.K.** conceived, designed and supervised experiments. M.K.L. provided reagents and critical feedback. **S.S.K.**, G.S.B. and S.E.L. wrote the manuscript; S.E.L. and **S.S.K.** prepared and organized the figures. G.S.B., M.L. and M.K.L. contributed to critical discussions and edited the manuscript. All authors discussed the results and commented on this manuscript.

## Khan-Boyle-Lacroix et al. Methods

*Abbreviations for subsequent sections:* WT, wild-type; APP, J20 APP transgenic mice;  $\alpha$ Syn, Tg12.2 transgenic mice;  $\alpha$ Syn-KO, SNCA-null mice.

**Transgenic animals.** Three transgenic lines were used: (i) Tg12.2 mice expressing the wild type form of human  $\alpha$ -synuclein under the control of the mouse prion promoter (Lee et al., 2002), (ii) SNCA-null mice (Abeliovich et al., 2000) and (iii) J20 (originally called hAPPJ20) mice (Mucke et al., 2000). SNCA-null mice were obtained from Jackson laboratories and backcrossed to C57BL6/J for greater than 10 generations. Every 6 months, the homozygous KO mice are outbred to wild-type C57BL6/J and homozygous KO mice are reconstituted from mating of heterozygote animals. Animals were then transferred from Michael K. Lee, University of Minnesota to Sylvain Lesné, University of Minnesota. Bigenic J20xTg12.2 mice resulted from the mating of Tg12.2 and J20 mice. All lines used were in the C57BL6 background strain. Both male and female animals were used in equal numbers for biochemical studies and Barnes Maze behavioral testing. All animal procedures and studies were reviewed and approved by the University of Minnesota Institutional Animal Care and Use Committee and Institutional Review Board

**Protein extractions.** Soluble aggregation-prone protein levels in brain tissue were analyzed using the extraction protocol previously described (Lesné et al., 2006; Sherman and Lesné, 2011), with a detailed 32-step-protocol explained in the latter. The goal of this lysis process is to fractionate proteins based on their cellular compartmentalization. The

sequential separation allows the recovery of a predicted protein in its compartment of 75-90% (Lesné et al., 2006; Larson et al., 2012b). Briefly, dissected frozen hemi-forebrain tissues (125-200 mg) are gently dissociated in NP40-lysis buffer (50 mM Tris-HCl [pH 7.6], 0.01% NP-40, 150 mM NaCl, 2mM EDTA, 0.1% SDS) and centrifuged at 800 x g, to separate extracellular proteins contained in the supernatant. The remaining loose pellet is then lysed with TNT-lysis buffer (50 mM Tris-HCl, pH 7.4, 150 mM NaCl, 0.1% Triton X-100), and centrifuged at 16,100 x g, to separate intracellular proteins present in the aqueous phase. The subsequent pellet is finally dissociated in RIPA-lysis buffer (50 mM Tris-HCl, pH 7.4, 150 mM NaCl, 0.5% Triton X-100, 1 mM EDTA, 3% SDS, 1% deoxycholate) and centrifuged at 16,100 x g, to separate membrane-bound proteins present in the supernatant. All supernatants were ultra-centrifuged for 20 minutes at 100,000 x g. Before analysis, fractions were depleted of endogenous immunoglobulins by incubating lysates with 50 µl of Protein A-Sepharose, Fast Flow® beads for one hour at 4° C, followed by 50 µl of Protein G-Sepharose, Fast Flow® beads (GE Healthcare Life Sciences). Protein amounts were determined with the Bicinchoninic acid protein assay (BCA Protein Assay, Pierce™).

**Antibodies.** The following primary antibodies were used in this study: 6E10 [1:2,000], 4D6 anti- $\alpha$ -Synuclein [1:500], LB509 [1:5,000–10,000], and Tau-5 (Catalog nos. SIG-803003, SIG-39720, SIG-39725 and SIG-39413, BioLegend), anti-MAP2 [1:500] (Catalog no. NB300-213, Novus), anti-Cyclin D1 [1:120], anti-MAP2 [1:2000] (Catalog nos. ab16663 and ab92434, Abcam), anti- $\beta$ -III-Tubulin (TUJ1) [1:5000] (gift from Anthony Spano, University of Virginia), anti-NeuN [1:500], anti-actin (C4) [1:10,000], anti-SYP

[1:25,000] (Catalog nos. MAB377 and MAB1501, EMD Millipore). anti-PCNA [1:200] anti-PSD95 [1:200], anti-GluN1 [1:1000], anti-GluN2A [1:1000], anti-GluN2B [1:1000] (Catalog nos. sc-56, sc-8575, sc-1467, sc-9058, and sc-9056, Santa Cruz Biotechnology), Phospho-Retinoblastoma (pS780) and Rab3A (Catalog nos. 8180S and 3930S, Cell Signaling Technologies), Iba [1:1,000] (Catalog no. 019-19741, Wako), GFAP [1:500] (Catalog no. 173006, Synaptic Systems), pS202-tau (CP13) [1:500], PG5 [1:500], MC1-tau [1:500], and PHF1 [1:500] (gifts from P. Davis, Albert Einstein College of Medicine, Yeshiva University), A11 [1:1000] and OC [1:2,000] (gift from R. Kaye, University of Texas Medical Branch), DW6 [1:500] (gift from D. Walsh, Harvard University).

The following secondary antibodies were used in this study: Alexa Fluor™ (Molecular Probes, Invitrogen) Goat-anti-Chicken 488 (Catalog no. A-11039), 568 (Catalog no. A-11041), 647 (Catalog no. A-21449), Goat-anti-Mouse 568 (Catalog no. A-11004), 647 (Catalog no. A-21235), Goat-anti-Rabbit 488 (Catalog no. A-11034), 555 (Catalog no. A-21435), 568 (Catalog no. A-11036), DyLight® Goat-anti-Mouse 405 (Catalog no. 35501BID), IRDye® (Li-COR) 800cw Goat anti-Rabbit (Catalog no. 925-32211), IRDye® (Li-COR) 680LT Goat anti-Mouse (Catalog no. 925-68020).

**A $\beta$  immunofluorescent staining and confocal imaging.** A series of mouse brain sagittal sections (30  $\mu$ m thick, n = 8 sections/animal) spaced at 400  $\mu$ m intervals was stained for deposited A $\beta$  plaques. Briefly, sections were rinsed with PBS, pretreated with 80% formic acid for 1 min at room temperature, pretreated with 0.1% TWEEN®20-

containing PBS, and blocked with PBS containing 5% normal goat serum before incubation at 4° C with 6E10 antibodies in blocking solution. Detection was performed as previously described (Lesné et al., 2005; Larson et al., 2012a; 2012b) using Alexa Fluor™ conjugated secondary antibodies (Molecular Probes, Invitrogen), treated for autofluorescence with 1% Sudan Black solution (Schnell et al., 1999) and coverslipped with ProLong-DAPI mounting medium (Molecular Probes). Digital images were obtained using an Olympus IX81 FluoView1000 microscope. Raw image z-stacks were analyzed using Imaris8.0 software suite (Bitplane Scientific Software, USA).

**Barnes circular maze.** The apparatus used was an elevated circular platform (0.91 m in diameter) with 20 holes (5 cm diameter) around the perimeter of the platform, one of which was connected to a dark escape recessed chamber (target box) (San Diego Instruments, USA). The maze was positioned in a room with large, simple visual cues attached on the surrounding walls. The protocol used here was published elsewhere (Sunyer et al., 2007; Larson et al., 2012b) (<http://www.nature.com/protocolexchange/protocols/349>). Briefly, mice were habituated to the training room prior to each training day for 30 minutes in their cages. In addition, on the first day mice were placed at the center of the maze in a bottomless opaque cylinder for 60 sec to familiarize the animals with the handling. Training sessions started 15 minutes later,. Acquisition consisted of 4 trials per day for 4 days separated by a 15 minute intertrial interval. Each mouse was positioned in the center of the maze in an opaque cylinder, which was gently lifted and removed to start the session. The mice were allowed 180 seconds to find the target box on the first trial; all trials were 3 minutes long.

At the end of the first 3 minutes, if the mouse failed to find the recessed escape box, it was gently guided to the chamber and allowed to stay in the target platform for 60 seconds. The location of the escape box was kept constant with respect to the visual cues, but the hole location of the target platform was changed randomly. An animal was considered to find the escape chamber when its back legs crossed the horizontal plane of the platform. An animal was considered to enter the escape chamber when the animal's entire body was in the escape chamber and no longer visible on the platform. Memory retention was tested 24 hours after the last training session (Probe trial day 5). The same parameters were collected during acquisition and retention phases using the ANY-maze software (Stoelting Co., USA).

**Primary neurons.** Primary neuron cultures were prepared as previously described (Seward et al., 2013; Norambuena et al., 2017).

**Preparation of Amyloid- $\beta$  oligomers.** A $\beta$ O<sub>s</sub> were prepared as previously described (Norambuena et al., 2017). Briefly, Lyophilized, synthetic A $\beta$ <sub>1-42</sub> (AnaSpec) was dissolved in 1,1,1,3,3,3-hexafluoro-2-propanol (Sigma-Aldrich) to ~1 mM and evaporated overnight at room temperature. The dried powder was resuspended for 5 minutes at room temperature in 40-50  $\mu$ l dimethylsulfoxide to ~1 mM and sonicated for 10 minutes in a water bath. To prepare oligomers, the dissolved, monomeric peptide was diluted to ~400  $\mu$ l (100  $\mu$ M final concentration) in Neurobasal medium (GIBCO), incubated 24-48 hours at 4° C with rocking, and then centrifuged at 14,000 g for 15 minutes to remove fibrils. For all experiments, A $\beta$ O<sub>s</sub> were diluted into tissue culture medium to a final concentration of

~1.5  $\mu\text{M}$  total  $\text{A}\beta_{1-42}$ .

**Complementary DNA constructs and shRNA sequences.** The control shRNA plasmid contained a scrambled sequence and was purchased from Addgene (Plasmid 1864; deposited by Dr David Sabatini).  $\alpha\text{Syn}$  shRNAs (shRNA 1: TRCN0000003736, shRNA 2: TRCN0000366590) were purchased from the RNAi consortium. Lentiviral shRNA efficiency was monitored by western blotting. An expression vector for human wild type  $\alpha\text{Syn}$ , under control of the synapsin promoter, was generated using the FSW plasmid. Primers used for insertion of the  $\alpha\text{-Syn}$  DNA were Forward: 3'-GG A CCG GTA TGG ATG TAT TCA TGA AAG G-5' and Reverse: 3'-AAG GCT AGC TTA GGC TTC AGG TTC GTA G-5'. Plasmids were validated by DNA sequencing, immunofluorescence, and western blotting. The vector FSW (with synapsin promoter) was kindly provided by Thomas Südhof from Stanford. Human wild type  $\alpha\text{Syn}$  expression was monitored by immunofluorescence or western blotting.

**Lentivirus production and infection.** Lentiviruses were prepared as previously described (Norambuena et al., 2017) with some modifications. Briefly, HEK293T17 cells were plated on 15 cm dishes until they reached 60-70% confluency. The cells then received a full media change using Opti-MEM lentiviral packaging reduced growth serum. The next day, the cells were transfected with 15  $\mu\text{g}$  total DNA plasmid which at a ratio of expression/shRNA vector (50%), packaging (pspax2) (37.5%) and envelope (pMD2.G) (12.5%) vectors, with 30 $\mu\text{l}$  each of P3000 Reagent and Lipofectamine 3000™ Reagent (ThermoFisher Scientific). Packing (pspax2) and envelope (pMD2.G) vectors were

obtained from Addgene. After 6 hours of incubation the media were replaced with full serum media and every 24 hours the lentiviral containing media were collected and stored at 4° C. The lentiviral containing media were then concentrated by centrifugation at 23,000rpm for 2 hours at 4° C using a Beckman SW28 swinging bucket rotor. Cells were infected at least 3 days before A $\beta$ O treatment at a 1/25 viral dilution. Transduction efficiency was monitored by Western blot or immunofluorescence.

**Measurements of glial density.** *Immunofluorescence.* Immunolabeling was performed to stain amyloid plaques, microglia and astrocytes. Brain tissue was permeabilized with 0.1% Triton<sup>TM</sup>-X100 then incubated in 10% Normal Goat serum to prevent nonspecific binding. Afterwards, the tissue was incubated with primary antibodies for 1 hour using the Biowave<sup>®</sup> Pro system (Pelco), followed by a series of PBS washes (3 x 6 mins), and with secondary antibodies for 1 hour.

*Confocal Imaging.* Triple-label immunofluorescence was performed as previously described (Larson et al., 2017) using Alexa Fluor<sup>TM</sup>-488, -555, -647–conjugated secondary antibodies (Molecular Probes, Invitrogen), treated for autofluorescence with 0.1% Sudan Black solution, and coverslipped with ProLong-DAPI mounting medium (Molecular Probes). Digital images were obtained using an Olympus IX81 FluoView1000 microscope. Raw image z-stacks were analyzed using Imaris7.x software suite (Bitplane Scientific Software).

*Cell counting & analysis.* Glial cells surrounding plaques at radii of interest were counted using Imaris software. The density of glial cells in the proximity of amyloid plaques within incremental radii of 5  $\mu$ m from the center of the plaque cores was then

compared among the three transgenic mice lines studied in 6 month old mice.

**Western blotting.** *Primary Neuron Sample Preparation* Cultured neurons were lysed using N-PER™ Neuronal Protein Extraction Reagent (ThermoFisher Scientific) following the manufacturer's instructions. N-PER™ was supplemented with Halt™ protease and phosphatase inhibitors (ThermoFisher Scientific). The protein concentrations were determined by using the Pierce™ BCA protein assay.

*Electrophoresis.* Protein separation was done using SDS-PAGE on freshly prepared 12% SDS-polyacrylamide gels, pre-cast 10-20% SDS-polyacrylamide Tris-Tricine gels, or 10.5-14% or 4-10.5% Tris-HCl gels (Bio-Rad). Protein levels were normalized by using 2-100 µg of protein per sample (depending on the targeted protein). The samples were resuspended with 4X Tricine loading buffer and boiled for 5 minutes prior to loading.

*Western blotting.* Proteins were transferred to 0.2 µm nitrocellulose membrane (Bio-Rad) following electrophoresis. For primary neuron experiments, membranes were blocked and antibodies were diluted into Odyssey Blocking Buffer (TBS version; LI-COR Biosciences, USA). For all other experiments, membranes were blocked in TBS containing 5% bovine serum albumin (BSA; Sigma) for 1-2 hours at room temperature, and probed with the appropriate antisera/antibodies diluted in 5% BSA-TBST (TBS with 0.1% Tween-20). Primary antibodies were probed with either anti-IgG immunoglobulins conjugated with biotin, HRP or IR dyes (LI-COR Biosciences). When biotin-conjugated secondary antibodies were used, HRP- or IR-conjugated Neutravidin® (Pierce) or ExtrAvidin® (Sigma) was added to amplify the signal. Blots were revealed on a LI-COR

Odyssey imaging platform (Li-Cor Biosciences).

*Stripping.* For reprobing, membranes were stripped using Restore™ Plus Stripping buffer (Pierce) for 5-180 min at room temperature, depending on the antibody affinity.

*Quantification.* Densitometry analyses were performed using the LI-COR Odyssey software. Each protein of interest was probed in 3 individual experiments under the same conditions. Quantification by software analysis, expressed as DLUs, followed determination of experimental conditions ascertaining linearity in the detection of the signal. This method allows for a dynamic range of ~100-fold above background. Respective averages were then determined across the triplicate Western blots. Normalization was performed against actin,  $\beta$ III-tubulin or NeuN, which were also measured in triplicate. The color of the signal detected at 680 nm (red by default on the Odyssey) was modified to magenta to allow colorblind individuals to distinguish both channels.

**Dot Blotting.** Two  $\mu$ g of extracellular-enriched or membrane-associated protein lysates were mixed with sterile filtered deionized water in a total volume of 2.5  $\mu$ L. Each sample was then adsorbed onto a nitrocellulose membrane until dry. Following a brief activation in 10% methanol/TBS, the membrane was boiled in PBS to enhance antigen detection as previously described (Sherman and Lesné, 2011). Membranes were blocked in TBS containing 5% BSA for 60 minutes, then moved to the appropriate primary antibodies for overnight incubation at 4° C. Following washes, anti-mouse IgG-IR800 (1:100,000) and anti-rabbit IgG-IR680 (1:150,000) secondary antibodies were used for detection with a LI-COR Odyssey imager. All steps were performed without detergent to enhance A11/OC

binding of oligomeric species as previously reported (Lesné et al., 2006; Fowler et al., 2014; Amar et al., 2017).

**Immunocytofluorescence microscopy.** Cultured neurons were labeled as previously described (Seward et al., 2013; Norambuena et al., 2017) with the following modifications. Depending on antibody vendors' recommendations, cells were fixed with either freshly made 4% paraformaldehyde for 15 minutes at room temperature or with methanol for 15 minutes at  $-20^{\circ}\text{C}$ . After 3 washes with PBS, samples were blocked in PBS containing 5% normal goat serum and 0.25% Tween-20 for one hour. After blocking, samples were incubated with primary antibodies at  $4^{\circ}\text{C}$  overnight. The next day, samples were washed 3 times with PBS, and then incubated for 1 hour in Alexa Fluor®-tagged goat anti-mouse, anti-rabbit, or anti-chicken IgG secondary antibodies (ThermoFisher Scientific). For some experiments 4',6-Diamidino-2-Phenylindole Dihydrochloride (DAPI; ThermoFisher Scientific) counterstaining was used between subsequent washes. Coverslips were then mounted onto microscope slides and allowed to dry overnight. Samples were then imaged using a Nikon Eclipse Ti inverted microscope equipped with a Yokogawa CSU-X1 spinning disk head, a 60x 1.4 NA Plan Apo objective; 405 nm, 488 nm, 561 nm and 640 nm lasers; and a Hamamatsu Flash 4.0 scientific CMOS camera. Analysis was performed using the Nikon software and ImageJ (<https://imagej.nih.gov/ij/plugins/cell-counter.html>).

Brain tissue sections were labeled for immunohistochemistry as previously described (Norambuena et al., 2017).

**Statistical Analyses.** When variables were non-normally distributed, nonparametric

statistics were used (Spearman rho correlation coefficients, Kruskal-Wallis non-parametric analysis of variance followed by Bonferroni-corrected two-group *posthoc* Mann-Whitney U tests). When variables were normally distributed, the following parametric statistics were used (one/two-way ANOVA followed by Bonferroni-corrected two-group *posthoc* Student t tests). Sample size was determined by power analysis to be able to detect statistically significant changes within a 20% variation of measured responses. Analyses were performed using JMP 12 or JMP 13 (SAS Institute, USA).

## Khan-Boyle-Lacroix et al. Introduction

Alzheimer's disease (AD) is classically defined by the co-occurrence of extracellular amyloid- $\beta$  ( $A\beta$ ) plaques and intracellular neurofibrillary tangles of tau. Although plaques and tangles are histopathological signatures of the disease, the soluble  $A\beta$  and tau aggregates that precede their formation are potently cytotoxic and they are therefore widely considered to be the primary drivers of neurodegeneration in AD. Soluble  $A\beta$  oligomers ( $A\beta$ Os) have been shown to directly induce memory deficits (Shankar et al., 2008; Reed et al., 2011), synaptic dysfunction, and neuronal cell-cycle re-entry, a prelude to neuronal death in AD (Varvel et al., 2008; Bhaskar et al., 2009; Seward et al., 2013; Bhaskar et al., 2014; Norambuena et al., 2017). Tau expression is required by many of the pathways aberrantly affected by  $A\beta$  (Roberson et al., 2007; Vossel et al., 2010; Bloom, 2014), supporting the notion that  $A\beta$ Os are signaling upstream of tau (Aarsland et al., 2003; Roberson et al., 2007; Vossel et al., 2010). Besides  $A\beta$  and tau, soluble alpha-synuclein ( $\alpha$ Syn) is also strongly linked to memory deficiencies in AD, as well as in Parkinson's disease (PD) and Lewy body dementia (LBD) (Aarsland et al., 2003; Hely et al., 2008; Overk et al., 2014; Adamowicz et al., 2017; Larson et al., 2017), suggesting an intrinsic contribution of  $\alpha$ Syn to the pathophysiology of AD. Despite this relationship and subsequent studies highlighted below, the role of  $\alpha$ Syn in AD remains particularly unclear, and its involvement in  $A\beta$ O and/or tau-induced AD pathogenesis is relatively understudied.

To date, several putative interactions have been identified linking  $\alpha$ Syn and  $A\beta$ . On

a cognitive level, overexpression of  $\alpha$ Syn in mutant APP transgenic mice exacerbates behavioral deficiencies (Masliah et al., 2001). The underlying mechanism responsible for this effect relies upon enhanced aggregation of  $\alpha$ Syn caused by A $\beta$  (Masliah et al., 2001). Expanding upon these findings, we recently identified and characterized distinct  $\alpha$ Syn aggregates induced by mutant APP expression in transgenic mice, which were associated to memory impairment through a transcriptional regulation of synapsin genes (Larson et al., 2017). By contrast, ablation of  $\alpha$ Syn in mThy1-APP mice was recently reported to alleviate learning deficits (Spencer et al., 2016). Hence, evidence suggests that  $\alpha$ Syn oligomerization, initiated by APP/A $\beta$  overexpression, contributes to synaptotoxicity and memory impairment in AD mouse models.

$\alpha$ Syn may also alter A $\beta$  solubility and plaque formation *in vivo*, although the reported findings are contradictory. Genetic ablation of  $\alpha$ Syn in Tg2576 APP mice resulted in increased plaque burden, although no other phenotypic change was reported (Kallhoff et al., 2007). By contrast, no difference in amyloid burden was reported in mThy1-APP mice after  $\alpha$ Syn depletion (Spencer et al., 2016). Overexpression of mutant  $\alpha$ Syn<sup>A53T</sup> in 3xTg-AD mice, on the other hand, resulted in enhanced A $\beta$  deposition (Clinton et al., 2010), whereas overexpression of mutant  $\alpha$ Syn<sup>A30P</sup> in Thy1-APPPS1 mice resulted in a reduction of A $\beta$  plaque burden and compromised synaptic integrity (Bachhuber et al., 2015). Therefore, the functional consequences induced by  $\alpha$ Syn on A $\beta$  aggregation and amyloid burden *in vivo* are ill defined and in dispute.

In an attempt to lift this controversial veil and to investigate the contribution of  $\alpha$ Syn to the central defining features of AD (i.e. amyloid deposition, synaptic dysfunction and subsequent cognitive dysfunction), we applied a bidirectional genetic approach to AD-

model transgenic mice and primary cortical neuron cultures. We generated bigenic mice that either co-express human APP with human wild-type  $\alpha$ Syn (APP/ $\alpha$ Syn), or APP transgenic animals lacking  $\alpha$ Syn (by ablating the murine *SNCA* gene, APP/ $\alpha$ Syn-KO). We then performed behavioral, histopathological, and candidate-driven protein expression analyses. Our results reveal bidirectional modulation of several key AD phenotypes by  $\alpha$ Syn. Human  $\alpha$ Syn expression in APP mice exacerbated memory deficits, increased soluble A $\beta$ O<sub>s</sub> and pathological tau proteins, and potentiated both synaptic protein loss and ectopic neuronal cell cycle re-entry (CCR), a frequent precursor of neuron death in AD. Ablation of  $\alpha$ Syn in APP mice prevented memory deficits, decreased conformationally altered tau molecules, prevented loss of postsynaptic GluN2A and Drebrin proteins, and ameliorated neuronal CCR. Thus, our results reveal a multi-faceted role for  $\alpha$ Syn in AD pathogenesis, and have direct implications for  $\alpha$ -synucleinopathies and tauopathies.

## Khan-Boyle-Lacroix et al. Results

### **$\alpha$ Syn overexpression decreases amyloid deposition but exacerbates behavioral deficits in APP mice**

Overexpression of mutant  $\alpha$ Syn ( $\alpha$ Syn<sup>A30P</sup> and  $\alpha$ Syn<sup>A53T</sup>) in APP transgenic mice can either result in diminished or enhanced amyloid burden, respectively (Clinton et al., 2010; Bachhuber et al., 2015), thereby generating a debate about the contribution of  $\alpha$ Syn on A $\beta$  pathology. Considering the distinct properties of mutant  $\alpha$ Syn compared to its wild-type isoform (Burré et al., 2012; 2015) ( $\alpha$ Syn<sup>WT</sup>), it also remains unclear whether human  $\alpha$ Syn<sup>WT</sup> can alter amyloid load. To begin assessing potential interplays between  $\alpha$ Syn and A $\beta$ , we crossed transgenic animals overexpressing  $\alpha$ Syn<sup>WT</sup> (TgI2.2 line, (Lee et al., 2002) with APP transgenic mice (J20 line, (Mucke et al., 2000) hereafter denoted APP/ $\alpha$ Syn. Overexpression of  $\alpha$ Syn did not alter early mortality seen in APP mice (**Fig. 1a**) nor did it alter forebrain full-length APP (fl-APP) and APP carboxyl terminal fragment (APP-CTF) protein abundance when compared to age-matched APP mice (**Supplementary Fig. 1**; as previously reported (Larson et al., 2017)). However, examination of amyloid burden at 6 months of age, when amyloid deposition is limited to the hippocampus in APP mice (Mucke et al., 2000), revealed striking differences (**Fig. 1b** and **Supplementary Fig. 1c, arrows**). Quantitation of plaque burden and density indicated a heavily reduced plaque load in APP/ $\alpha$ Syn mice when compared to APP mice (**Fig. 1c,d**) with the majority of plaque load reduction arising from fewer, small amyloid deposits <200  $\mu$ m<sup>2</sup> in size (**Fig. 1e**). These observations validate the changes induced by  $\alpha$ Syn<sup>A30P</sup> previously reported<sup>18</sup>.

Although APP/PS1 $\alpha$ Syn<sup>A30P</sup> bigenic animals displayed synaptic abnormalities suggestive of synapse loss (Bachhuber et al., 2015), it remained unknown whether these changes translate into cognitive deficits. In our 6-month-old APP/ $\alpha$ Syn mice, the reduced plaque load did not translate into ameliorated behavioral deficits when assessed by using the Barnes circular maze. Rather, APP/ $\alpha$ Syn animals displayed striking learning deficits (**Fig. 1f**) while APP and  $\alpha$ Syn mice were comparable to WT controls. Furthermore, while 6-month-old APP and  $\alpha$ Syn transgenic mice displayed subtle deficits in memory retention during the probe trial (as previously reported (Larson et al., 2012b)), APP/ $\alpha$ Syn mice remarkably suffered more pronounced impairment than both of these groups, with lower target quadrant occupancy and path efficiency (**Fig. 1g** and **Supplementary Figs. 2-3**). In addition, APP/ $\alpha$ Syn mice showed similar behavior to APP littermates, consistent with hyperactivity and a higher frequency of freezing episodes (**Supplementary Fig. 3a-c**). Altogether, these findings indicate that increased expression of  $\alpha$ Syn<sup>WT</sup> lowers A $\beta$  deposition and exacerbates cognitive deficits in APP mice.

### **$\alpha$ Syn ablation increases plaque load but rescues behavioral deficits**

Since overexpression of  $\alpha$ Syn<sup>WT</sup> in APP mice appeared to perturb multiple components of their phenotype, we next sought to investigate the effect of  $\alpha$ Syn ablation on amyloid deposition and learning deficits. Thus, we crossed APP mice with  $\alpha$ Syn knockout animals, hereafter denoted APP/ $\alpha$ Syn-KO. In contrast to APP/ $\alpha$ Syn mice, in which the overexpression of human  $\alpha$ Syn<sup>WT</sup> did not modify premature lethality, the early mortality defining APP mice was fully rescued in APP/ $\alpha$ Syn-KO mice (**Fig. 2a**). Second, where the APP/ $\alpha$ Syn mice showed decreased A $\beta$  deposition, amyloid burden and plaque density

were instead increased by 24% and 35% respectively in 6-month-old APP/ $\alpha$ Syn-KO mice (**Fig. 2b-d**). These changes were the result of an increased frequency in amyloid plaques  $< 200\mu\text{m}^2$  in size (**Fig. 2e**). Finally, spatial reference memory was assessed in these mice at 6-months of age using the Barnes circular maze. Although all groups learned the task similarly (**Fig. 2f**), only APP mice showed impaired spatial memory retention during the probe trial with lower target quadrant occupancy and poorer path efficiency compared to WT controls (**Fig. 2g** and **Supplementary Fig. 4d**). This deficit was reversed in APP/ $\alpha$ Syn-KO mice (**Fig. 2g** and **Supplementary Fig. 2**). Further supporting this phenotypic change, both hyperactivity and freezing behavior previously seen in APP mice were attenuated in APP/ $\alpha$ Syn-KO mice (**Supplementary Fig. 4a-c**) signifying a profound rescue of all behavioral components assessed. Of note,  $\alpha$ Syn-KO mice were indistinguishable from WT controls in each metric assessed (**Fig. 2a,f,g** and **Supplementary Figs. 2, 4**). Overall, these results indicate that ablation of *SNCA* in APP mice consistently rescued multiple central components of their phenotype, and are in sharp opposition to those of APP/ $\alpha$ Syn animals.

### **$\alpha$ Syn bidirectionally modulates the production and cellular distribution of soluble A $\beta$ O<sub>s</sub>**

The dramatic differences in amyloid burden and behavioral deficits observed among APP/ $\alpha$ Syn, APP and APP/ $\alpha$ Syn-KO mice, in absence of apparent changes in APP expression or APP processing (**Supplementary Fig. 1**), led us to hypothesize that the forebrain abundance of soluble A $\beta$ O<sub>s</sub> would also be altered. A11 and OC antibodies were used to detect soluble type I (non-fibrillar) and type II (pre-fibrillar) A $\beta$ O<sub>s</sub> by non-

denaturing dot blotting (Liu et al., 2015). 6E10 (anti APP/A $\beta$ ) and anti-actin antibodies were used as internal controls. Our analysis revealed subtle and consistent differences in A $\beta$ O<sub>s</sub> among APP, APP/ $\alpha$ Syn and APP/ $\alpha$ Syn-KO mice that complement the changes observed for deposited A $\beta$  (**Fig. 3**). In APP/ $\alpha$ Syn mice, which displayed a lower plaque burden than APP animals (**Fig. 1b**), forebrain lysates contained elevated OC<sup>+</sup> pre-fibrillar A $\beta$ O<sub>s</sub> in the extracellular-enriched fraction (EC) and decreased OC<sup>+</sup> pre-fibrillar A $\beta$ O<sub>s</sub> in the membrane-enriched fraction (MB). These changes imply the existence of a shift in the compartmentalization of these A $\beta$  assemblies between APP/ $\alpha$ Syn and APP animals. The opposite shift occurred in APP/ $\alpha$ Syn-KO mice, which harbor a higher amyloid plaque burden compared to APP mice (**Fig. 2b**). We found decreased detection profiles for A11, OC and 6E10 in the EC fractions of APP/ $\alpha$ Syn-KO forebrain lysates compared to APP mice. By contrast, OC and 6E10 immunoreactivity were elevated in the corresponding MB fraction of these animals, suggesting a redistribution of OC<sup>+</sup> pre-fibrillar A $\beta$ O<sub>s</sub> associated with enhanced plaque deposition. (**Fig. 3a,b**). Since prior studies suggested the existence of heterologous  $\alpha$ Syn-A $\beta$  hybrid oligomers, we performed co-immunoprecipitations with LB509. Although human  $\alpha$ Syn was readily pulled down, we could not reveal the presence of A $\beta$  within putative complexes using forebrain lysates from APP/ $\alpha$ Syn mice (**Fig. 3c**). Taken together, these results further support a bidirectional modulation of A $\beta$  aggregation in APP mice by  $\alpha$ Syn.

To reinforce these observations, we also hypothesized that this  $\alpha$ Syn-driven alteration of A $\beta$  deposition may result in a differential neuroimmune response. To broadly assess this, the cellular density of astrocytes and microglia in the close vicinity of amyloid plaques (50  $\mu$ m) was evaluated and compared across groups (**Supplementary Fig.**

**5a,b**). Our results indicated that  $\alpha$ Syn overexpression in APP mice led to a decrease in Iba1-positive microglia surrounding A $\beta$  deposits, whereas ablation of  $\alpha$ Syn augmented the density of astrocytes (**Supplementary Fig. 5c,b**). While these observations merit additional study, the changes in glial density paralleled those described for A $\beta$  plaque burden.

### **Early pathological features of tau are $\alpha$ Syn-dependent**

Because substantial evidence supports a role for tau in mediating A $\beta$ -induced toxicity (Rapoport et al., 2002; Roberson et al., 2007; Ittner et al., 2010; Nussbaum et al., 2012; Larson et al., 2012b; Seward et al., 2013; Bloom, 2014; Sherman et al., 2016; Amar et al., 2017), and since tau pathology is a histopathological signature of AD, we next sought to determine the state of tau in these animals. Using a well-established panel of antibodies against various pathological forms of tau (kind gift from Dr. Peter Davies), we assessed phosphorylation and conformational changes of tau in intracellular-enriched (IC) and membrane-enriched forebrain fractions as described earlier (Larson et al., 2012b; Sherman et al., 2016; Amar et al., 2017). We recently reported that young APP mice only display elevated tau hyper-phosphorylation at S202 and S416 (Amar et al., 2017), echoing the increase observed using an unbiased mass spectrometry approach by independent groups (Morris et al., 2015). Here, western blot analysis revealed no apparent pathological changes of tau detected within the intracellular-enriched fractions across genotypes, with the exception of MC1-tau immunoreactivity, which was reduced in APP/ $\alpha$ Syn-KO compared to APP and APP/ $\alpha$ Syn mice (**Fig. 4a,b**). By contrast, the introduction of  $\alpha$ Syn<sup>WT</sup> in APP mice substantially increased MC1 and CP13 anti-tau

immunoreactivity by ~2- and ~1.5-fold, respectively, in the membrane-enriched fraction (**Fig. 4c,d** and **Supplementary Fig. 6**). These biochemical changes were further supported by confocal image analysis using MC1 (**Fig. 4e**), which recognizes an early AD conformation requiring interaction between the N and C termini of tau (Jicha et al., 1997; Weaver et al., 2000), and CP13 (**Supplementary Fig. 6**), which recognizes tau phosphorylated at S202 (Weaver et al., 2000). Overall, these results indicate that  $\alpha$ Syn expression bidirectionally modulates the abundance of conformationally altered tau molecules detected by MC1 in APP mice.

### **GluN2A and Drebrin are bidirectionally modulated by $\alpha$ Syn**

Since synapse loss constitutes an early event that defines AD pathogenesis (Selkoe, 2002), and because A $\beta$ O $_s$  potently induce synapse loss in J20 mice (Hong et al., 2016), we next assessed whether synaptic protein integrity was modulated by  $\alpha$ Syn expression in APP animals. We selected several pre-synaptic (i.e.  $\alpha$ Syn, synaptophysin [SYP] and Ras-related protein Rab3A,) and post-synaptic (i.e. postsynaptic density protein 95 [PSD95], Drebrin and the N-Methyl-D-Aspartate receptor subunit GluN2A) proteins that are strongly implicated in AD pathophysiology as candidates for western blotting and immunofluorescence analysis (**Fig. 5**). As expected,  $\alpha$ Syn forebrain abundance was elevated in membrane-enriched fractions from APP/ $\alpha$ Syn bigenic mice when compared to APP animals, while  $\alpha$ Syn was absent in APP/ $\alpha$ Syn-KO mice (**Fig. 5a,b**). We previously reported that SYP and Rab3A protein expression was unchanged in young and middle-aged  $\alpha$ Syn transgenic mice compared to WT controls (**Supplementary Fig. 7** and as described earlier (Larson et al., 2012b; 2017). However, the expression of human  $\alpha$ Syn<sup>WT</sup>

in APP mice synergistically lowered the forebrain abundance of all synaptic proteins tested when compared to the APP parental line (**Fig. 5a,b**). Contrasting with APP/ $\alpha$ Syn mice, genetic ablation of endogenous  $\alpha$ Syn did not alter the protein expression of SYP, Rab3, or PSD95 compared to age-matched APP mice. Instead, forebrain lysates from APP/ $\alpha$ Syn-KO mice displayed higher protein amounts of postsynaptic markers drebrin and GluN2A than APP mice. These observations were further supported by immunofluorescent staining of synaptic markers SYP, GluN1 and GluN2B which revealed a qualitative reduction in SYP immunoreactivity in the hippocampus of APP/ $\alpha$ Syn mice whereas fluorescent detection of NMDA receptor subunits GluN1 and GluN2B appeared unchanged (**Fig. 5c**). Thus, these results demonstrate that overexpression of  $\alpha$ Syn<sup>WT</sup> exacerbates synaptic loss in APP mice, and that  $\alpha$ Syn specifically modulates GluN2A and Drebrin abundance in a bidirectional manner.

### **A $\beta$ -induced ectopic cell-cycle re-entry depends on $\alpha$ Syn**

In addition to A $\beta$ -mediated synaptic and cognitive deficits, A $\beta$ O<sub>s</sub> also induce ectopic CCR in post-mitotic neurons, initiating an early signaling event that results in dendritic abnormalities and precedes neuron loss in AD (Varvel et al., 2008; Bhaskar et al., 2009; Arendt, 2012; Bhaskar et al., 2014). We previously reported that neuronal CCR is a phenotypic feature of 6-month-old J20 mice (Seward et al., 2013), which led us to test whether  $\alpha$ Syn expression modulated A $\beta$ O-induced CCR in APP mice. CCR was determined by measuring the percentage of cortical neurons that also expressed nuclear cyclin D1, a protein that is required for G<sub>1</sub>/S phase transition during the cell cycle, as a surrogate for CCR (**Fig. 6**). We observed a robust increase in cyclin D1-positive cortical

neurons from J20 mice ( $n = 1092/3424$ , 31.06%) relative to their non-transgenic littermates ( $n = 253/4966$ , 5.09%; **Fig. 6b**), which is consistent with our previous report. In APP/ $\alpha$ Syn<sup>WT</sup> mice, however, neuronal cyclin D1 was markedly enhanced by ~1.5-fold ( $n = 1959/4064$ , 47.34%) relative to APP mice. Importantly, neuronal cyclin D1 in 6-month-old human wild-type  $\alpha$ Syn transgenic mice ( $n = 147/3209$ , 4.6%) did not significantly differ from non-transgenic animals, suggesting that the enhancement of CCR in the APP/ $\alpha$ Syn mice was not due to an additive effect (**Fig. 6b** and **Supplementary Fig. 8a**). On the other hand, genetic ablation of endogenous  $\alpha$ Syn in APP mice ameliorated neuronal CCR, with cyclin D1-positive neuron counts ( $n = 210/3835$ , 6.18%) indistinguishable from that of non-transgenic littermates (**Fig. 6a,b**). Hence, our results demonstrate bidirectional modulation of neuronal CCR by  $\alpha$ Syn *in vivo*.

To further assess the cellular consequences of  $\alpha$ Syn reduction, specifically in relation to A $\beta$ -induced increases in neuronal cyclin D1, we next measured A $\beta$ O-induced CCR after lentiviral depletion of  $\alpha$ Syn in primary cultures of mouse cortical neurons (**Supplementary Fig. 8b-c**). Strikingly, viral knockdown of  $\alpha$ Syn transcripts by two different shRNAs protected primary mouse cortical neurons from A $\beta$ O-induced increases in nuclear cyclin D1, as determined by quantitative confocal imaging (**Fig. 6c,d**) and immunoblotting (**Fig. 6e-h**). Contrary to previous observations (Spencer et al., 2016) this effect was independent of Rab3 as A $\beta$ O exposure did not alter the protein abundance of Rab3 under our experimental conditions (**Supplementary Fig. 7**). During the G<sub>1</sub>/S phase cell cycle transition, cyclin D1 forms a complex with the cyclin-dependent kinases CDK4/6, thereby activating the cyclin-CDK complex and relieving the repressor action of the retinoblastoma protein (Rb) via phosphorylation at serine 780 (S780) (Connell-

Crowley et al., 1997). Consistent with this canonical Cyclin D-CKD4/6 signaling cascade,  $\alpha$ Syn knockdown prevented the abnormal elevation of Rb phosphorylation at S780 (pRb) induced by A $\beta$ O (Fig. 6g). Finally, we also measured the protein abundance of the proliferating cell nuclear antigen (PCNA) following A $\beta$ O treatment, which is active during periods of DNA replication and synthesis. In agreement with independent studies (Bhaskar et al., 2009), we found that A $\beta$ O elevated PCNA protein amounts. By contrast,  $\alpha$ Syn knockdown prevented the elevation of PCNA caused by A $\beta$ O in primary cortical neurons (Fig. 6h). Together, these results demonstrate that  $\alpha$ Syn is also required for A $\beta$ O-induced neuronal CCR progression, likely by preventing the initial increase in cyclin D1 expression by A $\beta$ O.

### **Enhancement of CCR by $\alpha$ Syn in primary neurons is tau-dependent**

Based on the findings that  $\alpha$ Syn bidirectionally modulates pathological tau conformers *in vivo*, we explored whether the enhancement of A $\beta$ O-induced CCR by  $\alpha$ Syn was dependent on tau *in vitro*. Using the previously described experimental paradigm, we found that lentiviral knockdown of  $\alpha$ Syn abolished A $\beta$ O-induced MC1-reactive tau, whereas expression of human  $\alpha$ Syn<sup>WT</sup>, virally driven by the neuron-specific synapsin-1 promoter, exacerbated the accumulation of conformationally altered tau molecules induced by A $\beta$ O (Fig. 7a and Supplementary Fig. 9). These observations are consistent with the biochemical changes revealed in APP/ $\alpha$ Syn and APP/ $\alpha$ Syn-KO mice, further supporting a central role of  $\alpha$ Syn in modulating A $\beta$ -induced phenotypes. To assess if the enhancement of A $\beta$ -induced CCR by  $\alpha$ Syn was tau-dependent, we next overexpressed human  $\alpha$ Syn<sup>WT</sup> in primary cortical neurons from non-transgenic and tau-

KO mice, and quantified Cyclin D1-positive neurons following fluorescent immunostaining (**Fig. 7b-d**). Consistent with the CCR analysis of APP/ $\alpha$ Syn mice, lentiviral delivery of  $\alpha$ Syn in primary neurons from non-transgenic mice resulted in a substantial increase in Cyclin D1-positive neurons (29%) compared to neurons exposed to A $\beta$ O treatment alone (19.83%) or to viral control groups expressing eGFP (20.36%). In stark contrast to primary cultures derived from non-transgenic mice, we found virtually no cyclin D1-positive neurons in tau-KO mice in all treatment conditions, including in neurons transfected with  $\alpha$ Syn and treated with A $\beta$ O (**Fig. 7c,d, Supplementary Fig. 10**). Taken together, these results indicate that  $\alpha$ Syn, like tau, is required for A $\beta$ O-induced neuronal CCR.

# Khan-Boyle-Lacroix et al. Figures

Figure 1

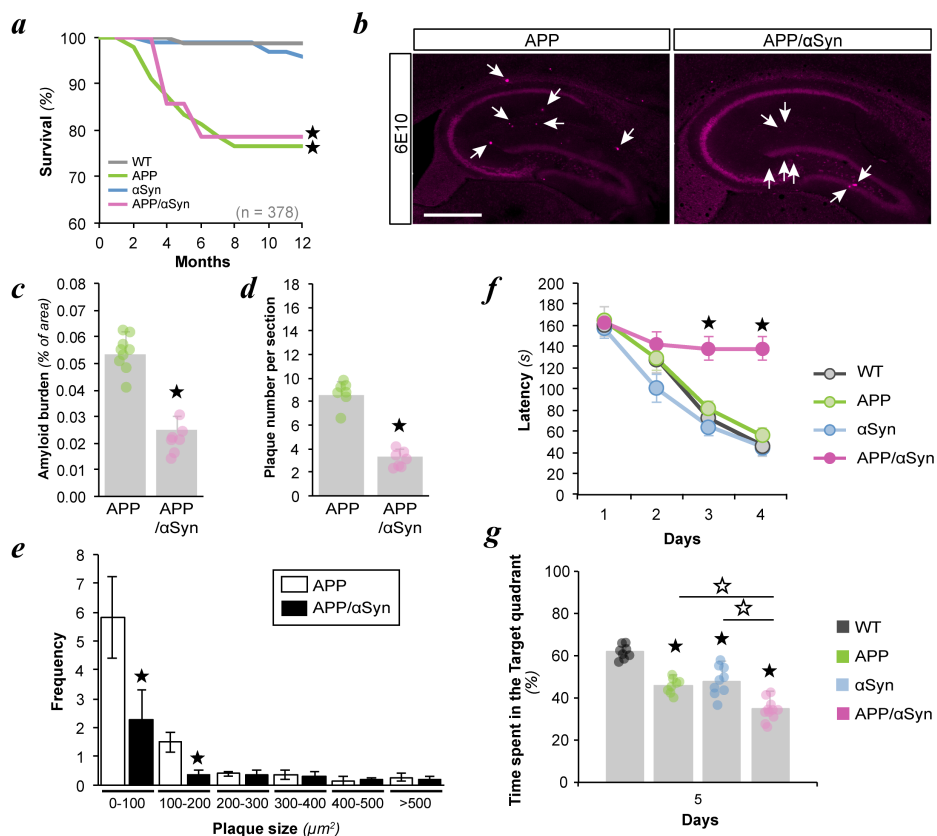


**Figure 1. Effects of human  $\alpha$ Syn<sup>WT</sup> overexpression on the phenotype of APP transgenic mice.** (a) Kaplan-Meier survival curves showing effect of the overexpression of human  $\alpha$ Syn<sup>WT</sup> on premature mortality in APP transgenic mice. All genotyped mice in the colony were included in the analysis ( $N = 378$ ,  $n_{\text{WT}} = 70$ ,  $n_{\text{APP}} = 92$ ,  $n_{\alpha\text{Syn}} = 87$ ,  $n_{\text{APP}/\alpha\text{Syn}} = 99$  mice). By Log-Rank comparison, both APP and APP/ $\alpha$ Syn mice differed from all other groups ( $\chi^2_{(3)} = 22.101$ ,  $\star P = 0.0001$  vs. WT). (b) Anti-A $\beta$  immunofluorescent labeling (6E10) was used to assess amyloid burden of the cortex and hippocampus of APP transgenic mice harvested after behavioral testing (6 months of age). White arrows indicate amyloid deposits. (c,d) Quantitation of the area covered by 6E10-immunoreactive deposits (c) and the number of amyloid plaques per section (d) detected

in APP and APP/ $\alpha$ Syn mice (Bars represent the mean  $\pm$  S.D.; *t* test, \**P* < 0.05, *n* = 8 sections/animal, *N* = 10-12 animals/genotype). **(e)** Comparison of plaque distribution between APP and APP/ $\alpha$ Syn mice binned by covered area (100  $\mu\text{m}^2$  increments). (Bars represent the mean  $\pm$  S.D.; *t* test, \**P* < 0.05, *n* = 8 sections/animal, *N* = 10-12 animals/genotype). **(f,g)** Influence of  $\alpha$ Syn overexpression on spatial reference memory in young mice. Six-month-old WT, APP,  $\alpha$ Syn and APP/ $\alpha$ Syn mice (*n* = 8-11 mice/genotype) were trained in the Barnes circular maze for 4 days. A probe trial (escape platform removed) was conducted 24 h after the last training session. During acquisition of the task, escape latency (*f*) was recorded. Two-way repeated-measures ANOVA revealed a significant effect of training ( $F_{(3,540)} = 34.228$ , *P* < 0.0001), of the transgene ( $F_{(3,540)} = 19.626$ , *P* < 0.0001) and a significant day\*transgene interaction ( $F_{(9,540)} = 3.688$ , *P* = 0.0002) for all mice. APP/ $\alpha$ Syn mice showed little ability to learn the task well ( $F_{(4,44)} = 8.56$ , *P* < 0.0001). During the probe trial on day 5 (*g*), APP mice showed poorer memory retention than any other group as confirmed by one-way ANOVA analysis ( $F_{(3,34)} = 24.596$ , *P* < 0.0001) followed by Student *t* test with Bonferroni correction, *P* < 0.0001. Data represent mean  $\pm$  S.E.M. (*f*) or S.D. (*g*) (*n* = 8-11 mice/age/genotype).

Figure 2

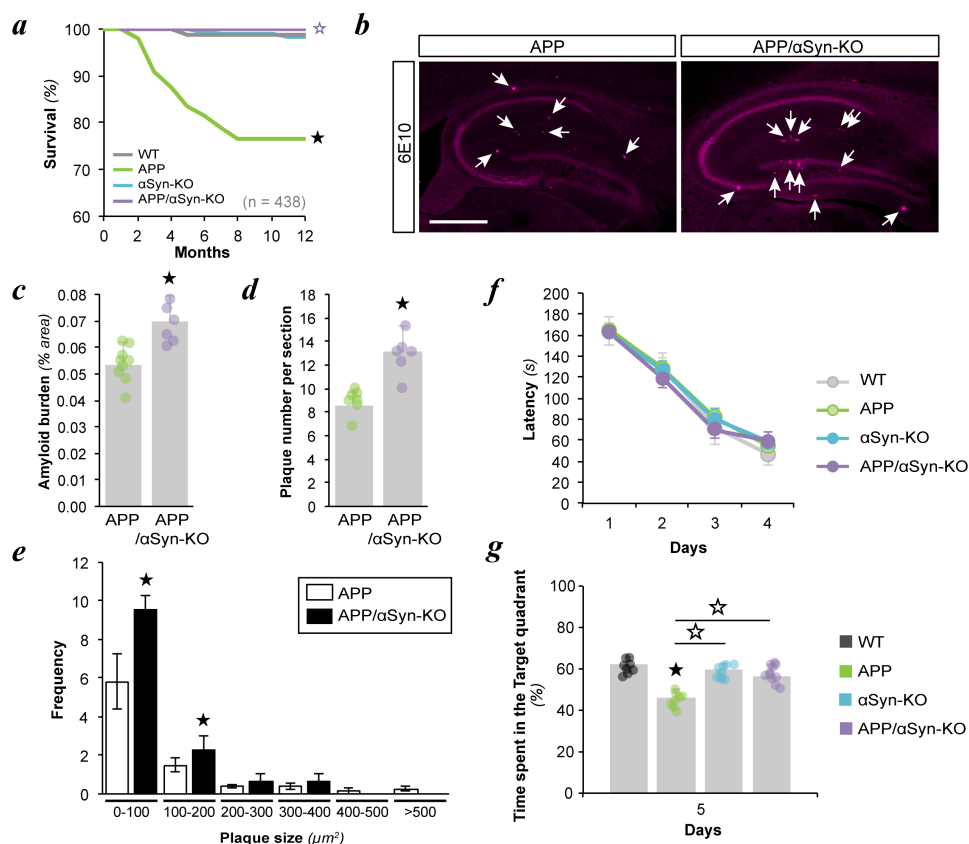


**Figure 2. Effects of  $\alpha$ Syn gene deletion on the phenotype of APP transgenic mice.** (a) Kaplan-Meier survival curves showing effect of the ablation of endogenous  $\alpha$ Syn on premature mortality in APP transgenic mice. All genotyped mice in the colony were included in the analysis ( $N = 438$ ,  $n_{WT} = 70$ ,  $n_{APP} = 92$ ,  $n_{\alpha Syn-KO} = 118$ ,  $n_{APP/\alpha Syn-KO} = 158$  mice). By Log-Rank comparison, only APP mice differed from all other groups ( $\chi^2_{(3)} = 18.784$ ,  $^*P = 0.0001$  vs. WT,  $^*P = 0.0001$  vs. APP). (b) Anti-A $\beta$  immunofluorescent labeling (6E10) was used to assess amyloid burden of the cortex and hippocampus of APP transgenic mice harvested after behavioral testing. White arrows indicate amyloid deposits. (c,d) Quantitation of the area covered by 6E10-immunoreactive deposits (c) and the number of amyloid plaques per section (d) detected in APP and APP/ $\alpha$ Syn-KO mice (Bars represent the mean  $\pm$  S.D.;  $t$  test,  $^*P < 0.05$ ,  $n = 8$  sections/animal,  $N = 10-12$

animals/genotype). **(e)** Comparison of plaque distribution between APP and APP/ $\alpha$ Syn-KO mice binned by covered area ( $100 \mu\text{m}^2$  increments). (Bars represent the mean  $\pm$  S.D.; *t* test, \* $P < 0.05$ ,  $n = 8$  sections/animal,  $N = 10-12$  animals/genotype). **(f,g)** Influence of SNCA deletion on spatial reference memory in young mice. Six-month-old WT, APP,  $\alpha$ Syn-KO and APP/ $\alpha$ Syn-KO mice ( $n = 8-11$  mice/genotype) were trained in the Barnes circular maze for 4 days. A probe trial (escape platform removed) was conducted 24 h after the last training session. During acquisition of the task, escape latency (*f*) was recorded. Two-way repeated-measures ANOVA revealed a significant effect of training ( $F_{(3,544)} = 74.124$ ,  $P < 0.0001$ ), no effect of genetic modification ( $F_{(3,544)} = 1.008$ ,  $P = 0.3886$ ), and a significant day\*transgene interaction ( $F_{(9,544)} = 2.796$ ,  $P = 0.0033$ ) for all four groups. During the probe trial on day 5 (*g*), APP mice showed poorer memory retention than any other group as confirmed by one-way ANOVA analysis ( $F_{(3,34)} = 7.354$ ,  $P = 0.0008$ ) followed by Student *t* test with Bonferroni correction,  $p < 0.0001$ . Data represent mean  $\pm$  S.E.M. (*f*) or S.D. (*g*) ( $n = 8-11$  mice/age/genotype).

Figure 3

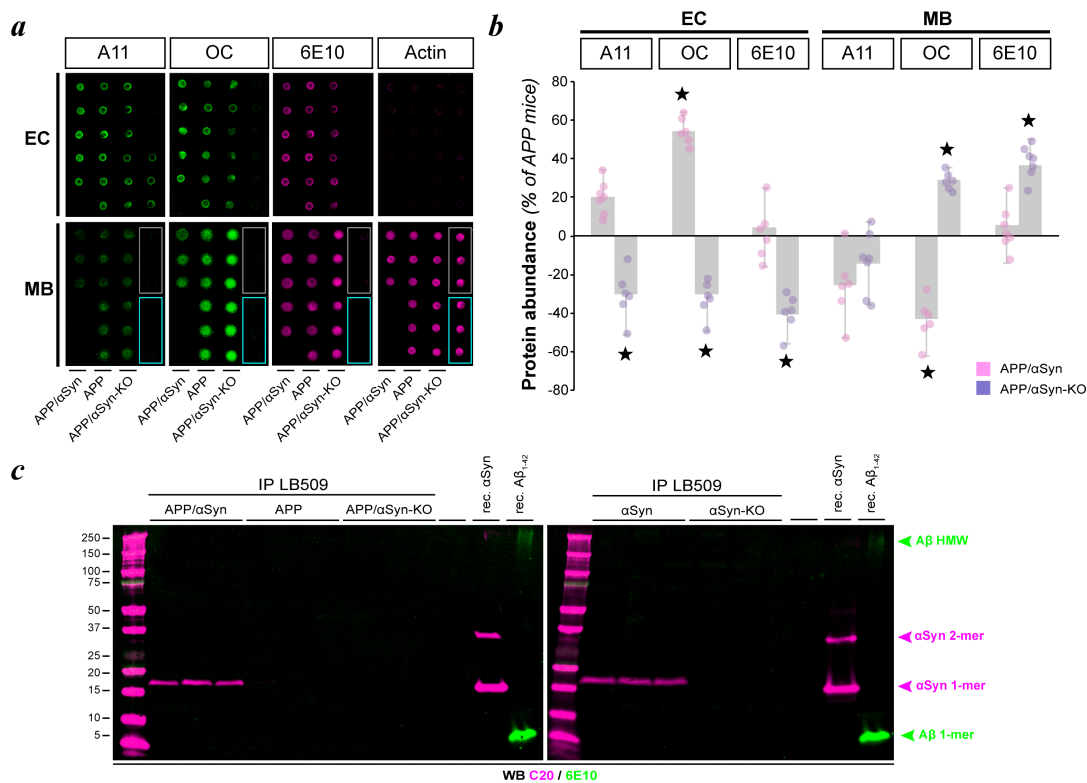


**Figure 3. Bidirectional redistribution of AβOs caused by αSyn in APP mice.** (a) Detection of oligomeric amyloid conformers in extracellular-enriched (EC) and membrane-enriched (MB) lysates from APP/αSyn, APP and APP/αSyn-KO mice by dot blot analysis using A11 and OC antibodies. 6E10 was also used to measure APP/Aβ abundance and actin was used as internal control. ( $n = 6$  animals/age/genotype). Note that only 3 (out of 6) APP/αSyn specimens were adsorbed onto the presented nitrocellulose membranes shown for A11, OC and Actin. Grey and teal rectangles correspond to WT and αSyn control lysates respectively. Note that Actin is not present in extracellular-enriched lysates as expected. (b) Normalized abundance of oligomeric species indicated a bidirectional redistribution of A11 and OC conformers in EC and MB extracts of APP animals. (Histograms represent the mean  $\pm$  S.D.; One-way ANOVA [ $F_{(2,18)}^{A11-EC} = 12.4110$ ,

$P = 0.0008$ ,  $F_{(2,18)}^{\text{OC-EC}} = 22.6278$ ,  $P < 0.0004$ ,  $F_{(2,18)}^{6\text{E}10\text{-EC}} = 8.5928$ ,  $P = 0.0037$  and  $F_{(2,18)}^{\text{A11-MB}} = 5.8887$ ,  $P = 0.0139$ ,  $F_{(2,18)}^{\text{OC-MB}} = 53.8985$ ,  $P < 0.0001$ ,  $F_{(2,18)}^{6\text{E}10\text{-MB}} = 5.131$ ,  $P = 0.0123$  respectively] followed by Student *t* test with Bonferroni correction; \* $P < 0.05$  vs. 6-month-old APP mice,  $n = 6$  animals/age/genotype). (c) Co-immunoprecipitation of A $\beta$  with  $\alpha$ Syn in membrane extracts from the forebrain of APP mice. A $\beta$  was detected with 6E10. Pre-aggregated synthetic human  $\alpha$ Syn and A $\beta_{1-42}$  were loaded as internal controls. Blot is representative of 3 experiments ( $n = 6$  mice/age/genotype).

**Figure 4**

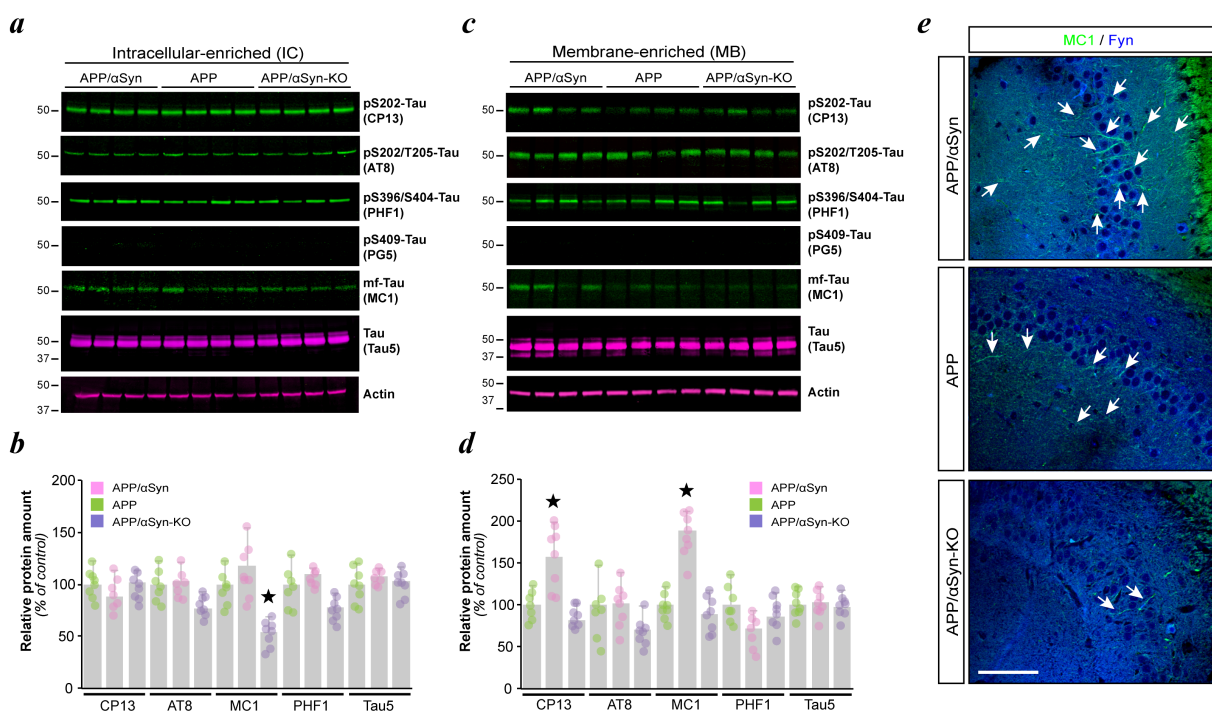


**Figure 4. Forebrain abundance of conformationally-altered tau molecules is bidirectionally controlled by  $\alpha$ Syn expression in APP mice. (a,b)** Representative Western blots (a) and quantitation (b) of soluble tau species detected in intracellular (IC)-enriched fractions from 6-month-old APP/ $\alpha$ Syn, APP and APP/ $\alpha$ Syn-KO mice. Histograms show mean  $\pm$  S.D.; One-way

ANOVA [ $F_{(2,23)} = 12.3071$ ,  $P = 0.0007$  for MC1-tau] followed by Student's  $t$  test,  $*P < 0.05$  vs. age-matched APP mice;  $n = 6-9$  mice/group. **(c,d)** Representative Western blots (c) and quantitation (d) of soluble tau species detected in membrane (MB)-enriched fractions from 6-month-old APP/ $\alpha$ Syn, APP and APP/ $\alpha$ Syn-KO mice. Histograms show mean  $\pm$  S.D.; One-way ANOVA [ $F_{(2,24)} = 8.7025$ ,  $P = 0.0042$  and  $F_{(2,24)} = 19.1536$ ,  $P < 0.0001$  for CP13- and MC1-tau respectively] followed by Student's  $t$  test,  $*P < 0.05$  vs. age-matched APP mice;  $n = 6-9$  mice/age/genotype. **(e)** Representative confocal images of CA3 hippocampal neurons immunostained for Fyn (blue) and MC1-Tau (green) revealed an aberrant accumulation and differential missorting of soluble tau species in apical dendrites of 6-month-old APP mice. Scale bar = 20  $\mu$ m.  $n = 6$  sections per animal;  $N = 6$  animals/age/genotype.

Figure 5

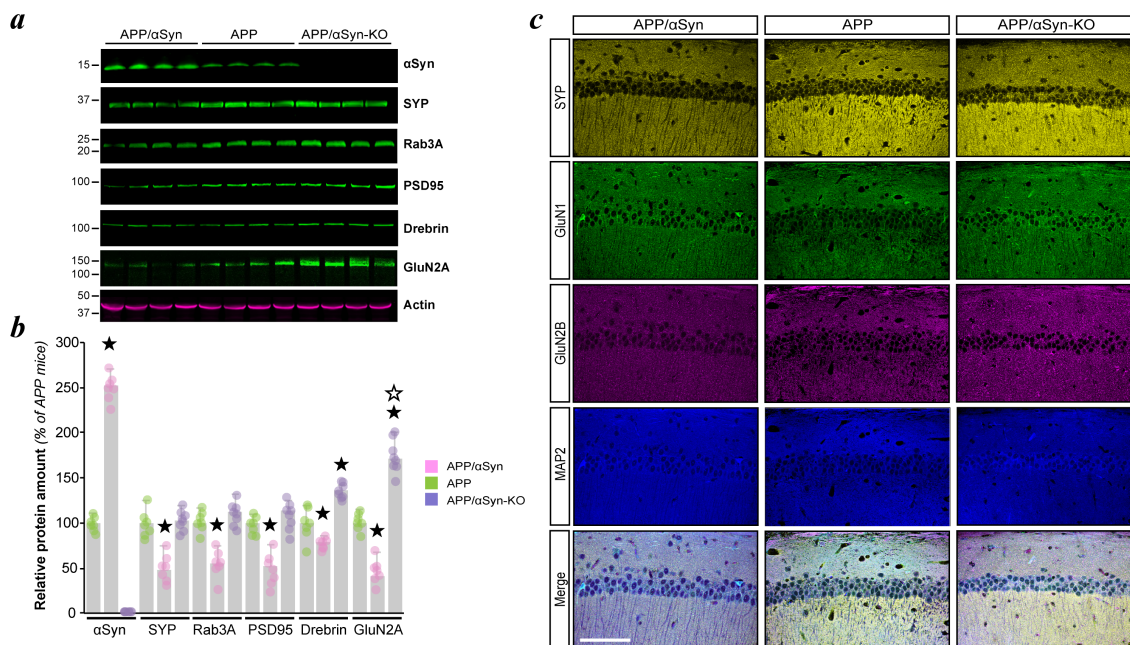


**Figure 5. Synaptic marker changes in APP/αSyn, APP and APP/αSyn-KO mice. (a,b)**

Representative Western blots (a) and quantitation (b) of pre- and postsynaptic proteins detected in membrane (MB)-enriched fractions from 6-month-old APP/αSyn, APP and APP/αSyn-KO mice.

Histograms show mean  $\pm$  S.D.; One-way ANOVA [ $F_{(2,21)}^{\alpha\text{Syn}} = 83.5965$ ,  $P < 0.0001$ ,  $F_{(2,21)}^{\text{SYP}} = 21.0623$ ,  $P < 0.0001$ ,  $F_{(2,21)}^{\text{Rab3A}} = 18.6904$ ,  $P < 0.0001$ ,  $F_{(2,21)}^{\text{PSD95}} = 29.3079$ ,  $P < 0.0001$ ,  $F_{(2,24)}^{\text{Drebrin}} = 15.1153$ ,  $P = 0.0001$  and  $F_{(2,23)}^{\text{GluN2A}} = 27.7055$ ,  $P < 0.0001$  respectively] followed by

Student's *t* test, \* $P < 0.05$  vs. age-matched APP mice, ; \* $P < 0.05$  vs. APP/αSyn mice;  $n = 6-9$

mice/group. (c) Representative confocal images of CA1 hippocampal neurons immunostained for synaptophysin (SYP, yellow), NMDA receptor subunits GluN1 (green) and GluN2B (magenta) and MAP2 (blue) revealed a marked reduction in SYP density in 6-month-old APP/αSyn mice

compared to APP or APP/ $\alpha$ Syn-KO animals. Scale bar = 20  $\mu$ m; n = 6 sections per animal; N = 6 animals/age/genotype.

**Figure 6**

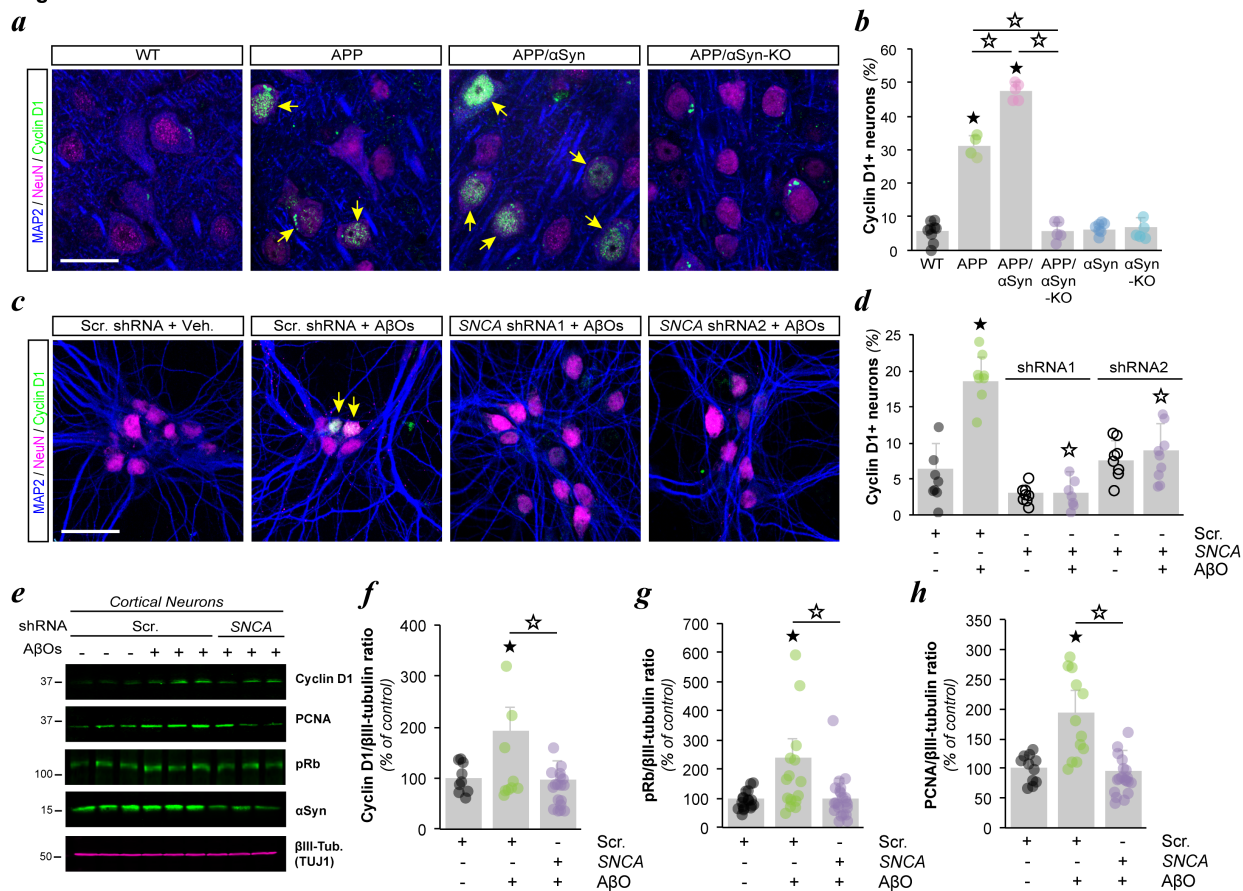


**Figure 6. Bidirectional regulation of cell cycle re-entry by  $\alpha$ Syn in APP mice and cultured**

**neurons.** (a,b) Representative confocal images (a) and quantitation (b) of cyclin D1 (green),

NeuN (magenta) and MAP2 (blue) from 6-month-old APP/ $\alpha$ Syn, APP and APP/ $\alpha$ Syn-KO mice.

Images were captured in the prefrontal cortex. Histograms show mean  $\pm$  S.D.; One-way ANOVA

[ $F_{(5,30)} = 210$ ,  $P < 0.0001$ ] followed by Student's  $t$  test, \* $P < 0.05$  vs. age-matched APP mice;  $n =$

6-9 mice/group. (c,d) Representative confocal images (a) and quantitation (b) of cyclin D1

(green), NeuN (magenta) and MAP2 (blue) from cultured primary cortical neurons exposed to 1.5

$\mu$ M A $\beta$ Os or vehicle for 24 hours. Neurons were also transfected with scrambled (Scr.) or SNCA

shRNAs (two separate shRNAs targeting  $\alpha$ Syn transcripts were used). Histograms show mean  $\pm$  S.D.; One-way ANOVA [ $F_{(5,37)} = 11.75$ ,  $P < 0.0001$ ] followed by Student's  $t$  test,  $*P < 0.05$  vs. neurons exposed to vehicle and Scr. shRNA;  $n = 8-9$  dishes/group. **(e-h)** Representative Western blots (e) and quantitation (f-h) of cell cycle markers detected in primary cortical neurons. Histograms show mean  $\pm$  S.D.; One-way ANOVA [ $F_{(2,30)} = 8.336$ ,  $P < 0.0013$ ,  $F_{(2,49)} = 4.84$ ,  $P < 0.0121$ ,  $F_{(2,35)} = 18.64$ ,  $P < 0.0001$ ] followed by Student's  $t$  test,  $*P < 0.05$  vs. age-matched APP mice;  $n = 8-9$  dishes/group.  $\alpha$ Syn shRNA 1 (TRCN000003736) and  $\alpha$ Syn shRNA 2 (TRCN0000366590) were used for **(c,d)**,  $\alpha$ Syn shRNA 1 was used for **(e-h)**.

**Figure 7**

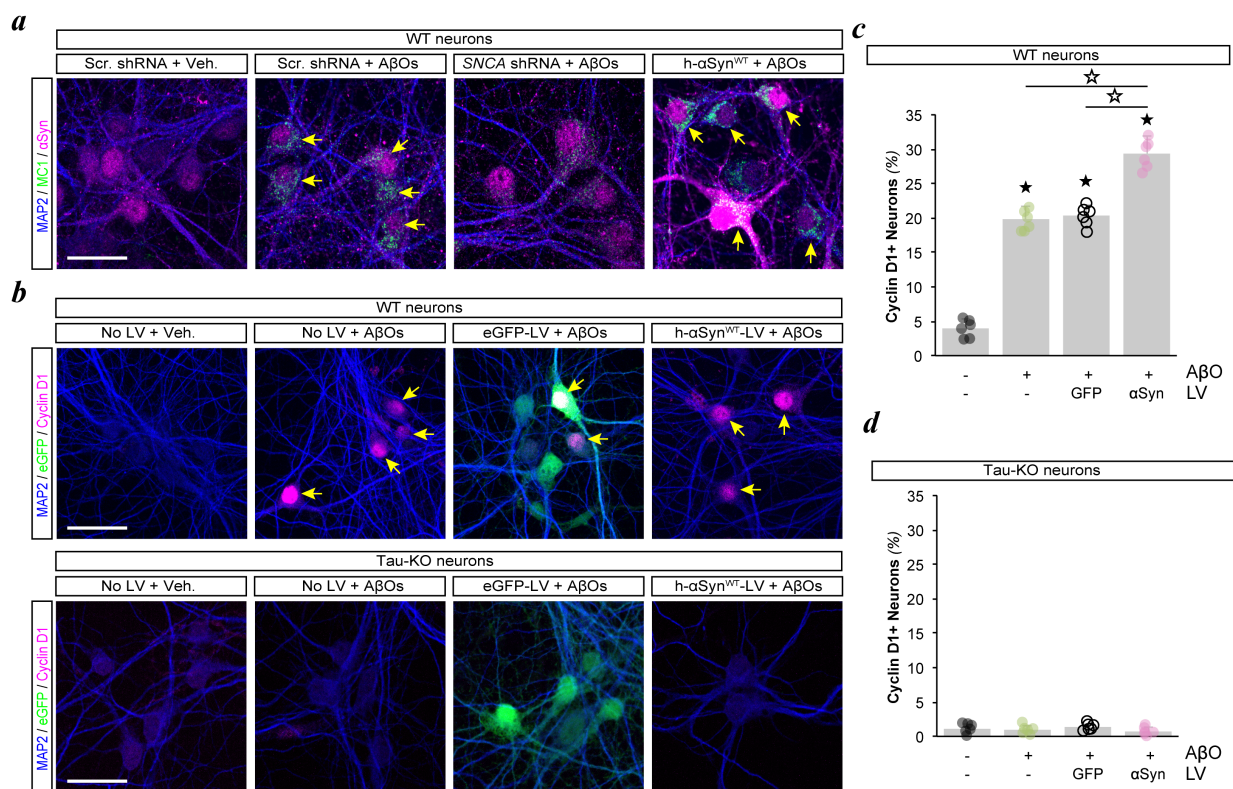


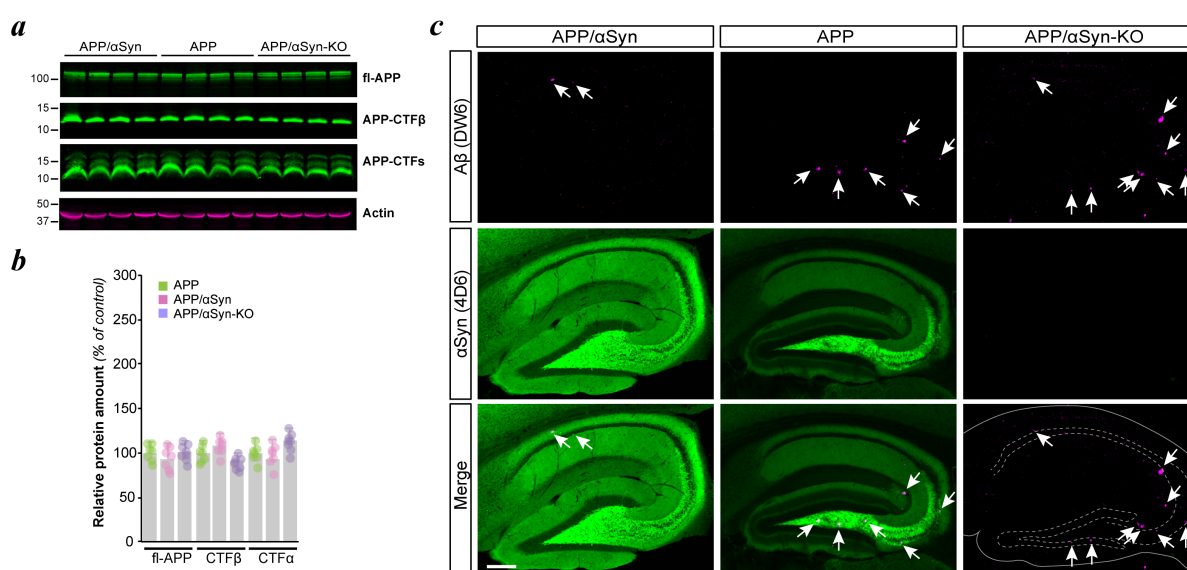
**Figure 7.  $\alpha$ Syn is required to cause A $\beta$ O-induced tau pathology in cultured neurons. (a)**

Representative confocal images of conformationally-altered tau molecules labeled with antibodies to a tau conformational variant (MC1; green),  $\alpha$ Syn (magenta) and MAP2 (blue) from wild type primary cortical neurons exposed to 1.5  $\mu$ M A $\beta$ O<sub>s</sub> or vehicle for 24 hours. Neurons were also transfected with scrambled (Scr.) or *SNCA* shRNAs. **(b)** Representative confocal images of eGFP (green), Cyclin D1 (magenta) and MAP2 (blue) from *MAPT*-null primary cortical neurons exposed to 1.5  $\mu$ M A $\beta$ O<sub>s</sub> or vehicle for 24 hours. Neurons were also transfected with lentiviruses expressing eGFP or human  $\alpha$ Syn<sup>WT</sup>. **(c,d)** Quantitation of Cyclin D1-positive neurons in wild-type (c) or *MAPT*-null (d) cortical neurons. Histograms show mean  $\pm$  S.D.; One-way ANOVA [ $F_{(7,40)} = 431.2, P < 0.0001$ ] followed by Student's *t* test,  $*P < 0.05$  vs. untransfected neurons exposed to vehicle;  $*P < 0.05$  vs. h- $\alpha$ Syn<sup>WT</sup> expressing neurons exposed to A $\beta$ O;  $n = 6$  dishes/group.

# Khan-Boyle-Lacroix et al. Supplemental

## Figures

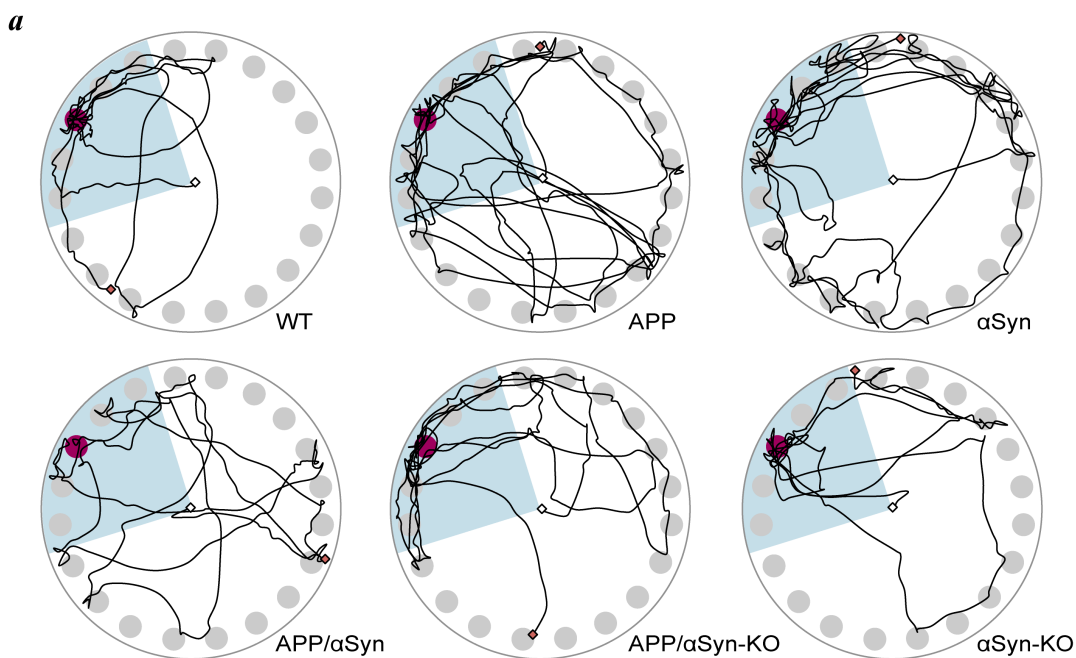
Supplementary Figure 1



**Supplementary Figure S1. Forebrain abundance of APP derivatives in APP/αSyn, APP and APP/αSyn-KO mice.** (a,b) Representative Western blots (a) and quantitation (b) of full-length APP (fl-APP), carboxyl terminal fragment beta (CTFβ) and total APP CTFs detected in membrane (MB)-enriched fractions from 6-month-old APP/αSyn, APP and APP/αSyn-KO mice. Histograms show mean ± S.D.; One-way ANOVA [ $F_{(2,18)} = 0.4849$ ,  $P = 0.6310$ ;  $F_{(2,18)} = 1.7053$ ,  $P = 0.2355$  and  $F_{(2,18)} = 1.4540$ ,  $P = 0.2837$  respectively] followed by Student's *t* test, \* $P < 0.05$  vs. age-

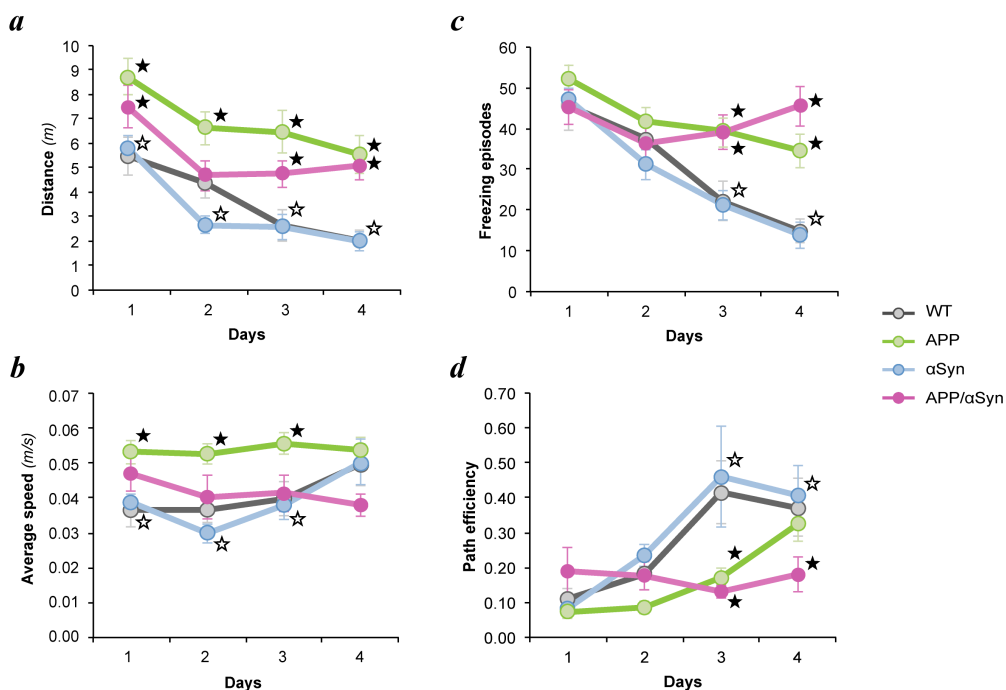
matched APP mice;  $n = 6-9$  mice/group. (c) Representative confocal images of hippocampi labeled for  $\alpha$ Syn (green; 4D6 antibody) and amyloid deposits (magenta, DW6 antibody) from 6-month-old APP/ $\alpha$ Syn, APP and APP/ $\alpha$ Syn-KO mice. Arrows indicate DW6-positive A $\beta$  deposits. Note the absence of Lewy bodies in APP/ $\alpha$ Syn mice. Scale bars = 200  $\mu$ m.

**Supplementary Figure 2**



**Supplementary Figure S2. Paths used by animals during the retention phase of the Barnes circular maze.** (a) Representative path tracings for WT, APP,  $\alpha$ Syn, APP/ $\alpha$ Syn, APP/ $\alpha$ Syn-KO and  $\alpha$ Syn-KO mice during the probe trial. White and red diamonds indicate the starting and final position of the animals during the 180 seconds of the task. The target hole and quadrant are colored in plum and blue respectively.

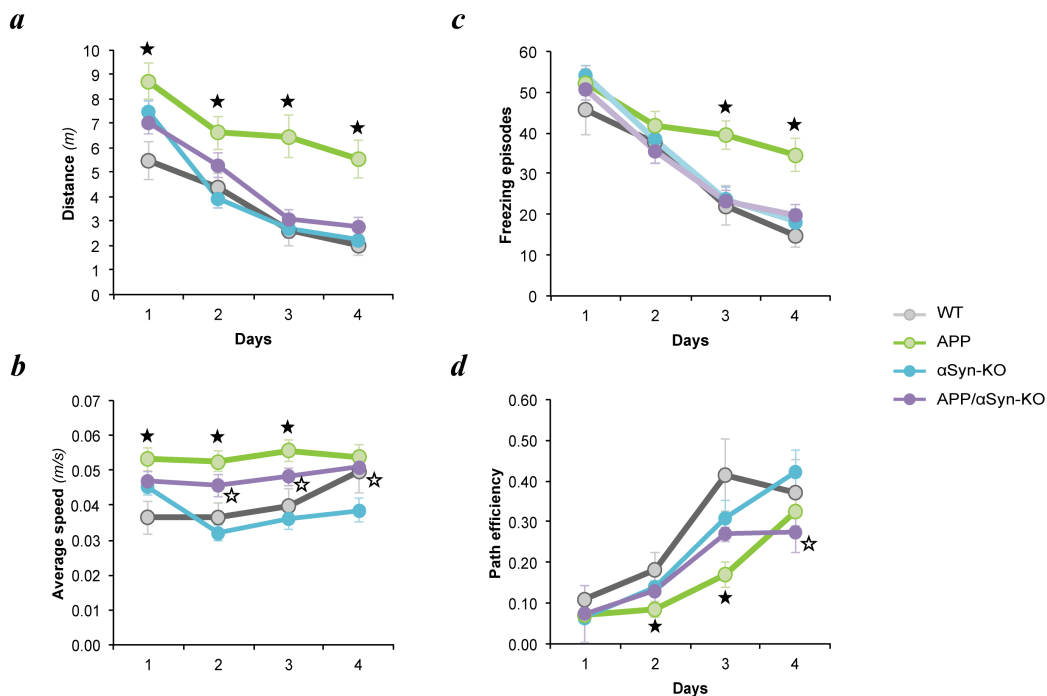
Supplementary Figure 3



**Supplementary Figure S3. Comparative behavioral analysis of 6-month-old WT, APP, αSyn and APP/αSyn mice.** (a) Distance travelled during the learning phase of the spatial task. Two-way repeated-measures ANOVA revealed a significant effect of training ( $F_{(3,540)} = 16.033$ ,  $P < 0.0001$ ), of the transgene ( $F_{(3,540)} = 33.652$ ,  $P < 0.0001$ ), but no significant day\*transgene interaction ( $F_{(9,540)} = 1.465$ ,  $P = 0.1594$ ) for all 4 groups. APP and APP/αSyn mice ran more than WT mice on 3 out of the 4 training days ( $*P < 0.05$ ). APP/αSyn mice ran more than αSyn mice on all 4 training days ( $*P < 0.05$ ). (b) Average speed displayed by the mice during the learning phase of the task. Two-way repeated-measures ANOVA revealed a significant effect of transgene ( $F_{(3,540)} = 12.544$ ,  $P < 0.0001$ ), no effect of training ( $F_{(3,540)} = 0.469$ ,  $P = 0.7040$ ), and a significant

day\*transgene interaction ( $F_{(9,540)} = 1.974, P = 0.0410$ ) for all 4 groups. APP mice were faster than WT ( $*P < 0.05$ ) and  $\alpha$ Syn ( $*P < 0.05$ ) mice on 3 out of the 4 training days. The data presented in (a) and (b) are consistent with the hyperactivity phenotype ascribed to APP animals (Cheng et al., 2007). (c) Occurrence of freezing episodes during the learning phase of the spatial task. Two-way repeated-measures ANOVA revealed a significant effect of training ( $F_{(3,540)} = 12.643, P < 0.0001$ ), of the transgene ( $F_{(3,540)} = 16.788, P < 0.0001$ ), and a significant day\*transgene interaction ( $F_{(9,540)} = 2.748, P = 0.0040$ ) for all 4 groups. APP and APP/ $\alpha$ Syn mice froze more often than WT ( $*P < 0.05$ ) and  $\alpha$ Syn ( $*P < 0.05$ ) mice during the last 2 days of the 4 training days, suggestive of enhanced anxiety. (d) Measure of path efficiency displayed by the mice during the learning phase of the task. Two-way repeated-measures ANOVA revealed a significant effect of transgene ( $F_{(3,540)} = 5.783, P = 0.0007$ ), of training ( $F_{(3,540)} = 8.627, P < 0.0001$ ), and a significant day\*transgene interaction ( $F_{(9,540)} = 2.188, P = 0.0220$ ) for all 4 groups. APP and APP/ $\alpha$ Syn mice displayed less efficient paths than WT ( $*P < 0.05$ ) and  $\alpha$ Syn ( $*P < 0.05$ ) mice on two of the four training days.

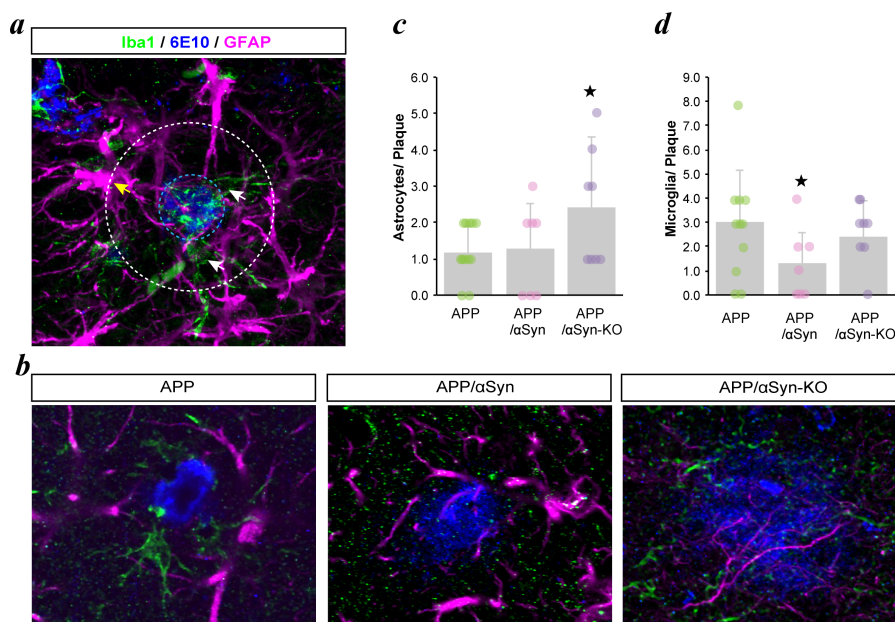
Supplementary Figure 4



**Supplementary Figure S4. Comparative behavioral analysis of 6-month-old WT, APP,  $\alpha$ Syn-KO and APP/ $\alpha$ Syn-KO mice.** (a) Distance travelled during the learning phase of the spatial task. Two-way repeated-measures ANOVA revealed a significant effect of training ( $F_{(3,544)} = 38.313$ ,  $P < 0.0001$ ), of the transgene ( $F_{(3,544)} = 29.356$ ,  $P < 0.0001$ ), and a significant day\*transgene interaction ( $F_{(9,544)} = 3.261$ ,  $P = 0.0007$ ) for all 4 groups. Only APP mice ran more than WT mice throughout the four training days ( $*P < 0.05$ ). (b) Average speed displayed by the mice during the learning phase of the task. Two-way repeated-measures ANOVA revealed a significant effect of transgene ( $F_{(3,544)} = 22.800$ ,  $P < 0.0001$ ), no effect of training ( $F_{(3,544)} = 0.288$ ,  $P = 0.8339$ ), and no significant day\*transgene interaction ( $F_{(9,544)} = 1.812$ ,  $P = 0.0634$ ) for all 4 groups. APP mice were faster than WT mice on 3 out of the 4 training days ( $*P < 0.05$ ). APP/ $\alpha$ Syn-KO were faster than

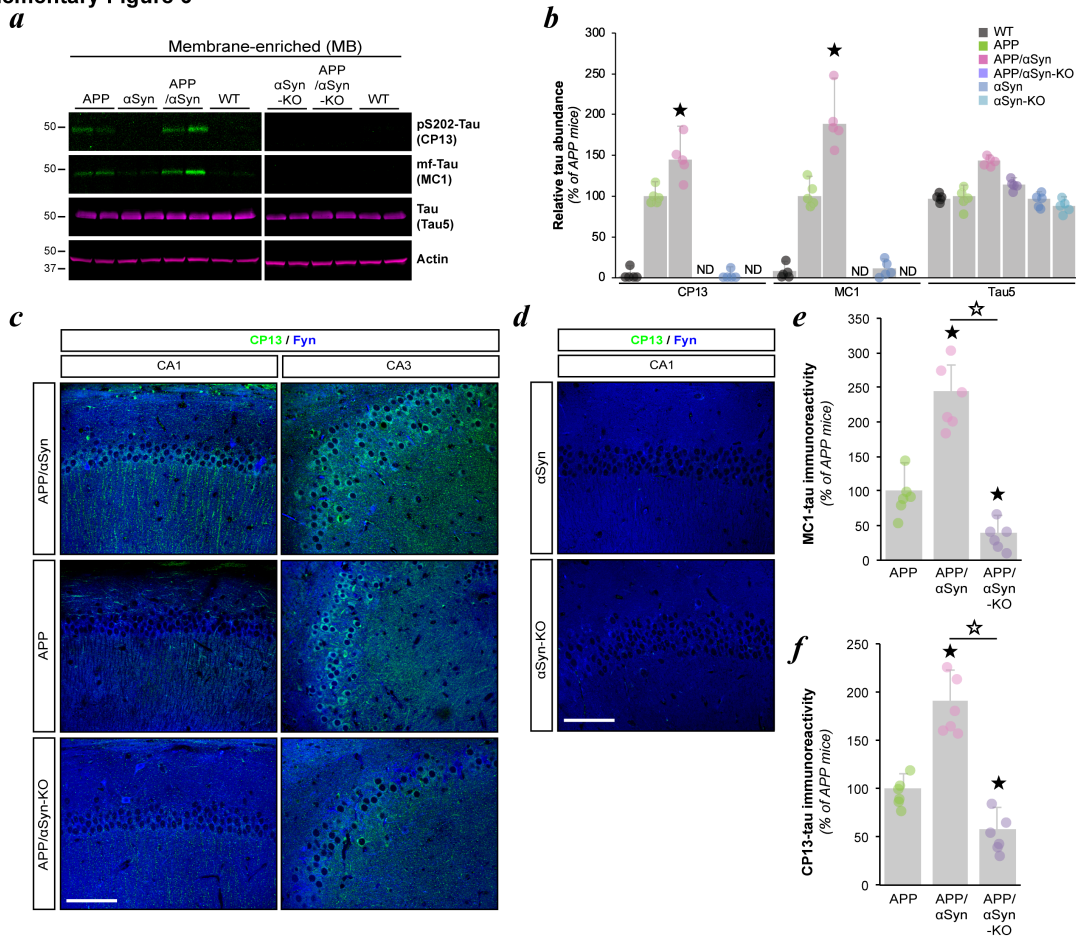
$\alpha$ Syn-KO mice on 3 out the 4 training days ( $^*P < 0.05$ ). **(c)** Occurrence of freezing episodes during the learning phase of the spatial task. Two-way repeated-measures ANOVA revealed a significant effect of training ( $F_{(3,544)} = 45.449, P < 0.0001$ ), of the transgene ( $F_{(3,544)} = 11.363, P < 0.0001$ ), and a significant day\*transgene interaction ( $F_{(9,544)} = 3.116, P = 0.0012$ ) for all four groups. Only APP mice froze more often than WT mice during the last 2 days of the 4 training days ( $^*P < 0.05$ ), suggestive of enhanced anxiety. **(d)** Measure of path efficiency displayed by the mice during the learning phase of the task. Two-way repeated-measures ANOVA revealed a significant effect of transgene ( $F_{(3,544)} = 6.768, P = 0.0002$ ), of training ( $F_{(3,544)} = 36.67,8 P < 0.0001$ ), but no significant day\*transgene interaction ( $F_{(9,544)} = 1.548, P = 0.1279$ ) for all 4 groups. APP mice ran less efficient paths than WT mice on 2 of the 4 training days ( $^*P < 0.05$ ) and APP/ $\alpha$ Syn-KO mice ran less efficient paths than  $\alpha$ Syn-KO mice on the last day of the training period ( $^*P < 0.05$ ).

Supplementary Figure 5



**Supplementary Figure S5.  $\alpha$ Syn expression alters glial density in the hippocampus of APP mice.** (a-d) Representative confocal images (a,b) and quantitation (c,d) of microglia positive to Iba1 (green), astrocytes detected with GFAP (magenta) and amyloid deposits (blue) from 6-month-old APP/ $\alpha$ Syn, APP and APP/ $\alpha$ Syn-KO mice. Z-stacks were captured in the hippocampi of all animals studied and used to perform cellular counts. Single Z-plane images are shown. Histograms show mean  $\pm$  S.D.; One-way ANOVA [ $F_{(5,24)} = 8.9792$ ,  $P = 0.0067$  and  $F_{(5,24)} = 12.2829$ ,  $P = 0.0025$  for astrocytic and microglial counts respectively] followed by Student's t test, \* $P < 0.05$  vs. age-matched APP mice;  $n = 6-9$  mice/age/genotype.

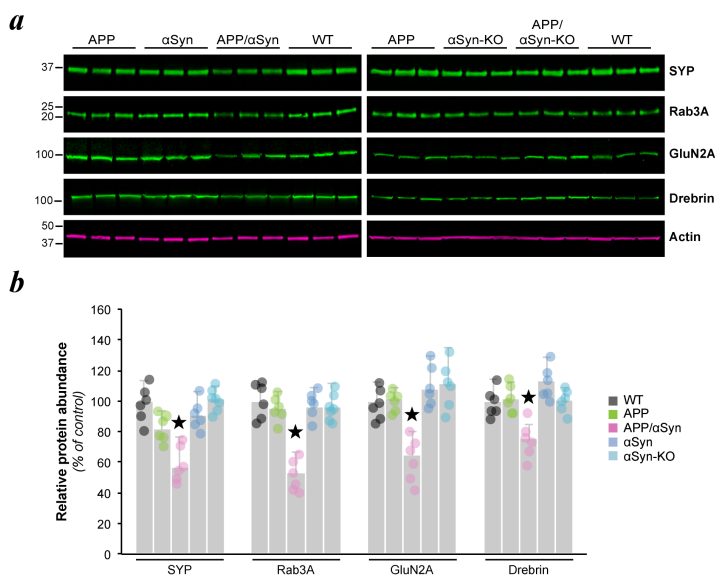
Supplementary Figure 6



**Supplementary Figure S6. Hippocampal tau pathology is bidirectionally altered by  $\alpha$ Syn expression in APP mice.** (a,b) Representative Western blots (a) and quantitation (b) of MC1- and CP13-tau detected in membrane (MB)-enriched fractions from 6-month-old mice. Histograms show mean  $\pm$  S.D.; One-way ANOVA [ $F_{(5,30)} = 17.3481$ ,  $P = 0.0026$  and  $F_{(5,30)} = 19.7232$ ,  $P < 0.0001$  respectively] followed by Student's  $t$  test,  $*P < 0.05$  vs. age-matched APP mice;  $n = 5$  mice/age/genotype. (c,d) Representative confocal images of hippocampal neurons immunostained for Fyn (blue) and pS202-Tau (CP13, green) revealed an aberrant accumulation and differential missorting of soluble tau species in somatodendritic compartments of pyramidal neurons of 6-month-old APP/ $\alpha$ Syn, APP, APP/ $\alpha$ Syn-KO (c) and  $\alpha$ Syn,  $\alpha$ Syn-KO (d) mice. Scale bars = 50  $\mu$ m. (e,f) Quantitation of MC1- (e) and CP13-tau (f) immunoreactivity in CA3

hippocampal fields. Histograms show mean  $\pm$  S.D.; One-way ANOVA [ $F_{(2,18)} = 36.2747$ ,  $P < 0.0001$  and  $F_{(2,18)} = 34.4679$ ,  $P < 0.0001$  respectively] followed by Student's  $t$  test,  $^*P < 0.05$  vs. age-matched APP mice,  $^*P < 0.05$  vs. age-matched APP/ $\alpha$ Syn mice;  $n = 6$  sections per animal;  $N = 6$  animals/age/genotype.

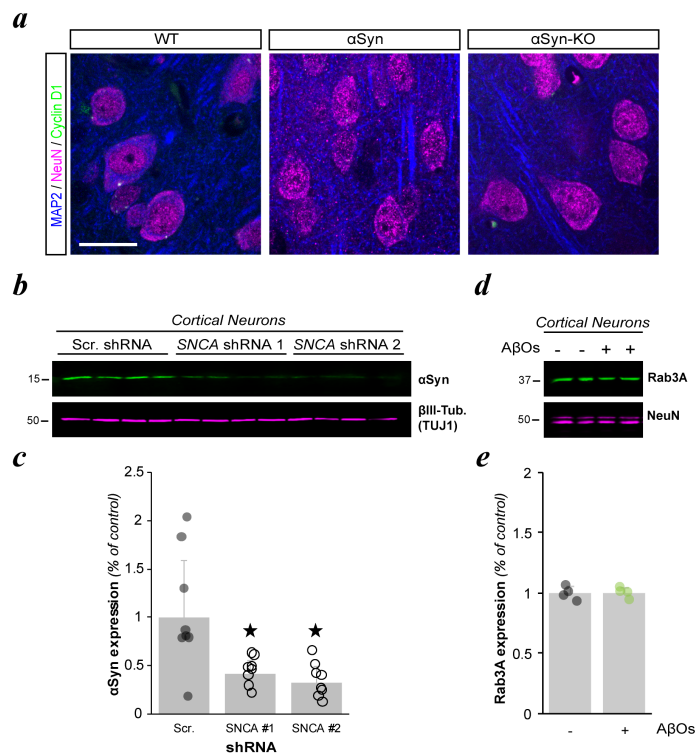
**Supplementary Figure 7**



**Supplementary Figure S7. Forebrain abundance of pre- and postsynaptic proteins in WT, APP,  $\alpha$ Syn,  $\alpha$ Syn-KO and APP/ $\alpha$ Syn mice. (a,b) Representative Western blots (a) and quantitation (b) of the presynaptic markers SYP and Rab3A, and the postsynaptic marker, GluN2A, detected in membrane (MB)-enriched fractions from 6-month-old mice. Histograms show mean  $\pm$  S.D.; One-way ANOVA [ $F_{(4,30)} = 6.6070$ ,  $P = 0.0023$ ;  $F_{(4,30)} = 11.3043$ ,  $P < 0.0001$ ;  $F_{(4,30)}$**

= 4.8234,  $P = 0.0051$  and  $F_{(4,30)} = 6.7021$ ,  $P = 0.0008$  respectively] followed by Student's  $t$  test,  $*P < 0.05$  vs. age-matched APP mice;  $n = 6$  mice/age/genotype.

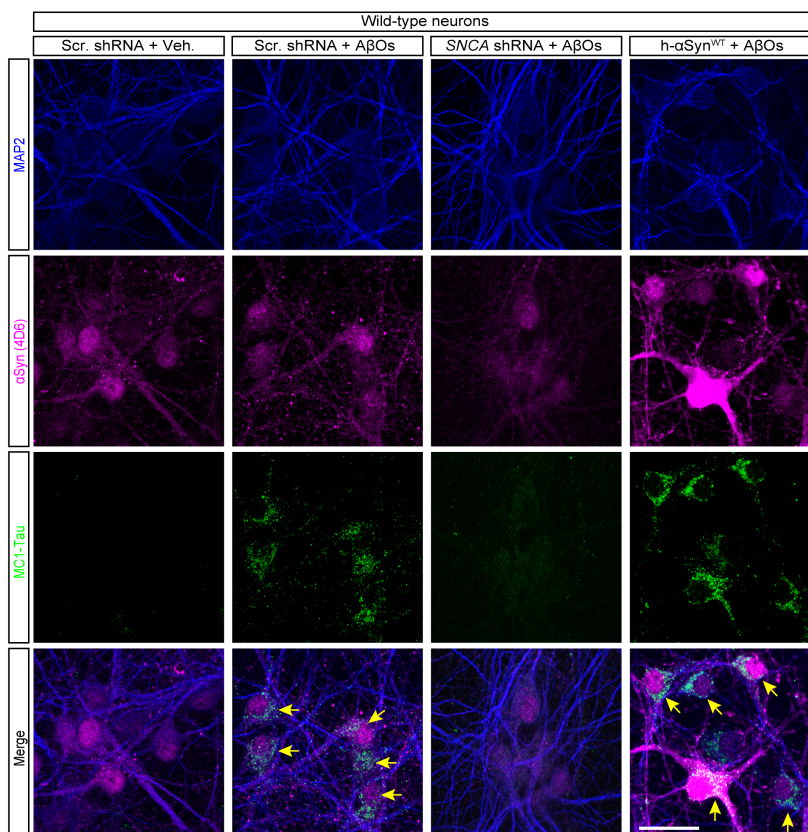
### Supplementary Figure 8



**Supplementary Figure S8. Bidirectional regulation of cell cycle re-entry by αSyn in APP mice and cultured neurons.** (a) Representative confocal images of cyclin D1 (green), NeuN (magenta) and MAP2 (blue) from 6-month-old WT, αSyn and αSyn-KO mice. Images were captured from the prefrontal cortex. (b,c) Representative Western blots (b) and quantitation (c) of αSyn and βIII-tubulin detected in lysates from primary cortical neurons. Histograms show mean ± S.D.; One-way ANOVA [ $F_{(2,18)} = 27.84$ ,  $P < 0.0001$ ] followed by Student's  $t$  test,  $*P < 0.05$  vs. neurons expressing the scrambled shRNA;  $n = 8-9$  dishes/group. (d,e) Representative Western

blots (d) and quantitation (e) of Rab3A and NeuN detected in lysates from primary cortical neurons exposed to 1.5  $\mu\text{M}$  A $\beta$ O or vehicle for 24 hours. Histograms show mean  $\pm$  S.D.; *t* test, \**P* < 0.05 vs. vehicle-treated neurons; *n* = 4 dishes/group.

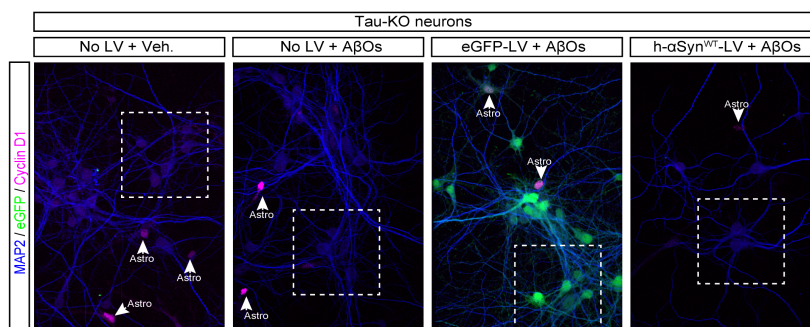
Supplementary Figure 9



**Supplementary Figure S9. Tau pathology is bidirectionally altered by  $\alpha\text{Syn}$  expression in cultured neurons exposed to A $\beta$ O.**

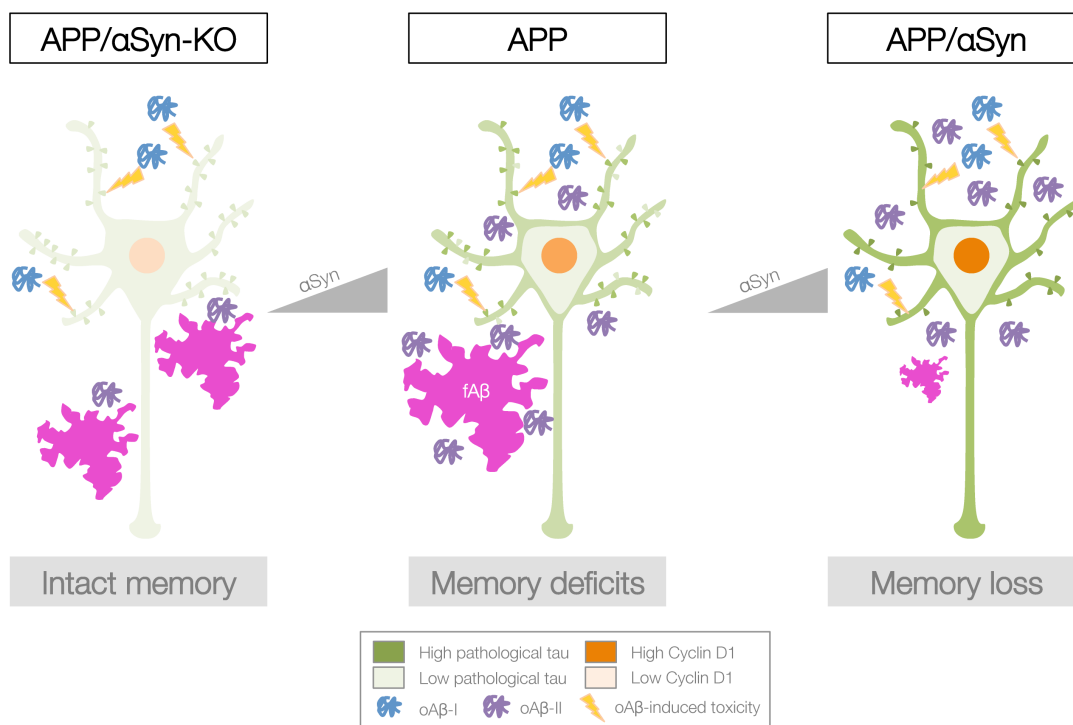
(a) Representative confocal images of primary cortical neurons immunostained for MAP2 (blue), conformationally altered tau (MC1, green) and  $\alpha\text{Syn}$  (4D6, magenta) revealed an aberrant accumulation of soluble tau conformers in somatodendritic compartments of cultured neurons treated with 1.5  $\mu\text{M}$  A $\beta$ O or vehicle for 24 hours. Scale bars = 20  $\mu\text{m}$ ; *n* = 9 dishes/group.

## Supplementary Figure 10



**Supplementary Figure S10. Ablation of MAPT inhibits Cyclin D1 expression in cultured neurons exposed to A $\beta$ O<sub>s</sub>.** Representative wide-field confocal images of primary cortical neurons immunostained for MAP2 (blue) and Cyclin D1 (magenta) revealed the absence of immunoreactivity for Cyclin D1 in tau KO neurons. Only astrocytes (white arrowheads) readily expressed Cyclin D1 in these cultures. Dashed squares correspond to the fields of view shown in Fig. 7.

Supplementary Figure 11



### Supplementary Figure S11. Proposed model of the role of alpha-synuclein in APP

**transgenic mice.** In young APP mice, synaptic and cognitive deficits are caused by soluble Aβ oligomers, including soluble non-fibrillar type-I (AβO-I, blue) and prefibrillar type II (AβO-II, purple). AβO-II are mostly sequestered in the vicinity of amyloid plaques formed of fibrillar Aβ (fAβ), while AβO-I are more abundant away from deposits. Tau pathology (green) is subtle and restricted to local changes in dendrites and axons. Cyclin D1 (orange) expression is readily detectable in a large subset of neurons. In young APP/αSyn mice, amyloid burden is reduced thereby preventing the sequestration of AβO-II assemblies, which exacerbate tau pathology and cyclin D1 expression in neurons. These deleterious changes translate into greater cognitive impairment. In young APP/αSyn-KO mice, amyloid deposition is enhanced at the expense of

soluble A $\beta$ Os resulting in reduced tau pathology, cyclin D1 expression and improved memory function.

## Khan-Boyle-Lacroix et al. Discussion

Our findings reveal a multifaceted role for  $\alpha$ Syn in modulating central components of the phenotype defining AD mouse models and introduce several important implications. While overexpression of human  $\alpha$ Syn<sup>WT</sup> had no impact on animal mortality in APP mice, *SNCA* gene deletion abolished the premature death phenotype seen in APP animals. This surprising result is reminiscent of the protection conferred by deletion of the *MAPT* gene encoding for tau in APP mice (Roberson et al., 2007). Like tau elimination (Roberson et al., 2007; Hoover et al., 2010; Ittner et al., 2010),  $\alpha$ Syn elimination in AD model mice rescued cognitive and synaptic deficits, highlighting a central role for  $\alpha$ Syn in AD pathophysiology.

Previous studies have reported conflicting results about the effect of  $\alpha$ Syn expression on A $\beta$  deposition in mice (Kallhoff et al., 2007; Clinton et al., 2010; Bachhuber et al., 2015; Spencer et al., 2016). Under conditions where mutant human  $\alpha$ Syn<sup>A30P</sup> or  $\alpha$ Syn<sup>A53T</sup> is overexpressed in APP transgenic mice, amyloid plaque burden was either reduced (Bachhuber et al., 2015) or increased (Clinton et al., 2010) respectively. Under conditions where *SNCA* is ablated, amyloid plaque load was either increased (Kallhoff et al., 2007) or unchanged (Spencer et al., 2016). Although the use of different APP transgenic lines across these studies potentially impacted the outcomes, it is unlikely that this factor alone was responsible for the opposing findings observed, and thus, the role of  $\alpha$ Syn on A $\beta$  deposition remained uncertain. Consequently, the relationship between amyloid burden changes mediated by  $\alpha$ Syn and other symptoms, such as behavioral deficits, when reported, were also unclear. Here we found that modest overexpression of

human  $\alpha$ Syn<sup>WT</sup> in APP mice resulted in decreased A $\beta$  deposition and exacerbated memory deficits in the Barnes circular maze. Overexpression of human  $\alpha$ Syn<sup>WT</sup> in APP mice also led to higher amounts of extracellular soluble A $\beta$  oligomers. By contrast, and in spite of an increase in A $\beta$  plaque load, spatial memory impairment was dramatically improved in 6-month-old APP mice whose *SNCA* gene was deleted. Moreover, this functional rescue was associated with decreased amounts of extracellular A $\beta$ Os in APP/ $\alpha$ Syn-KO forebrains. These findings support earlier observations that increased A $\beta$  fibril formation, and subsequent lowering of A $\beta$  oligomers, reduce functional deficits in APP mice (Cheng et al., 2007).

While in a different context, parallels could be drawn between our results and the findings reported from the Elan AN-1792 human clinical trials, where subjects were immunized with an adjuvanted formulation of synthetic A $\beta$ <sub>1-42</sub> peptide with the goal to reduce amyloid burden (Nicoll et al., 2003; Holmes et al., 2008; Vellas et al., 2009). Similarly to our APP/ $\alpha$ Syn mice, human subjects had a substantial reduction in plaque load, but their cognitive abilities did not improve, and instead, either remained stable or worsened over time. The results of the Elan AN-1792 trial were instrumental to the then budding assertion that soluble A $\beta$  assemblies are far more responsible than large, insoluble A $\beta$  deposits (i.e. amyloid plaques) for the cognitive deficits observed in AD. Taken together, our work may resolve the debate surrounding the impact of  $\alpha$ Syn on the AD phenotype of APP transgenic mice, and implicates  $\alpha$ Syn as a bidirectional modulator of A $\beta$  solubility and aggregation as well as A $\beta$ -induced cognitive deficits.

Beyond this controversy, our work also expands upon a very recent report that  $\alpha$ Syn ablation rescues neurodegeneration, and learning and synaptic deficits in the mThy1-

APP<sub>751</sub> AD model mice (Spencer et al., 2016). At first glance, the protective effects provided by  $\alpha$ Syn ablation by Spencer and colleagues appear in agreement with our observations, but notable differences exist between both studies. For instance, in contrast to the rescue of A $\beta$ -induced Rab3 depletion observed in mThy1-APP<sub>751</sub>/ $\alpha$ Syn-KO mice and in primary neurons, we found no difference in Rab3A following  $\alpha$ Syn ablation *in vivo* and *in vitro*. Instead, forebrain Rab3A protein amounts were lowered by half following  $\alpha$ Syn overexpression in APP mice. These results are consistent with earlier work demonstrating that neither  $\alpha$ Syn<sup>WT</sup> overexpression nor  $\alpha$ Syn ablation alters Rab3A protein abundance in mouse synaptosomes. It is also worth reiterating that the studies performed in mThy1-APP<sub>751</sub> mice did not report a change in amyloid burden caused by  $\alpha$ Syn ablation in contrast to the present study in which amyloid burden was elevated in APP/ $\alpha$ Syn-KO, in agreement with an earlier report performed in Tg2576 mice (Kallhoff et al., 2007).

There is substantial evidence to support a role for tau in mediating A $\beta$ -induced toxicity (Rapoport et al., 2002; Roberson et al., 2007; Ittner et al., 2010; Jin et al., 2011; Nussbaum et al., 2012; Larson et al., 2012b; Seward et al., 2013; Bloom, 2014; Sherman et al., 2016; Amar et al., 2017). We therefore assessed whether overexpression or deletion of  $\alpha$ Syn affects tau pathological changes caused by A $\beta$  *in vivo* and *in vitro*. Unexpectedly, we found little difference across APP, APP/ $\alpha$ Syn and APP/ $\alpha$ Syn-KO mice, except for two early markers of tau pathology, CP13 and MC1. The accumulation of pS202-Tau and misfolded Tau in membrane-enriched lysates from  $\alpha$ Syn-overexpressing APP mice is notable because it is consistent with the aberrant missorting of tau to the postsynaptic site (Amar et al., 2017) and subsequent synaptic dysfunction (Hoover et al.,

2010; Ittner and Götz, 2011). Confocal imaging of both pathological tau forms confirmed prominent dendritic labeling of pyramidal neurons in the hippocampi from APP/ $\alpha$ Syn compared to APP littermates. However, only conformationally altered tau molecules reactive with MC1 were bidirectionally controlled by  $\alpha$ Syn. Previous studies have described interactions between  $\alpha$ Syn and tau at multiple levels. At a genetic level, genome-wide association studies reported linkages between the genes encoding for tau and  $\alpha$ Syn, and PD pathogenesis (Simón-Sánchez et al., 2009). At a cellular level, insoluble  $\alpha$ Syn and tau proteins co-exist in DLB cases (Iseki et al., 2003; Colom-Cadena et al., 2013) and recent evidence suggests that  $\alpha$ Syn oligomers and tau oligomers, defined by their respective conformationally altered states, co-occur in brains from PD and LBD patients (Sengupta et al., 2015). At a molecular level, fibrillar and oligomeric  $\alpha$ Syn are capable of inducing tau phosphorylation, tau oligomerization and tangles formation *in vitro* (Lasagna-Reeves et al., 2010; Waxman and Giasson, 2011). Moreover, different strains of fibrillar  $\alpha$ Syn seeds were identified to cause tau aggregation *in vivo* and *in vitro* (Guo et al., 2013). Based on these observations, it is worth considering the possibility that  $\alpha$ Syn regulates or stabilizes the misfolded state of tau, or vice versa. Considering the rapid accumulation of evidence linking  $\alpha$ Syn to tau, future studies will be required to decipher the mechanistic and functional details of this molecular interaction in greater detail.

By analyzing both pre-synaptic and post-synaptic proteins, we identified a novel bidirectional modulatory role of  $\alpha$ Syn on GluN2A, a unique feature of our study. The measurements of SYP protein abundance in the forebrain of APP/ $\alpha$ Syn recapitulated the original findings observed in Thy1-APP<sup>PS1</sup>/ $\alpha$ Syn<sup>A30P</sup> animals reported by Bachhuber and

coworkers (Bachhuber et al., 2015), suggesting that overexpression of both wild-type and mutant  $\alpha$ Syn exacerbate pre-synaptic injury in APP mice. Our studies further expand this interpretation to additional pre-synaptic and post-synaptic proteins, including Rab3A, PSD95, Drebrin and GluN2A, indicating a generalized alteration of synaptic elements. Surprisingly, the relative protein abundance of SYP and PSD95, two central molecules defining pre-synaptic and post-synaptic terminals, was indistinguishable between APP and APP/ $\alpha$ Syn-KO mice. However, the protein abundance of GluN2A and Drebrin detected in forebrain tissues from APP/ $\alpha$ Syn-KO mice surpassed that measured in APP mice, thereby providing a molecular insight for the behavioral rescue observed in these animals. Indeed, the bidirectional effect of  $\alpha$ Syn on both postsynaptic proteins is consistent with  $\alpha$ Syn-induced modulation of memory deficits observed in APP transgenic mice. Although these changes merit further evaluation, the effects of  $\alpha$ Syn ablation on GluN2A and the NMDAR anchor, Drebrin, are compelling considering that both postsynaptic proteins are implicated in brain executive function and synaptic plasticity (Ivanov et al., 2009; Kannangara et al., 2015). Loss of the F-actin binding Drebrin has long been associated with memory impairment (Counts et al., 2012) and AD (Harigaya et al., 1996; Hatanpää et al., 1999). Because Drebrin is a key regulator of dendritic spine morphogenesis (Shirao and González-Billault, 2013; Jung et al., 2015), increased Drebrin may contribute to the protective effects on memory retention in APP/ $\alpha$ Syn-KO mice by expanding spine size and receptor integration at the postsynaptic membrane. The identification of the exact mechanism by which Drebrin and GluN2A are modulated by  $\alpha$ Syn will require additional studies but we speculate it could involve degradation or potentially transcriptional regulation since  $\alpha$ Syn has been shown to affect both gene

transcription and protein degradation(Cuervo et al., 2004; Larson et al., 2017).

In addition to synaptic and tau alterations, we also made the novel observation that  $\alpha$ Syn expression is required for A $\beta$ O-induced neuronal CCR. In line with our *in vivo* behavioral and synaptic protein results,  $\alpha$ Syn<sup>WT</sup> overexpression in APP transgenic mice and in cultured neurons exposed to A $\beta$ O<sub>s</sub> exacerbated neuronal CCR. Overexpression alone, as in the human transgenic  $\alpha$ Syn parental line, was not sufficient to induce neuronal CCR in 6-month old mice, suggesting that the phenotype in APP/ $\alpha$ Syn mice is the product of synergism between A $\beta$ O<sub>s</sub> and  $\alpha$ Syn. We also found that genetic ablation of  $\alpha$ Syn, or  $\alpha$ Syn lentiviral knockdown using RNA interference, lowered or prevented A $\beta$ O-induced CCR in cultured neurons. Our findings thus suggest that  $\alpha$ Syn is necessary, but not sufficient to induce ectopic CCR *in vivo* and *in vitro*. Unlike our observations in wild type neurons, when we tested for enhancement of A $\beta$ O-induced CCR by  $\alpha$ Syn in tau null neurons, we found that  $\alpha$ Syn<sup>WT</sup> overexpression, in combination with A $\beta$ O exposure, did not promote neuronal CCR. Our results also indicate that  $\alpha$ Syn and tau somehow work coordinately to modulate neuronal CCR. Taken together, these findings therefore imply that  $\alpha$ Syn-mediated CCR constitutes a key feature of AD, and possibly to other  $\alpha$ synucleinopathies in which neuronal CCR has been detected (Jordan-Sciutto et al., 2003; Höglinger et al., 2007; Stone et al., 2011). Additionally, it is tempting to speculate that  $\alpha$ Syn oligomers represent a trigger of neuronal CCR in PD, but further studies will be needed to test this hypothesis.

In conclusion, the findings reported here highlight an underappreciated and multifaceted role of  $\alpha$ Syn in AD pathogenesis. Considering the bidirectional effects of  $\alpha$ Syn on both A $\beta$  and tau, targeting  $\alpha$ Syn in AD may prove a viable therapeutic strategy.

## **Chapter 3: Future Directions**

## Future Directions

My results in conjunction with work from the Lesné lab show that  $\alpha$ Syn modulates the AD phenotype in several ways: by (1) decreasing amyloid deposition and inversely worsening memory retention of APP mice, (2) increasing soluble extracellular A $\beta$  oligomers and fibrils, (3) promoting MC1- and CP13-tau production, (4) depleting synaptic protein levels of GlutN2A and Drebrin, and (5) promoting tau-dependent ectopic neuronal cell cycle re-entry by A $\beta$ Os. Each modulation by  $\alpha$ Syn represents a novel observation, and therefore functional links among each observation should be extrapolated in future studies. This section will offer future potential experimental directions for each of the primary findings.

This study chose to focus on the effects of bidirectional  $\alpha$ Syn expression in APPJ20 mice to determine the effects of  $\alpha$ Syn on behavior. The results could be considered counterintuitive because there was a commensurate decrease in amyloid deposition despite a worsening in Barnes maze performance of the APPJ20/ $\alpha$ Syn bigenic mice. A follow-up study should determine if these observations hold true in other strains of mutant APP mice, such as the Tg2576. The Tg2576 mice would be particularly worthwhile to characterize under this context because, consistent with our reported observations, an increase in amyloid deposition was observed in these mice when they were crossbred to  $\alpha$ Syn KO mice (Kallhoff et al., 2007). Conversely, it would also be interesting to determine if targeting tau or cell cycle regulators in the bigenic mice would also ameliorate behavioral symptoms. For instance, would conditional KO of cyclin D1 in neurons prevent a decline in Barnes maze performance in APP mice? Alternatively, would passive immunization

against MC1-tau in APPJ20 mice have a similar effect to  $\alpha$ Syn ablation?

The Lesné lab results identify an increase in extracellular A $\beta$ O and A $\beta$  fibrils by dot blot analysis, despite no difference in APP production or cleavage. Additionally, the increase in A $\beta$  was likely not the result of a direct interaction between  $\alpha$ Syn and A $\beta$ , based on the co-immunoprecipitation data. How then does  $\alpha$ Syn promote an increase in A $\beta$  oligomerization? One possible explanation would be through a modulation of the inflammatory response. Indeed, we demonstrate altered behavior of GFAP astrocytes and Iba1-microglia near amyloid plaques. The change in the inflammatory response could result in an increased production of cytokines that may promote Amyloid- $\beta$  oligomerization. Conversely, the results here do not exclude the possibility of a potential feedback loop between Amyloid- $\beta$  and tau (Bloom, 2014). To rule out this possibility, it would be worthwhile to perform a dot blot experiment comparing the APPJ20 parental strain to bigenic mice where tau is genetically ablated. According to the amyloid cascade hypothesis of AD, under these conditions the production of extracellular Amyloid- $\beta$  should remain the same between APPJ20 and APPJ20/Tau-KO mice.

The results we observed of  $\alpha$ Syn on tau phosphorylation and conformation are perhaps the most perplexing. For instance,  $\alpha$ Syn bi-directionally modulates immunoreactivity against MC1-tau, an epitope that recognizes an early conformational change in tau that is elevated in AD pathology. However, no differences were detected in tau phosphorylated at serine 409 (PG5), serine 202/205 (AT8), or serine 396/404 (PHF1). Hence, the data imply that a specific conformational change in tau, MC1-reactivity, is primarily responsible for synaptic dysfunction in APPJ20 mice and in A $\beta$ O-treated primary cortical neurons. However, the results presented here do not exclude the possibility that

other, transient tau phosphorylation events precede MC1 reactivity, and may be necessary for subsequent tau neurotoxicity. Therefore, future studies should determine if phosphorylation at specific sites, for instance, serine 416, tyrosine 18, or serine 262, are necessary for the production of MC1-tau. This could be accomplished by quantifying immunofluorescent detection of MC1-tau in A $\beta$ O-treated primary neuronal cultures from tau-KO mice, following viral expression of human phospho-null tau constructs.

Overexpression of  $\alpha$ Syn resulted in a significant depletion of SYP, Rab3A, PSD95, Drebrin, and GluN2A. Intriguingly,  $\alpha$ Syn-KO specifically restored expression levels of Drebrin and GluN2A. Future experiments should more thoroughly characterize changes at synapses. For instance, immunofluorescent characterization of dendritic spines or presynaptic boutons would help to determine if the depletion of synaptic protein expression levels observed in this study result in synapse loss. Additionally, since both Drebrin and GluN2A are associated with NMDA receptors (see Discussion), another possible area of future study would be to determine the distribution of synaptic and extra-synaptic NMDA receptors across the different bigenic mice. Since extra-synaptic NMDA receptors are postulated to contribute to synaptotoxicity in AD, it is hypothesized that extra-synaptic NMDA would be elevated in APPJ20/ $\alpha$ Syn mice, and reduced in APP/ $\alpha$ Syn-KOs, relative to the APPJ20 parental strain.

Finally, my results show that  $\alpha$ Syn bi-directionally alters a mechanism that precludes neuronal death in AD, ectopic neuronal cell cycle re-entry (CCR). The enhancement of CCR by  $\alpha$ Syn in bigenic mice appeared to reflect synergism between  $\alpha$ Syn and A $\beta$ , since no CCR was detected in the parental I2.2 WT  $\alpha$ Syn overexpression mice. Interestingly, the modulatory effect of  $\alpha$ Syn was only present in neurons expressing endogenous tau;

when  $\alpha$ Syn was overexpressed in tau-KO neurons, no enhancement in CCR was observed, even when overexpression was combined with A $\beta$ O exposure. Therefore, these results suggest that the bi-directional modulation of CCR by  $\alpha$ Syn cannot circumvent an interaction between A $\beta$ O and tau. Future studies should expand upon these observations, by investigating the relationship between  $\alpha$ Syn and tau. While we did not test for a direct interaction,  $\alpha$ Syn and tau binding has been previously reported (Jensen et al., 1999). Thus, perhaps a direct interaction between  $\alpha$ Syn and tau is required for the induction of CCR by A $\beta$ O. Conversely, the link between CCR and synaptic protein loss is currently unclear. Future studies should therefore determine if cell cycle inhibition would prevent A $\beta$ O-induced depletion of either GlutN2A or Drebrin.

In summary, the results presented in this thesis offer novel insights into  $\alpha$ Syn pathophysiology, specifically in the context of AD. Potential avenues for further investigation offer a greater understanding of neuronal dysfunction in AD and establish  $\alpha$ Syn as an essential component of the deleterious amyloid-cascade. Given that  $\alpha$ Syn pathophysiology is frequently observed in other neurodegenerative disorders, these results, in combination with subsequent studies in the context of those synucleinopathies, may also provide further insight into the many causes of synaptic dysfunction and neuronal loss in the brain.

## **Chapter 4: References**

## References

- Aarsland D, Andersen K, Larsen JP, Lolk A (2003) Prevalence and Characteristics of Dementia in Parkinson Disease. *Arch Neurol* 60:387–392.
- Abeliovich A, Schmitz Y, Fariñas I, Choi-Lundberg D, Ho WH, Castillo PE, Shinsky N, Verdugo JM, Armanini M, Ryan A, Hynes M, Phillips H, Sulzer D, Rosenthal A (2000) Mice lacking alpha-synuclein display functional deficits in the nigrostriatal dopamine system. *Neuron* 25:239–252.
- Adamowicz DH, Roy S, Salmon DP, Galasko DR, Hansen LA, Masliah E, Gage FH (2017) Hippocampal  $\alpha$ -Synuclein in Dementia with Lewy Bodies Contributes to Memory Impairment and Is Consistent with Spread of Pathology. *J Neurosci* 37:1675–1684.
- Ahn TB, Kim SY, Kim JY, Park SS, Lee DS, Min HJ, Kim YK, Kim SE, Kim J-M, Kim H-J, Cho J, Jeon BS (2008) alpha-Synuclein gene duplication is present in sporadic Parkinson disease. *Neurology* 70:43–49.
- Allsop D, Landon M, Kidd M (1983) The isolation and amino acid composition of senile plaque core protein. *Brain Research* 259:348–352.
- Amar F, Sherman MA, Rush T, Larson M, Boyle G, Chang L, Götz J, Buisson A, Lesné SE (2017) The amyloid- $\beta$  oligomer A $\beta$ \*56 induces specific alterations in neuronal signaling that lead to tau phosphorylation and aggregation. *Science Signaling* 10:eaal2021.

Arendt T (2012) Cell Cycle Activation and Aneuploid Neurons in Alzheimer's Disease.

Mol Neurobiol 46:125–135.

Arendt T, Brückner MK, Mosch B, Lösche A (2010) Selective cell death of hyperploid neurons in Alzheimer's disease. The American Journal of Pathology 177:15–20

Available at:

<http://www.pubmedcentral.nih.gov/articlerender.fcgi?artid=2893646&tool=pmcentrez&rendertype=abstract>.

Bachhuber T, Katzmarski N, McCarter JF, Loreth D, Tahirovic S, Kamp F, Abou-Ajram C, Nuscher B, Serrano-Pozo A, Müller A, Prinz M, Steiner H, Hyman BT, Haass C, Meyer-Luehmann M (2015) Inhibition of amyloid- $\beta$  plaque formation by  $\alpha$ -synuclein. Nature Medicine 21:802–807.

Bartels T, Choi JG, Selkoe DJ (2011)  $\alpha$ -Synuclein occurs physiologically as a helically folded tetramer that resists aggregation. Nature 477:107–110.

Bendor JT, Logan TP, Edwards RH (2013) The function of  $\alpha$ -synuclein. Neuron 79:1044–1066.

Bertini I, Gupta YK, Luchinat C, Parigi G, Peana M, Sgheri L, Yuan J (2007)

Paramagnetism-based NMR restraints provide maximum allowed probabilities for the different conformations of partially independent protein domains. J Am Chem Soc 129:12786–12794.

Bhaskar K, Maphis N, Xu G, Varvel NH, Kokiko-Cochran ON, Weick JP, Staugaitis SM, Cardona A, Ransohoff RM, Herrup K, Lamb BT (2014) Microglial derived tumor

necrosis factor- $\alpha$  drives Alzheimer's disease-related neuronal cell cycle events. *Neurobiology of Disease* 62:273–285.

Bhaskar K, Miller M, Chludzinski A, Herrup K, Zagorski M, Lamb BT (2009) The PI3K-Akt-mTOR pathway regulates A $\beta$  oligomer induced neuronal cell cycle events. *Mol Neurodegeneration* 4:14–18.

Blessed G, Tomlinson BE, Roth M (1968) The association between quantitative measures of dementia and of senile change in the cerebral grey matter of elderly subjects. *Br J Psychiatry* 114:797–811.

Bloom GS (2014) Amyloid- $\beta$  and tau: the trigger and bullet in Alzheimer disease pathogenesis. *JAMA Neurol* 71:505–508.

Braak H, Braak E (1991) Neuropathological staging of Alzheimer-related changes. *Acta Neuropathol* 82:239–259 Available at: <http://link.springer.com/10.1007/BF00308809>.

Burré J, Sharma M, Südhof TC (2012) Systematic mutagenesis of  $\alpha$ -synuclein reveals distinct sequence requirements for physiological and pathological activities. *J Neurosci* 32:15227–15242.

Burré J, Sharma M, Südhof TC (2014)  $\alpha$ -Synuclein assembles into higher-order multimers upon membrane binding to promote SNARE complex formation. *Proc Natl Acad Sci USA* 111:E4274–E4283.

- Burré J, Sharma M, Südhof TC (2015) Definition of a molecular pathway mediating  $\alpha$ -synuclein neurotoxicity. *J Neurosci* 35:5221–5232.
- Burré J, Sharma M, Tsetsenis T, Buchman V, Etherton MR, Südhof TC (2010) Alpha-synuclein promotes SNARE-complex assembly in vivo and in vitro. *Science* 329:1663–1667.
- Bussell R, Eliezer D (2003) A structural and functional role for 11-mer repeats in alpha-synuclein and other exchangeable lipid binding proteins. *Journal of Molecular Biology* 329:763–778.
- Bussell R, Ramlall TF, Eliezer D (2005) Helix periodicity, topology, and dynamics of membrane-associated alpha-synuclein. *Protein Sci* 14:862–872.
- Bussièrè T, Giannakopoulos P, Bouras C, Perl DP, Morrison JH, Hof PR (2003) Progressive degeneration of nonphosphorylated neurofilament protein-enriched pyramidal neurons predicts cognitive impairment in Alzheimer's disease: Stereologic analysis of prefrontal cortex area 9. *J Comp Neurol* 463:281–302.
- Castillo-Carranza DL, Guerrero-Munoz MJ, Sengupta U, Gerson JE, Kaye R (2018)  $\alpha$ -Synuclein Oligomers Induce a Unique Toxic Tau Strain. *Biological Psychiatry*.
- Chandra S, Chen X, Rizo J, Jahn R, Südhof TC (2003) A broken alpha-helix in folded alpha-synuclein. *J Biol Chem* 278:15313–15318.
- Cheng IH, Scarce-Levie K, Legleiter J, Palop JJ, Gerstein H, Bien-Ly N, Puoliväli J, Lesné S, Ashe KH, Muchowski PJ, Mucke L (2007) Accelerating amyloid-beta

fibrillization reduces oligomer levels and functional deficits in Alzheimer disease mouse models. *J Biol Chem* 282:23818–23828.

Clinton LK, Blurton-Jones M, Myczek K, Trojanowski JQ, LaFerla FM (2010) Synergistic Interactions between Abeta, tau, and alpha-synuclein: acceleration of neuropathology and cognitive decline. *J Neurosci* 30:7281–7289.

Cole NB, Murphy DD, Grider T, Rueter S, Brasaemle D, Nussbaum RL (2002) Lipid droplet binding and oligomerization properties of the Parkinson's disease protein alpha-synuclein. *J Biol Chem* 277:6344–6352.

Colom-Cadena M, Gelpi E, Martí MJ, Charif S, Dols-Icardo O, Blesa R, Clarimón J, Lleó A (2013) MAPT H1 haplotype is associated with enhanced  $\alpha$ -synuclein deposition in dementia with Lewy bodies. *Neurobiology of Aging* 34:936–942.

Connell-Crowley L, Harper JW, Goodrich DW (1997) Cyclin D1/Cdk4 regulates retinoblastoma protein-mediated cell cycle arrest by site-specific phosphorylation. *Mol Biol Cell* 8:287–301.

Counts SE, He B, Nadeem M, Wu J, Scheff SW, Mufson EJ (2012) Hippocampal drebrin loss in mild cognitive impairment. *Neurodegener Dis* 10:216–219.

Crowther RA, Jakes R, Spillantini MG, Goedert M (1998) Synthetic filaments assembled from C-terminally truncated alpha-synuclein. *FEBS Lett* 436:309–312.

- Cuervo AM, Stefanis L, Fredenburg R, Lansbury PT, Sulzer D (2004) Impaired degradation of mutant alpha-synuclein by chaperone-mediated autophagy. *Science* 305:1292–1295.
- Davidson WS, Jonas A, Clayton DF, George JM (1998) Stabilization of alpha-synuclein secondary structure upon binding to synthetic membranes. *J Biol Chem* 273:9443–9449.
- Dawson HN, Ferreira A, Eyster MV, Ghoshal N, Binder LI, Vitek MP (2001) Inhibition of neuronal maturation in primary hippocampal neurons from tau deficient mice. *Journal of Cell Science* 114:1179–1187.
- Diao J, Burré J, Vivona S, Cipriano DJ, Sharma M, Kyoung M, Südhof TC, Brunger AT (2013) Native  $\alpha$ -synuclein induces clustering of synaptic-vesicle mimics via binding to phospholipids and synaptobrevin-2/VAMP2. *eLife* 2:e00592.
- Dixit R, Ross JL, Goldman YE, Holzbaur ELF (2008) Differential regulation of dynein and kinesin motor proteins by tau. *Science* 319:1086–1089 Available at: <http://www.pubmedcentral.nih.gov/articlerender.fcgi?artid=2866193&tool=pmcentrez&rendertype=abstract>.
- Duka T, Rusnak M, Drolet RE, Duka V, Wersinger C, Goudreau JL, Sidhu A (2006) Alpha-synuclein induces hyperphosphorylation of Tau in the MPTP model of parkinsonism. *FASEB J* 20:2302–2312.
- Duka V, Lee J-H, Credle J, Wills J, Oaks A, Smolinsky C, Shah K, Mash DC, Masliah E, Sidhu A (2013) Identification of the Sites of Tau Hyperphosphorylation and

Activation of Tau Kinases in Synucleinopathies and Alzheimer's Diseases Reddy H, ed. PLoS ONE 8:e75025–11.

Eliezer D, Kutluay E, Bussell R, Browne G (2001) Conformational properties of alpha-synuclein in its free and lipid-associated states. *Journal of Molecular Biology* 307:1061–1073.

Engler H, Forsberg A, Almkvist O, Blomquist G, Larsson E, Savitcheva I, Wall A, Ringheim A, Långström B, Nordberg A (2006) Two-year follow-up of amyloid deposition in patients with Alzheimer's disease. *Brain* 129:2856–2866.

Fortin DL, Troyer MD, Nakamura K, Kubo S-I, Anthony MD, Edwards RH (2004) Lipid rafts mediate the synaptic localization of alpha-synuclein. *J Neurosci* 24:6715–6723.

Fowler SW, Chiang ACA, Savjani RR, Larson ME, Sherman MA, Schuler DR, Cirrito JR, Lesné SE, Jankowsky JL (2014) Genetic modulation of soluble A $\beta$  rescues cognitive and synaptic impairment in a mouse model of Alzheimer's disease. *J Neurosci* 34:7871–7885.

George JM, Jin H, Woods WS, Clayton DF (1995) Characterization of a novel protein regulated during the critical period for song learning in the zebra finch. *Neuron* 15:361–372.

Glenner GG, Wong CW (1984a) Alzheimer's disease: initial report of the purification and characterization of a novel cerebrovascular amyloid protein. *Biochemical and Biophysical Research Communications* 120:885–890.

Glennner GG, Wong CW (1984b) Alzheimer's disease and Down's syndrome: sharing of a unique cerebrovascular amyloid fibril protein. *Biochemical and Biophysical Research Communications* 122:1131–1135.

Goate A, Chartier-Harlin MC, Mullan M, Brown J, Crawford F, Fidani L, Giuffra L, Haynes A, Irving N, James L (1991) Segregation of a missense mutation in the amyloid precursor protein gene with familial Alzheimer's disease. *Nature* 349:704–706.

Goedert M, Spillantini MG, Jakes R, Rutherford D, Crowther RA (1989a) Multiple isoforms of human microtubule-associated protein tau: sequences and localization in neurofibrillary tangles of Alzheimer's disease. *Neuron* 3:519–526.

Goedert M, Spillantini MG, Potier MC, Ulrich J, Crowther RA (1989b) Cloning and sequencing of the cDNA encoding an isoform of microtubule-associated protein tau containing four tandem repeats: differential expression of tau protein mRNAs in human brain. *The EMBO Journal* 8:393–399.

Goldgaber D, Lerman MI, McBride OW, Saffiotti U, Gajdusek DC (1987) Characterization and chromosomal localization of a cDNA encoding brain amyloid of Alzheimer's disease. *Science* 235:877–880.

Götz J, Chen F, van Dorpe J, Nitsch RM (2001) Formation of neurofibrillary tangles in P301I tau transgenic mice induced by Aβ<sub>42</sub> fibrils. *Science* 293:1491–1495.

Gratuzze M, Cisbani G, Cicchetti F, Planel E (2016) Is Huntington's disease a tauopathy? *Brain* 139:1014–1025.

Grundke-Iqbal I, Iqbal K, Tung YC, Quinlan M, Wisniewski HM, Binder LI (1986)

Abnormal phosphorylation of the microtubule-associated protein tau ( $\tau$ ) in Alzheimer cytoskeletal pathology. *Proceedings of the National Academy of Sciences* 83:4913–4917.

Guo JL, Covell DJ, Daniels JP, Iba M, Stieber A, Zhang B, Riddle DM, Kwong LK, Xu Y,

Trojanowski JQ, Lee VM-Y (2013) Distinct  $\alpha$ -synuclein strains differentially promote tau inclusions in neurons. *CELL* 154:103–117 Available at:

<http://www.pubmedcentral.nih.gov/articlerender.fcgi?artid=3820001&tool=pmcentrez&rendertype=abstract>.

Haggerty T, Credle J, Rodriguez O, Wills J, Oaks AW, Masliah E, Sidhu A (2011)

Hyperphosphorylated Tau in an  $\alpha$ -synuclein-overexpressing transgenic model of Parkinson's disease. *Eur J Neurosci* 33:1598–1610.

Hamilton RL (2000) Lewy Bodies in Alzheimer ' s Disease : A Neuropathological Review

of 145 Cases Using  $\alpha$ -Synuclein Immunohistochemistry. 384:378–384.

Harigaya Y, Shoji M, Shirao T, Hirai S (1996) Disappearance of actin-binding protein,

drebrin, from hippocampal synapses in Alzheimer's disease. *J Neurosci Res* 43:87–92.

Hashimoto M, Bar-on P, Ho G, Takenouchi T, Rockenstein E, Crews L, Masliah E

(2004)  $\beta$ -Synuclein Regulates Akt Activity in Neuronal Cells. *J Biol Chem* 279:23622–23629.

- Hatanpää K, Isaacs KR, Shirao T, Brady DR, Rapoport SI (1999) Loss of proteins regulating synaptic plasticity in normal aging of the human brain and in Alzheimer disease. *J Neuropathol Exp Neurol* 58:637–643.
- Hely MA, Reid WGJ, Adena MA, Halliday GM, Morris JGL (2008) The Sydney multicenter study of Parkinson's disease: the inevitability of dementia at 20 years. *Mov Disord* 23:837–844.
- Herrup K, Yang Y (2007) Cell cycle regulation in the postmitotic neuron: oxymoron or new biology? *Nat Rev Neurosci* 8:368–378 Available at: <http://www.ncbi.nlm.nih.gov/pubmed/17453017>.
- Hippius H, Neundörfer G (2003) The discovery of Alzheimer's disease. *Dialogues Clin Neurosci* 5:101–108.
- Holmes C, Boche D, Wilkinson D, Yadegarfar G, Hopkins V, Bayer A, Jones RW, Bullock R, Love S, Neal JW, Zotova E, Nicoll JA (2008) Long-term effects of A $\beta$ 42 immunisation in Alzheimer's disease: follow-up of a randomised, placebo-controlled phase I trial. *The Lancet* 372:216–223.
- Hong S, Beja-Glasser VF, Nfonoyim BM, Frouin A, Li S, Ramakrishnan S, Merry KM, Shi Q, Rosenthal A, Barres BA, Lemere CA, Selkoe DJ, Stevens B (2016) Complement and microglia mediate early synapse loss in Alzheimer mouse models. *Science* 352:712–716.
- Hoover BR, Reed MN, Su J, Penrod RD, Kotilinek LA, Grant MK, Pitstick R, Carlson GA, Lanier LM, Yuan L-L, Ashe KH, Liao D (2010) Tau Mislocalization to Dendritic

Spines Mediates Synaptic Dysfunction Independently of Neurodegeneration.

Neuron 68:1067–1081 Available at:

<http://linkinghub.elsevier.com/retrieve/pii/S0896627310009724>.

Horowitz PM, LaPointe N, Guillozet-Bongaarts AL, Berry RW, Binder LI (2006) N-terminal fragments of tau inhibit full-length tau polymerization in vitro. *Biochemistry* 45:12859–12866.

Höglinger GU, Breunig JJ, Depboylu C, Rouaux C, Michel PP, Alvarez-fischer D, Boutillier A-L, Degregori J, Oertel WH, Rakic P, Hirsch EC (2007) The pRb / E2F cell-cycle pathway mediates cell death in Parkinson ' s disease. 104:1–6.

Hsu LJ, Mallory M, Xia Y, Veinbergs I, Hashimoto M, Yoshimoto M, Thal LJ, Saitoh T, Masliah E (1998) Expression pattern of synucleins (non-Abeta component of Alzheimer's disease amyloid precursor protein/alpha-synuclein) during murine brain development. *Journal of Neurochemistry* 71:338–344.

Igbavboa U, Sun GY, Weisman GA, He Y, Wood WG (2009) Amyloid beta-protein stimulates trafficking of cholesterol and caveolin-1 from the plasma membrane to the Golgi complex in mouse primary astrocytes. *Neuroscience* 162:328–338

Available at:

<http://www.pubmedcentral.nih.gov/articlerender.fcgi?artid=3083247&tool=pmcentrez&rendertype=abstract>.

- Iseki E, Togo T, Suzuki K, Katsuse O, Marui W, de Silva R, Lees A, Yamamoto T, Kosaka K (2003) Dementia with Lewy bodies from the perspective of tauopathy. *Acta Neuropathol* 105:265–270.
- Ittner A et al. (2016) Site-specific phosphorylation of tau inhibits amyloid- $\beta$  toxicity in Alzheimer's mice. *Science* 354:904–908.
- Ittner LM, Götz J (2011) Amyloid- $\beta$  and tau--a toxic pas de deux in Alzheimer's disease. *Nat Rev Neurosci* 12:65–72 Available at:  
<http://www.ncbi.nlm.nih.gov/pubmed/21193853>.
- Ittner LM, Ke YD, Delerue F, Bi M, Gladbach A, van Eersel J, Wölfing H, Chieng BC, Christie MJ, Napier IA, Eckert A, Staufenbiel M, Hardeman E, Götz J (2010) Dendritic Function of Tau Mediates Amyloid- $\beta$  Toxicity in Alzheimer's Disease Mouse Models. *CELL* 142:387–397.
- Ivanov A, Esclapez M, Pellegrino C, Shirao T, Ferhat L (2009) Drebrin A regulates dendritic spine plasticity and synaptic function in mature cultured hippocampal neurons. *Journal of Cell Science* 122:524–534.
- Jeganathan S, Bergen von M, Brutlach H, Steinhoff H-J, Mandelkow E (2006) Global hairpin folding of tau in solution. *Biochemistry* 45:2283–2293.
- Jenkins SM, Johnson GV (1998) Tau complexes with phospholipase C-gamma in situ. *Neuroreport* 9:67–71.

- Jensen PH, Hager H, Nielsen MS, Hojrup P, Gliemann J, Jakes R (1999) alpha-synuclein binds to Tau and stimulates the protein kinase A-catalyzed tau phosphorylation of serine residues 262 and 356. *J Biol Chem* 274:25481–25489.
- Ji H, Liu YE, Jia T, Wang M, Liu J, Xiao G, Joseph BK, Rosen C, Shi YE (1997) Identification of a breast cancer-specific gene, BCSG1, by direct differential cDNA sequencing. *Cancer Res* 57:759–764.
- Jicha GA, Bowser R, Kazam IG, Davies P (1997) Alz-50 and MC-1, a new monoclonal antibody raised to paired helical filaments, recognize conformational epitopes on recombinant tau. *J Neurosci Res* 48:128–132.
- Jin M, Shepardson N, Yang T, Chen G, Walsh D, Selkoe DJ (2011) Soluble amyloid beta-protein dimers isolated from Alzheimer cortex directly induce Tau hyperphosphorylation and neuritic degeneration. *Proc Natl Acad Sci USA* 108:5819–5824.
- Jo E, McLaurin J, Yip CM, St George-Hyslop P, Fraser PE (2000) alpha-Synuclein membrane interactions and lipid specificity. *J Biol Chem* 275:34328–34334.
- Jonsson T et al. (2012) A mutation in APP protects against Alzheimer's disease and age-related cognitive decline. *Nature* 488:96–99 Available at: <http://www.ncbi.nlm.nih.gov/pubmed/22801501>.
- Jordan-Sciutto KL, Dorsey R, Chalovich EM, Hammond RR, Achim CL (2003) Expression patterns of retinoblastoma protein in Parkinson disease. *J Neuropathol Exp Neurol* 62:68–74.

- Jung G, Kim E-J, Cicvaric A, Sase S, Gröger M, Höger H, Sialana FJ, Berger J, Monje FJ, Lubec G (2015) Drebrin depletion alters neurotransmitter receptor levels in protein complexes, dendritic spine morphogenesis and memory-related synaptic plasticity in the mouse hippocampus. *Journal of Neurochemistry* 134:327–339.
- Kallhoff V, Peethumnongsin E, Zheng H (2007) Lack of  $\alpha$ -synuclein increases amyloid plaque accumulation in a transgenic mouse model of Alzheimer's disease. *Mol Neurodegeneration* 2:6–7.
- Kang J, Lemaire HG, Unterbeck A, Salbaum JM, Masters CL, Grzeschik KH, Multhaup G, Beyreuther K, Müller-Hill B (1987) The precursor of Alzheimer's disease amyloid A4 protein resembles a cell-surface receptor. *Nature* 325:733–736.
- Kannangara TS, Eadie BD, Bostrom CA, Morch K, Brocardo PS, Christie BR (2015) GluN2A  $-/-$  Mice Lack Bidirectional Synaptic Plasticity in the Dentate Gyrus and Perform Poorly on Spatial Pattern Separation Tasks. *Cereb Cortex* 25:2102–2113.
- King ME, Kan H-M, Baas PW, Erisir A, Glabe CG, Bloom GS (2006) Tau-dependent microtubule disassembly initiated by prefibrillar beta-amyloid. *J Cell Biol* 175:541–546 Available at:  
<http://www.pubmedcentral.nih.gov/articlerender.fcgi?artid=2064590&tool=pmcentrez&rendertype=abstract>.
- Kochanek KD, Murphy SL, Xu J, Tejada-Vera B (2016) Deaths: Final Data for 2014. *Natl Vital Stat Rep* 65:1–122.

Kontopoulos E, Parvin JD, Feany MB (2006) Alpha-synuclein acts in the nucleus to inhibit histone acetylation and promote neurotoxicity. *Human Molecular Genetics* 15:3012–3023.

Kosik KS, Joachim CL, Selkoe DJ (1986) Microtubule-associated protein tau (tau) is a major antigenic component of paired helical filaments in Alzheimer disease. *Proceedings of the National Academy of Sciences* 83:4044–4048.

Kumar DKV, Choi SH, Washicosky KJ, Eimer WA, Tucker S, Ghofrani J, Lefkowitz A, McColl G, Goldstein LE, Tanzi RE, Moir RD (2016) Amyloid- $\beta$  peptide protects against microbial infection in mouse and worm models of Alzheimer's disease. *Science Translational Medicine* 8:340ra72–340ra72.

Larson M, Sherman MA, Amar F, Nuvolone M, Schneider JA, Bennett DA, Aguzzi A, Lesné SE (2012a) The complex PrP(c)-Fyn couples human oligomeric A $\beta$  with pathological tau changes in Alzheimer's disease. *J Neurosci* 32:16857–71a.

Larson ME, Greimel SJ, Amar F, LaCroix M, Boyle G, Sherman MA, Schley H, Miel C, Schneider JA, Kaye R, Benfenati F, Lee MK, Bennett DA, Lesné SE (2017) Selective lowering of synapses induced by oligomeric  $\alpha$ -synuclein exacerbates memory deficits. *Proc Natl Acad Sci USA* 114:E4648–E4657.

Larson ME, Sherman MA, Greimel S, Kuskowski M, Schneider JA, Bennett DA, Lesné SE (2012b) Soluble  $\alpha$ -Synuclein Is a Novel Modulator of Alzheimer's Disease Pathophysiology. *Journal of Neuroscience* 32:10253–10266.

Lasagna-Reeves CA, Castillo-Carranza DL, Guerrero-Munoz MJ, Jackson GR, Kaye R (2010) Preparation and Characterization of Neurotoxic Tau Oligomers.

Biochemistry 49:10039–10041.

Lee MK, Stirling W, Xu Y, Xu X, Qui D, Mandir AS, Dawson TM, Copeland NG, Jenkins NA, Price DL (2002) Human  $\alpha$ -synuclein-harboring familial Parkinson's disease-linked Ala-53  $\rightarrow$  Thr mutation causes neurodegenerative disease with  $\alpha$ -synuclein aggregation in transgenic mice. Proceedings of the National Academy of Sciences 99:8968–8973.

Lee VM, Goedert M, Trojanowski JQ (2001) Neurodegenerative tauopathies. Annu Rev Neurosci 24:1121–1159.

Lesné S, Kotilinek L, Ashe KH (2008) Plaque-bearing mice with reduced levels of oligomeric amyloid-beta assemblies have intact memory function. Neuroscience 151:745–749.

Lesné S, Ali C, Gabriel C, Croci N, MacKenzie ET, Glabe CG, Plotkine M, Marchand-Verrecchia C, Vivien D, Buisson A (2005) NMDA receptor activation inhibits alpha-secretase and promotes neuronal amyloid-beta production. J Neurosci 25:9367–9377.

Lesné S, Koh MT, Kotilinek L, Kaye R, Glabe CG, Yang A, Gallagher M, Ashe KH (2006) A specific amyloid-beta protein assembly in the brain impairs memory. Nature 440:352–357.

- Leugers CJ, Lee G (2010) Tau potentiates nerve growth factor-induced mitogen-activated protein kinase signaling and neurite initiation without a requirement for microtubule binding. *J Biol Chem* 285:19125–19134.
- Lewis J, Dickson DW, Lin WL, Chisholm L, Corral A, Jones G, Yen SH, Sahara N, Skipper L, Yager D, Eckman C, Hardy J, Hutton M, McGowan E (2001) Enhanced neurofibrillary degeneration in transgenic mice expressing mutant tau and APP. *Science* 293:1487–1491 Available at:  
<http://www.pubmedcentral.nih.gov/articlerender.fcgi?artid=PMC4249520>.
- Liu P, Reed MN, Kotilinek LA, Grant MKO, Forster CL, Qiang W, Shapiro SL, Reichl JH, Chiang ACA, Jankowsky JL, Wilmot CM, Cleary JP, Zahs KR, Ashe KH (2015) Quaternary Structure Defines a Large Class of Amyloid- $\beta$  Oligomers Neutralized by Sequestration. *CellReports* 11:1760–1771.
- Ma H, Lesné S, Kotilinek L, Steidl-Nichols JV, Sherman M, Younkin L, Younkin S, Forster C, Sergeant N, Delacourte A, Vassar R, Citron M, Kofuji P, Boland LM, Ashe KH (2007) Involvement of beta-site APP cleaving enzyme 1 (BACE1) in amyloid precursor protein-mediated enhancement of memory and activity-dependent synaptic plasticity. *Proceedings of the National Academy of Sciences* 104:8167–8172.
- Maroteaux L, Campanelli JT, Scheller RH (1988) Synuclein: a neuron-specific protein localized to the nucleus and presynaptic nerve terminal. *Journal of Neuroscience* 8:2804–2815.

- Masliah E, Rockenstein E, Veinbergs I, Sagara Y, Mallory M, Hashimoto M, Mucke L (2001)  $\beta$ -Amyloid peptides enhance  $\alpha$ -synuclein accumulation and neuronal deficits in a transgenic mouse model linking Alzheimer's disease and Parkinson's disease. *Proceedings of the National Academy of Sciences* 98:12245–12250.
- Merrick SE, Trojanowski JQ, Lee VM (1997) Selective destruction of stable microtubules and axons by inhibitors of protein serine/threonine phosphatases in cultured human neurons. *Journal of Neuroscience* 17:5726–5737.
- Mori F, Tanji K, Yoshimoto M, Takahashi H, Wakabayashi K (2002) Immunohistochemical comparison of alpha- and beta-synuclein in adult rat central nervous system. *Brain Research* 941:118–126.
- Morris M, Knudsen GM, Maeda S, Trinidad JC, Ioanoviciu A, Burlingame AL, Mucke L (2015) Tau post-translational modifications in wild-type and human amyloid precursor protein transgenic mice. *Nature Neuroscience* 18:1183–1189.
- Mucke L, Yu GQ, Masliah E, Mallory M, Rockenstein EM, Tatsuno G, Hu K, Kholodenko D, Johnson-Wood K, McConlogue L (2000) High-level neuronal expression of abeta 1-42 in wild-type human amyloid protein precursor transgenic mice: synaptotoxicity without plaque formation. *20:4050–4058* Available at: <http://www.ncbi.nlm.nih.gov/pubmed/10818140>.
- Mullan M, Crawford F, Axelman K, Houlden H, Lilius L, Winblad B, Lannfelt L (1992) A pathogenic mutation for probable Alzheimer's disease in the APP gene at the N-terminus of beta-amyloid. *Nat Genet* 1:345–347.

- Murrell J, Farlow M, Ghetti B, Benson MD (1991) A mutation in the amyloid precursor protein associated with hereditary Alzheimer's disease. *Science* 254:97–99.
- Nakajo S, Shioda S, Nakai Y, Nakaya K (1994) Localization of phosphoneuroprotein 14 (PNP 14) and its mRNA expression in rat brain determined by immunocytochemistry and in situ hybridization. *Brain Res Mol Brain Res* 27:81–86.
- Nelson PT, Braak H, Markesbery WR (2009) Neuropathology and Cognitive Impairment in Alzheimer Disease: A Complex but Coherent Relationship. *J Neuropathol Exp Neurol* 68:1–14.
- Nemani VM, Lu W, Berge V, Nakamura K, Onoa B, Lee MK, Chaudhry FA, Nicoll RA, Edwards RH (2010) Increased expression of alpha-synuclein reduces neurotransmitter release by inhibiting synaptic vesicle reclustering after endocytosis. *Neuron* 65:66–79.
- Neve RL, Harris P, Kosik KS, Kurnit DM, Donlon TA (1986) Identification of cDNA clones for the human microtubule-associated protein tau and chromosomal localization of the genes for tau and microtubule-associated protein 2. *Brain Research* 387:271–280.
- Nicoll JAR, Wilkinson D, Holmes C, Steart P, Markham H, Weller RO (2003) Neuropathology of human Alzheimer disease after immunization with amyloid-beta peptide: a case report. *Nature Medicine* 9:448–452.
- Norambuena A, Wallrabe H, McMahon L, Silva A, Swanson E, Khan SS, Baerthlein D, Kodis E, Oddo S, Mandell JW, Bloom GS (2017) mTOR and neuronal cell cycle

reentry: How impaired brain insulin signaling promotes Alzheimer's disease. *Alzheimers Dement* 13:152–167.

Nuscher B, Kamp F, Mehnert T, Odoy S, Haass C, Kahle PJ, Beyer K (2004) Alpha-synuclein has a high affinity for packing defects in a bilayer membrane: a thermodynamics study. *J Biol Chem* 279:21966–21975.

Nussbaum JM, Schilling S, Cynis H, Silva A, Swanson E, Wangsanut T, Tayler K, Wiltgen B, Hatami A, Rönicke R, Reymann K, Hutter-Paier B, Alexandru A, Jagla W, Graubner S, Glabe CG, Demuth H-U, Bloom GS (2012) Prion-like behaviour and tau-dependent cytotoxicity of pyroglutamylated amyloid- $\beta$ . *Nature* 485:651–655  
Available at: <http://www.ncbi.nlm.nih.gov/pubmed/22660329>.

Outeiro TF, Kontopoulos E, Altmann SM, Kufareva I, Strathearn KE, Amore AM, Volk CB, Maxwell MM, Rochet J-C, McLean PJ, Young AB, Abagyan R, Feany MB, Hyman BT, Kazantsev AG (2007) Sirtuin 2 inhibitors rescue alpha-synuclein-mediated toxicity in models of Parkinson's disease. *Science* 317:516–519.

Overk CR, Cartier A, Shaked G, Rockenstein E, Ubhi K, Spencer B, Price DL, Patrick C, Desplats P, Masliah E (2014) Hippocampal neuronal cells that accumulate alpha-synuclein fragments are more vulnerable to A $\beta$  oligomer toxicity via mGluR5 - implications for dementia with Lewy bodies. 9:1–18.

Park SM, Ahn KJ, Jung HY, Park JH, Kim J (2004) Effects of novel peptides derived from the acidic tail of synuclein (ATS) on the aggregation and stability of fusion proteins. *Protein Eng Des Sel* 17:251–260.

- Park SM, Jung HY, Chung KC, Rhim H, Park JH, Kim J (2002) Stress-induced aggregation profiles of GST-alpha-synuclein fusion proteins: role of the C-terminal acidic tail of alpha-synuclein in protein thermosolubility and stability. *Biochemistry* 41:4137–4146.
- Perrin RJ, Woods WS, Clayton DF, George JM (2000) Interaction of human alpha-Synuclein and Parkinson's disease variants with phospholipids. Structural analysis using site-directed mutagenesis. *J Biol Chem* 275:34393–34398.
- Petersen RC, Stevens JC, Ganguli M, Tangalos EG, Cummings JL, DeKosky ST (2001) Practice parameter: Early detection of dementia: Mild cognitive impairment (an evidence-based review): Report of the Quality Standards Subcommittee of the American Academy of Neurology. *Neurology* 56:1133–1142.
- Rapoport M, Dawson HN, Binder LI, Vitek MP, Ferreira A (2002) Tau is essential to beta-amyloid-induced neurotoxicity. *Proceedings of the National Academy of Sciences* 99:6364–6369.
- Reed MN, Hofmeister JJ, Jungbauer L, Welzel AT, Yu C, Sherman MA, Lesné S, Ladu MJ, Walsh DM, Ashe KH, Cleary JP (2011) Cognitive effects of cell-derived and synthetically derived A $\beta$  oligomers. *Neurobiology of Aging* 32:1784–1794.
- Reiman EM et al. (2012) Brain imaging and fluid biomarker analysis in young adults at genetic risk for autosomal dominant Alzheimer's disease in the presenilin 1 E280A kindred: a case-control study. *The Lancet Neurology* 11:1048–1056.

- Rentz DM, Locascio JJ, Becker JA, Moran EK, Eng E, Buckner RL, Sperling RA, Johnson KA (2010) Cognition, reserve, and amyloid deposition in normal aging. *Ann Neurol* 67:353–364.
- Roberson ED, Scearce-Levie K, Palop JJ, Yan F, Cheng IH, Wu T, Gerstein H, Yu GQ, Mucke L (2007) Reducing Endogenous Tau Ameliorates Amyloid  $\beta$ -Induced Deficits in an Alzheimer's Disease Mouse Model. *Science* 316:750–754.
- Sapir T, Frotscher M, Levy T, Mandelkow E-M, Reiner O (2012) Tau's role in the developing brain: implications for intellectual disability. *Human Molecular Genetics* 21:1681–1692.
- Schell H, Hasegawa T, Neumann M, Kahle PJ (2009) Nuclear and neuritic distribution of serine-129 phosphorylated alpha-synuclein in transgenic mice. *Neuroscience* 160:796–804.
- Schnell SA, Staines WA, Wessendorf MW (1999) Reduction of lipofuscin-like autofluorescence in fluorescently labeled tissue. *J Histochem Cytochem* 47:719–730.
- Scott D, Roy S (2012)  $\alpha$ -Synuclein inhibits intersynaptic vesicle mobility and maintains recycling-pool homeostasis. *J Neurosci* 32:10129–10135.
- Selkoe DJ (2002) Alzheimer's Disease Is a Synaptic Failure. *Science* 298:789–791.
- Sengupta U, Guerrero-Munoz MJ, Castillo-Carranza DL, Lasagna-Reeves CA, Gerson JE, Paulucci-Holthauzen AA, Krishnamurthy S, Farhed M, Jackson GR, Kaye R

(2015) Pathological interface between oligomeric alpha-synuclein and tau in synucleinopathies. *Biological Psychiatry* 78:672–683.

Seward ME, Swanson E, Norambuena A, Reimann A, Cochran JN, Li R, Roberson ED, Bloom GS (2013) Amyloid- $\beta$  signals through tau to drive ectopic neuronal cell cycle re-entry in Alzheimer's disease. *Journal of Cell Science* 126:1278–1286 Available at: <http://www.ncbi.nlm.nih.gov/pubmed/23345405>.

Shankar GM, Li S, Mehta TH, Garcia-Munoz A, Shepardson NE, Smith I, Brett FM, Farrell MA, Rowan MJ, Lemere CA, Regan CM, Walsh DM, Sabatini BL, Selkoe DJ (2008) Amyloid-beta protein dimers isolated directly from Alzheimer's brains impair synaptic plasticity and memory. *Nature Medicine* 14:837–842 Available at: <http://www.pubmedcentral.nih.gov/articlerender.fcgi?artid=2772133&tool=pmcentrez&rendertype=abstract>.

Sherman MA, LaCroix M, Amar F, Larson ME, Forster C, Aguzzi A, Bennett DA, Ramsden M, Lesné SE (2016) Soluble Conformers of A $\beta$  and Tau Alter Selective Proteins Governing Axonal Transport. *J Neurosci* 36:9647–9658.

Sherman MA, Lesné SE (2011) Detecting a $\beta$ \*56 oligomers in brain tissues. *Methods Mol Biol* 670:45–56.

Shirao T, González-Billault C (2013) Actin filaments and microtubules in dendritic spines. *Journal of Neurochemistry* 126:155–164.

Simón-Sánchez J et al. (2009) Genome-wide association study reveals genetic risk underlying Parkinson's disease. *Nat Genet* 41:1308–1312.

- Singleton AB et al. (2003) Alpha-Synuclein Locus Triplication Causes Parkinson's Disease. *Science* 302:2003.
- Spencer B, Desplats PA, Overk CR, Valera-Martin E, Rissman RA, Wu C, Mante M, Adame A, Florio J, Rockenstein E, Masliah E (2016) Reducing Endogenous  $\alpha$ -Synuclein Mitigates the Degeneration of Selective Neuronal Populations in an Alzheimer's Disease Transgenic Mouse Model. *Journal of Neuroscience* 36:7971–7984.
- Spires-Jones TL, Stoothoff WH, de Calignon A, Jones PB, Hyman BT (2009) Tau pathophysiology in neurodegeneration: a tangled issue. *Trends in Neurosciences* 32:150–159.
- Stone JG, Siedlak SL, Tabaton M, Hirano A, Castellani RJ, Santocanale C, Perry G, Smith MA, Zhu X, Lee H-G (2011) The cell cycle regulator phosphorylated retinoblastoma protein is associated with tau pathology in several tauopathies. *J Neuropathol Exp Neurol* 70:578–587.
- Sunyer B, Patil S, Höger H, Lubec G (2007) Barnes maze, a useful task to assess spatial reference memory in the mice.
- Swanson E, Breckenridge L, McMahon L, Som S, McConnell I, Bloom GS (2017) Extracellular Tau Oligomers Induce Invasion of Endogenous Tau into the Somatodendritic Compartment and Axonal Transport Dysfunction. *Alzheimer's Dis* 58:803–820.

- Tanzi RE, Gusella JF, Watkins PC, Bruns GA, St George-Hyslop P, Van Keuren ML, Patterson D, Pagan S, Kurnit DM, Neve RL (1987) Amyloid beta protein gene: cDNA, mRNA distribution, and genetic linkage near the Alzheimer locus. *Science* 235:880–884.
- Tobe T, Nakajo S, Tanaka A, Mitoya A, Omata K, Nakaya K, Tomita M, Nakamura Y (1992) Cloning and characterization of the cDNA encoding a novel brain-specific 14-kDa protein. *Journal of Neurochemistry* 59:1624–1629.
- Tucker KL, Meyer M, Barde YA (2001) Neurotrophins are required for nerve growth during development. *Nature Neuroscience* 4:29–37.
- Tyan S-H, Shih AY-J, Walsh JJ, Maruyama H, Sarsoza F, Ku L, Eggert S, Hof PR, Koo EH, Dickstein DL (2012) Amyloid precursor protein (APP) regulates synaptic structure and function. *Mol Cell Neurosci* 51:43–52.
- Uéda K, Fukushima H, Masliah E, Xia Y, Iwai A, Yoshimoto M, Otero DA, Kondo J, Ihara Y, Saitoh T (1993) Molecular cloning of cDNA encoding an unrecognized component of amyloid in Alzheimer disease. *Proceedings of the National Academy of Sciences* 90:11282–11286.
- Varvel NH, Bhaskar K, Patil AR, Pimplikar SW, Herrup K, Lamb BT (2008) Aβ Oligomers Induce Neuronal Cell Cycle Events in Alzheimer's Disease. *Journal of Neuroscience* 28:10786–10793.
- Vellas B, Black R, Thal LJ, Fox NC, Daniels M, McLennan G, Tompkins C, Leibman C, Pomfret M, Grundman M, AN1792 (QS-21)-251 Study Team (2009) Long-term

follow-up of patients immunized with AN1792: reduced functional decline in antibody responders. *Curr Alzheimer Res* 6:144–151.

Volles MJ, Lee SJ, Rochet JC, Shtilerman MD, Ding TT, Kessler JC, Lansbury PT (2001) Vesicle permeabilization by protofibrillar alpha-synuclein: implications for the pathogenesis and treatment of Parkinson's disease. *Biochemistry* 40:7812–7819.

Vossel KA, Zhang K, Brodbeck J, Daub AC, Sharma P, Finkbeiner S, Cui B, Mucke L (2010) Tau Reduction Prevents A $\beta$ -Induced Defects in Axonal Transport. *Science* 330:198–198.

Wang L, Das U, Scott DA, Tang Y, McLean PJ, Roy S (2014)  $\alpha$ -synuclein multimers cluster synaptic vesicles and attenuate recycling. *Curr Biol* 24:2319–2326.

Wang W et al. (2011) A soluble  $\alpha$ -synuclein construct forms a dynamic tetramer. *Proc Natl Acad Sci USA* 108:17797–17802.

Waxman EA, Giasson BI (2011) Induction of intracellular tau aggregation is promoted by  $\alpha$ -synuclein seeds and provides novel insights into the hyperphosphorylation of tau. *J Neurosci* 31:7604–7618.

Weaver CL, Espinoza M, Kress Y, Davies P (2000) Conformational change as one of the earliest alterations of tau in Alzheimer's disease. *NBA* 21:719–727.

Weingarten MD, Lockwood AH, Hwo SY, Kirschner MW (1975) A protein factor essential for microtubule assembly. *Proceedings of the National Academy of Sciences* 72:1858–1862 Available at:

[http://www.pubmedcentral.nih.gov/articlerender.fcgi?artid=432646&tool=pmcentrez  
&rendertype=abstract](http://www.pubmedcentral.nih.gov/articlerender.fcgi?artid=432646&tool=pmcentrez&rendertype=abstract).

West MJ, Coleman PD, Flood DG, Troncoso JC (1994) Differences in the pattern of hippocampal neuronal loss in normal ageing and Alzheimer's disease. *344:769–772*  
Available at: <http://linkinghub.elsevier.com/retrieve/pii/S0140673694923388>.

Withers GS, George JM, Banker GA, Clayton DF (1997) Delayed localization of synelfin (synuclein, NACP) to presynaptic terminals in cultured rat hippocampal neurons. *Brain Res Dev Brain Res 99:87–94*.

Witman GB, Cleveland DW, Weingarten MD, Kirschner MW (1976) Tubulin requires tau for growth onto microtubule initiating sites. *Proceedings of the National Academy of Sciences 73:4070–4074*.

Woerman AL, St hr J, Aoyagi A, Rampersaud R, Krejciova Z, Watts JC, Ohyama T, Patel S, Widjaja K, Oehler A, Sanders DW, Diamond MI, Seeley WW, Middleton LT, Gentleman SM, Mordes DA, S dhof TC, Giles K, Prusiner SB (2015) Propagation of prions causing synucleinopathies in cultured cells. *Proceedings of the National Academy of Sciences 112:E4949–E4958*.

Wood JG, Mirra SS, Pollock NJ, Binder LI (1986) Neurofibrillary tangles of Alzheimer disease share antigenic determinants with the axonal microtubule-associated protein tau (tau). *Proceedings of the National Academy of Sciences 83:4040–4043*.

Wu K-P, Kim S, Fela DA, Baum J (2008) Characterization of conformational and dynamic properties of natively unfolded human and mouse alpha-synuclein

ensembles by NMR: implication for aggregation. *Journal of Molecular Biology* 378:1104–1115.

Yoshiyama Y, Lee VM, Trojanowski JQ (2001) Frontotemporal dementia and tauopathy. *Curr Neurol Neurosci Rep* 1:413–421.

Yu S, Li X, Liu G, Han J, Zhang C, Li Y, Xu S, Liu C, Gao Y, Yang H, Uéda K, Chan P (2007) Extensive nuclear localization of alpha-synuclein in normal rat brain neurons revealed by a novel monoclonal antibody. *Neuroscience* 145:539–555.